

**Size controlled retinal differentiation of human  
induced pluripotent stem cells in shaking  
microwells**

Thesis submitted for the degree of

**Doctor of Engineering in Biochemical Engineering**

**Vishal Surendra Sharma**

**The Advanced Centre for Biochemical Engineering**

**Department of Biochemical Engineering**

**University College London**

## **Declaration**

**I, Vishal Surendra Sharma, confirm that the work presented in this thesis is my own. Where information has been derived from other sources, I confirm that this has been indicated in the thesis.**

## Acknowledgments

Thank you to my supervisor Dr Farlan Veraitch for recruiting me to the Regenerative Medicine group and this doctoral training programme. The advice, vision and enthusiasm you have shared have given flight to my ideas and provided support throughout. Thank you also to my second supervisor Professor Gary Lye your knowledge and wisdom have helped focus my efforts and inspire me to reach for new horizons.

At UCL my gratitude goes to Ludmilla Ruban who has trained me in stem cell culture with selfless dedication making the work herein possible. My thanks go to Amelia, and Dae for sharing their knowledge on retinal differentiation protocols and more. Thanks also to the rest of the Regenmed lab Owen, Tristan, Shahz, Nat, Kate and Iwan, Giulia, Ben, John, Rui and Zuming. Your kind and practical words of advice, precisely chilled alcohol and cake in times of daily need have helped me reach the finish line! Thanks also to the rest of my EngD cohort who have made the past few years so much fun to look back on. I would also like to thank Professor Pete Coffey and his lab at the Institute of Ophthalmology for showing kind generosity in teaching me the fine art of cryosectioning! My gratitude also goes to my masters students Leonard Leung and Rose Kinsella for their enthusiastic efforts during their summer placement with me.

Thank you to Kunal, Sheena, Kishen, Hanish and Minesh you have been there for me without question and are the best friends I could wish for and you're unconditional support will always be remembered. Thanks to the Samanta family for fun breaks and tasty meals to sustain Anoushka and I during the exams and writing months. Eternal gratitude goes to my parents, you're love and support is a true blessing and one to which I owe everything. Thanks also to my lovely sisters Alpa and Jyoti and Brother-in-law, Matt for their unwavering support, optimism and belief. A heartfelt thank you also goes to my wonderful fiancé Anoushka for being my study buddy, enduring and enjoying too many lab themed dates and for providing much needed joy every single day.

Finally, I would like to thank my sponsors UCL and the Engineering and Physical Sciences Research Council for their support.

## Abstract

Human induced pluripotent stem cells (hiPSC) have the potential to provide patient and disease specific cells for research and act as therapeutic agents in unlimited supply. To translate lab-scale research toward clinical applications we need to reduce variability from complex differentiation protocols which often include xenogeneic components. A move toward more defined culture systems will improve predictability and process control as well as reduce risks of exposure to animal pathogens. Cell therapy development, also requires flexibility in scalability as cell numbers for therapies vary greatly between disease indications. Improved control over the microenvironment at the lab scale would offer more defined parameters amenable to scale up with better flexibility, reduced waste and more precision.

This thesis describes the use of forced aggregation to improve the initiation of differentiation combined with culture in pre-validated and scalable, 24 microwell plates on shaking platforms, for stem cell differentiation toward retinal lineages. Using an established hiPSC line (MSU001) we show using forced aggregation to form embryoid bodies (EBs) promotes efficient initiation of differentiation. We next determined 2 EB sizes (5K and 10K cells/EB) which improved initiation of retinal differentiation compared to scraped EBs as demonstrated by >3fold increase in expression of early eye field transcription factor Rax at day 3 of culture. The 5K and 10K EBs also facilitated the adaption of an adherent protocol for retinal differentiation to an orbital shaken suspension culture system. Size controlled EBs also enabled the selection of a permissive shaking speed (120rpm) suitable for orbital shaken culture for initiating retinal differentiation with 5K and 10K EBs. Furthermore orbital shaken culture enabled elimination of the undefined xenogeneic ingredients of Matrigel, from the culture system.

This thesis demonstrates that combining size control for hiPSC derived EBs and orbital shaken culture is a feasible method for the initiation of retinal differentiation. By facilitating removal of xenogeneic materials from the culture system; the combination of orbital shaken culture with size controlled EBs may be of value to other complex stem cell differentiation systems to improve the initiation of differentiation whilst providing the potential for scalability.

## Table of Contents

**Initiation of retinal differentiation in size-controlled human induced pluripotent stem cell derived embryoid bodies on an orbital shaken microwell platform.** Error!  
Bookmark not defined.

<b>Declaration.....</b>	<b>2</b>
<b>Acknowledgments .....</b>	<b>3</b>
<b>Abstract.....</b>	<b>4</b>
<b>List of Figures.....</b>	<b>8</b>
<b>List Tables.....</b>	<b>12</b>
<b>List of Abbreviations .....</b>	<b>14</b>
<b>Chapter 1.0 Introduction.....</b>	<b>17</b>
1.1 The emergence of pluripotent stem cells.....	17
1.2 Human embryonic stem cells .....	18
1.3 The emergence of induced pluripotent stem cells .....	20
1.4 IPS derivation and culture refinement.....	21
1.5 hiPSC Characterisation.....	25
1.6 Stem cell differentiation with embryoid bodies .....	27
1.7 The case for orbitally shaken culture systems for retinal differentiation .....	32
1.8 Engineering and flow characteristics in shaken microwells .....	35
1.9 The eye and in vitro retinogenesis as a biological model to investigate stem cell differentiation .....	40
1.10 Cues for directed differentiation of pluripotent stem cells into retinal cells ....	47
1.11 Project Aims & Objectives .....	58
<b>2.0 Materials and Methods.....</b>	<b>61</b>
2.1 Pluripotent stem cell culture and maintenance .....	61
2.2 Aggregation of stem cells and aggregate/EB processing .....	64
2.3 Retinal differentiation.....	65
2.4 Analytical techniques for retinal differentiation.....	67
2.5 Immunocytochemistry .....	71
2.6 Gene expression analyses .....	72

2.7 Mycoplasma Testing and Karyotyping .....	74
<b>3.0 Stem Cell Aggregation Efficiency and EB Size Control .....</b>	<b>78</b>
3.1 Introduction .....	78
3.2 Characterisation of EB Formation.....	80
3.3 The impact of aggregation technique on EB size.....	87
3.4 Pluripotency and differentiation capacity of EBs.....	91
3.5 Differentiation capacity of EBs .....	91
3.6 Summary .....	92
<b>4.0 Establishing an orbitally shaken culture protocol to initiate retinal differentiation .....</b>	<b>97</b>
4.1 Introduction & Aims .....	97
4.2 Establishing a range of viable EB sizes permissive to retinal differentiation in suspension culture .....	99
4.3 Selection of orbital shaking frequencies for EB culture.....	104
4.4 Characterizing the impact of EB size on initiation of retinal differentiation in suspension cultures.....	110
4.5 Summary .....	113
<b>5.0 The impact of size controlled EBs and orbital shaking on the progression of retinal differentiation over 21 days in a matrigel-free culture .....</b>	<b>114</b>
5.1 Introduction .....	114
5.2 Characterising the impact of orbital shaking culture on retinal differentiation	116
5.3 Immunocytochemistry analyses show retinal marker expression in orbital shaken cultures is comparable to that of static culture.....	125
5.4 QPCR Analyses of retinal differentiation in adherent and orbital shaken cultures .....	131
5.5 Day 15: QPCR Analyses of EFTFs and POU5F1 expression.....	135
5.6 Day 21: QPCR Analyses of EFTFs and POU5F1 expression.....	140
5.7 Summary .....	147
<b>6.0 Orbital shaken culture of EBs for retinal differentiation with a feeder free cell line .....</b>	<b>150</b>
6.1 Introduction .....	150
6.2 Forced aggregation maintains consistent EB formation sizes with BJ hiPSC derived EBS which express early retinal markers at day 3 .....	151

6.3 Orbital shaken cultures support initiation of retinal differentiation in the feeder free cell line BJ hiPS derived EBs.....	154
6.4 QPCR analyses for retinal differentiation in orbital shaken cultures with BJ hiPSC derived EBs .....	159
6.5 Summary .....	162
<b>7.0 Conclusions and future work.....</b>	<b>163</b>
7.1 Conclusions .....	163
7.2 Future work .....	168
<b>Appendix I .....</b>	<b>172</b>
<b>AppendixII.....</b>	<b>173</b>
<b>Bibliography .....</b>	<b>181</b>

## **List of Figures**

### **Chapter 1**

- 1.1 Common methods for EB formation
- 1.2 Structural features of the retina linked to transcriptional control and key differentiation protocols
- 1.3 Environmental cues and bioprocessing factors impacting pluripotent stem cell fate decisions
- 1.4 Overview of optic cup morphogenesis and extracellular matrix components
- 1.5 Overview of experimental approach

### **Chapter 2**

- 2.1 Micrographs of EBs with illustrated lines to show average size measurement method
- 2.2 Karyotypic Analysis of MSU001 and BJ hiPSC lines

### **Chapter 3**

- 3.1 Micrographs of stem cell aggregates at 24 hours
- 3.2 Numbers of cells per EB without taking size distribution into account
- 3.3 Live and dead cell counts for scraped versus forced aggregation for MSU001 hiPSC
- 3.4 Size distribution plots of variation in EB size between aggregation techniques at 24 hours
- 3.5 Size distribution plots of variation in EB size between aggregation techniques at 48 hours
- 3.6 Fluorescent micrographs of stem cell aggregates at 24 hours
- 3.7 Expression of pluripotency markers and early retinal transcription factors at day 3 in MSU001 EBs formed by scraped or forced aggregation with 1000 cells/EB

- 3.8 Pluripotency marker expression by immunocytochemistry in MSU001 hiPSC colonies
- 3.9 Pluripotency marker expression by immunocytochemistry of BJ hiPSC colonies

#### **Chapter 4**

- 4.1 Micrographs of hiPSC cells before and after forced aggregation at 0 and 24 hours for EBs made of 5K, 10K, 15K and 20K cells
- 4.2 Micrographs of hiPSC stem cell aggregates cultured in retinal differentiation medium in rotary suspension at different speeds at day 7
- 4.3 Size distribution plots of 5K and 10K EBs at day 3 of culture
- 4.4 Relative normalized expression of early retinal transcription factor genes, Pax6, Rx, Six 3 and Otx2 and pluripotency marker POU5F1 in differentiated EBs at day 3

#### **Chapter 5**

- 5.1 Representative micrographs of MSU001 retinal EBs made from 5K or 10K cells at days 3, 10, and 21 of retinal differentiation culture
- 5.2 Size distribution of retinal EBs formed of 5K or 10K cells per EB between days 3 and 21 of culture
- 5.3 A comparison of the size distributions of MSU001 EBs with different starting sizes through retinal differentiation at day 10 and day 15
- 5.4 Cell quantification of retinal EBs and LDH activity in suspension cultures
- 5.5 Pluripotency marker POU5F1, early retinal transcription marker Otx2 and photoreceptor precursor marker Crx expression in adherent EBs made from 5K cells at day 10 of retinal differentiation culture
- 5.6 Pluripotency marker POU5F1, early retinal transcription marker Otx2 and photoreceptor precursor marker Crx expression in adherent retinal EBs made from 10K cells at day 10 of retinal differentiation culture

- 5.7 Pluripotency marker POU5F1, early retinal transcription marker Otx2 and photoreceptor precursor marker Crx expression in adherent EBs made from 5K and 10K cells at day 15 of retinal differentiation culture
- 5.8 Immunocytochemistry of cross-sections of orbital shaken EBs made from 5K cells at days 10, 15 and 21 of retinal differentiation culture
- 5.9 Immunocytochemistry of cross-sections of orbital shaken EBs made from 10K cells at days 10, 15 and 21 of retinal differentiation culture
- 5.10 The impact of varying EB size on expression of retinal differentiation markers in adherent and orbital shaking systems at day 10 of retinal differentiation culture
- 5.11 A size matched EB comparison of the impact of orbital shaking on expression of retinal differentiation markers in adherent and orbital shaking systems at day 10 of retinal differentiation culture
- 5.12 The impact of EB size on expression of retinal differentiation markers in adherent and orbital shaken cultures at day 15 for 5K and 10K EBs
- 5.13 The impact of orbital shaking on expression of retinal differentiation markers in adherent and orbital shaken cultures at day 15 for 5K and 10K EBs.
- 5.14 The Impact of EB size on expression of retinal differentiation markers in adherent and orbital shaken cultures at day 21
- 5.15 The impact of orbital shaken culture on retinal differentiation markers at day 21 of retinal differentiation culture
- 5.16 Clustergram showing the relative levels of normalized gene expression for pluripotency marker POU5F1 and retinal markers Otx2, Crx, Rho and Nrl across different EB sizes, retinal differentiation culture techniques at days 10,15 and 21

## **Chapter 6**

- 6.1 i) Micrograph of BJ retinal EBs (10K cells/EB) at day 3 of retinal differentiation and ii) relative expression of early retinal transcription factor

genes Pax 6, Rx, Otx2 and Six3 with pluripotency marker POU5F1, in BJ EBs formed by scraped or forced aggregation (10K cells/EB) at day 3

- 6.2 Micrograph images of BJ EBs formed of 10K cells/EB in adherent or orbital shaken suspension cultures at days 10 and 15 of retinal differentiation culture
- 6.3 Expression of Otx2 and Crx in adherent and orbital suspension BJ EBs made from 10K cells at day 15 of retinal differentiation culture
- 6.4 Immunohistochemistry of adherent BJ EBs made from 10K cells/EB at day 15 of retinal differentiation culture, showing expression of rod photoreceptor marker Rho
- 6.5 Relative expression of early retinal transcription factor Otx2, photoreceptor precursor marker Crx, rod photoreceptor markers Nrl and Rho with pluripotency marker POU5F1, in differentiated BJ EBs made from 10K cells at days 10 and 15 in adherent and orbital shaken retinal differentiation cultures

# List Tables

## Chapter 1

- 1.1 Components of conventional culture highlighting motivating factors for the development of chemically defined medium
- 1.2 Comparison of methods to induce pluripotency highlighting genomic integration risks relative to reprogramming efficiencies
- 1.3 International stem cell banks in the International Stem Cell Banking Initiative
- 1.4 A comparison of key retinal differentiation protocols and the exogenous molecules used to induce target retinal cell types and number of culture days required to express retinal markers where reported
- 1.5 Table 1.5 Image size reference table showing  $\mu\text{m}/\text{pixel}$  measurements used to calculate EB sizes

## Chapter 2

- 2.1 Primary antibodies used for immunocytochemistry to assess pluripotency and retinal differentiation
- 2.2 Secondary antibodies used against the primary antibodies in assessing pluripotency and differentiation marker expression.
- 2.3 List of primers used to quantify expression of key markers of retinal differentiation.

## Chapter 3

- 3.1 EB volume calculations at 24 hrs and 48 hrs

## Chapter 4

- 4.1 Cell numbers needed per EB size using the Aggrewell protocol.
- 4.2 Cell numbers required per EB size in relation to feasibility, showing numbers of experiments possible from each size

4.3 Parameters and calculations used to determine the critical shaking speed ( $N_{Cr}$ ) for the minimal and maximal working volumes of 24 well microwells used for EB culture

## List of Abbreviations

- a* Specific mass transfer area,  $m^{-1}$
- a<sub>o</sub>* constant of proportionality (=1.4 for water)
- AMD** Age-related macular degeneration
- aFGF** Alpha fibroblastic growth factor
- ANOVA** Analysis of variance
- B27** Serum-free supplement for neural cell culture
- bFGF** Basic fibroblastic growth factor
- BMP** Bone morphogenic protein
- C<sub>L</sub><sup>\*</sup>* Saturation concentration of oxygen in gas/liquid interface
- C<sub>L</sub>* Saturation concentration of oxygen in bulk phase
- cdNA** Complementary deoxyribose nucleic acid
- CHI99021** Inhibitor of Glycogen synthase kinase-3B (GSK-3)
- CHX10** synonym for visual system homeobox transcription factor 2 (VSX2)
- CRX** Cone rod homeobox transcription factor
- d* Diameter (m)
- d<sub>i</sub>* Inner diameter (m)
- d<sub>o</sub>* Orbital diameter (m)
- D<sub>w</sub>** Well diameter (m)
- DAPI** 4,6-diamidino-2-phenylindole
- DAPT** GSI-IX, LY-374973, N-[N-(3,5-Difluorophenacetyl)-L-alanyl]-S-phenylglycine t-butyl ester (Notch signalling suppression)
- DKK-1** Dickkopf-1, Dickkopf-related protein-1
- DMEM** Dulbecco's modified eagle medium
- DMSO** Dimethyl sulphoxide
- DNA** Deoxyribonucleic acid
- DPBS** Dulbecco's phosphate buffered saline
- EB** Embryoid body or stem cell aggregate
- ECM** Extracellular matrix
- EDTA** Ethylenediaminetetraacetic acid
- EFTF** Early eye field transcription factors
- ESC** Embryonic stem cell

**FBS** Foetal bovine serum

**FGF** Fibroblastic growth factor

**Fr** Froude number ( $2(\pi N^2 d/g)$ ), dimensionless

**Fr<sub>do</sub>** Froude number as defined with orbital diameter as characteristic length, dimensionless

**Fr<sub>a</sub>** Froude number as defined with axial length as characteristic length, dimensionless

**g** Acceleration due to gravity  $9.81 \text{ ms}^{-1}$

**GMP** Good manufacturing practice

**gDNA** Genomic DNA

**GSK-3** Glycogen synthase kinase 3

**h** Fluid height (m)

**hESC** Human Embryonic stem cells

**hiPSC** Human induced pluripotent stem cells

**ICC** Immunohistochemistry

**IGF** Insulin-like growth factor

**k<sub>L</sub>** Mass transfer coefficient,  $\text{ms}^{-1}$

**k<sub>La</sub>** Volumetric mass transfer coefficient,  $\text{h}^{-1}$

**KSR** Knockout serum replacement

**L<sub>O<sub>2</sub></sub>** Oxygen solubility

**LHX2** LIM Homeobox Protein

**MEF** Mouse embryonic fibroblast

**N** Shaker rotational speed,  $\text{s}^{-1}$

**N2** Chemically defined, serum-free supplement based on Bottenstein's N-1 formulation

**n<sub>crit</sub>** Critical agitation rate =  $\sqrt{((\sigma \cdot d)/(4 \cdot \pi \cdot V_L \cdot \rho \cdot d_o))}$ ,  $\text{s}^{-1}$

**NEAA** Non essential amino acids

**NRL** Neural Retina Leucine Zipper

**NRQ** Normalized relative quantity

**NRT** No reverse transcriptase

**NTC** No template control

**OTR** Oxygen transfer rate,  $\text{mML}^{-1}\text{h}^{-1}$

**OTX2** Orthodenticle Homeobox 2 gene

**Ph** Phase number =  $d_o/d (1+3\log_{10}(\text{Re}_f))$ , dimensionless

**PAX6** Paired box protein 6 gene

**PCR** Polymerase chain reaction

**Ph** Phase number,

$d_0/d \{ 1 + 3 \log_{10} [ (\rho(2\pi N)/\mu)(d^2/4) ((1 - \sqrt{1 - (4/\pi)(V_L^{1/3}/d)^2})^2) ] \}$

dimensionless

**PO<sub>2</sub>** Oxygen partial pressure (kPa)

**QPCR** Quantitative real-time PCR

**RA** Retinoic acid

**Re** Reynolds number  $(\rho N d^2)/\eta$ , dimensionless

**RHO** Rhodopsin

**RNA** Ribonucleic acid

**RPE** Retinal pigment epithelium

**RT-PCR** Reverse transcription PCR (semi-quantitative)

**RX/ RAX** Retina and anterior neural fold homeobox

**SAG Hh** Smoothened agonist Hedgehog

**Shh** Sonic hedgehog protein

**SIX 3** Six Oculis Homeobox Homolog 3

**SIX 6** Six Oculis Homeobox Homolog 6

**T3** Triiodothyronine

**TE buffer** Tris-EDTA buffer

**TGF $\beta$**  Transforming growth factor  $\beta$

**V<sub>L</sub>** Vessel fill volume, m<sup>-3</sup>

**XAV939** 3,5,7,8-Tetrahydro-2-[4-(trifluoromethyl)phenyl]-4H-thiopyrano[4,3-d]pyrimidin-4-one (Wnt/  $\beta$  Catenin inhibitor)

### **Greek symbol units**

**$\sigma$**  Surface tension, Nm<sup>-1</sup>

**$\rho$**  Density of liquid Kgm<sup>-3</sup>

## Chapter 1: Introduction

### 1.1 The emergence of pluripotent stem cells

The origins of the term ‘stem cells’ in the scientific literature can be credited to an 18<sup>th</sup> Century Zoologist Ernst Haeckel, who first described the concept of ‘*stamzelle*’ in 1868 which gave rise to the English translation of ‘stem cell’. In his work Haeckel describes morphogenesis as a concise recapitulation of phylogeny where unicellular units give rise to multicellular organisms, describing stem cells as naïve, undifferentiated cells able to give rise to all other cell types of the body (Haeckel 1868). Almost a century passed between the publication of Haeckel’s concepts and a demonstration of the potential use of stem cells in medicine by James Till and Ernest McCulloch in 1963. Till & McCulloch showed bone marrow cells donated to irradiated recipient mice, formed clonal colonies of erythroid and myeloid cells matched to the donor mice to repopulate their haematopoietic systems (Becker, A.J. McCulloch, E.A. Till 1963). Their work set the foundations of our understanding of the haematopoietic system, which depends on populations of stem cells that possess the ability to self-renew and give rise to differentiated (blood) cells (Becker, A.J. McCulloch, E.A. Till 1963).

Stem cell’s potential to aid repair in the body was demonstrated in the 60’s, but decades passed before there was substantial evidence of their pluripotent potential – the capacity to develop into virtually any specialised cell type in the body. Pluripotency was first demonstrated in mouse embryonic stem cells (mESC) by their ability to participate in the normal embryogenesis of chimeric animals and form teratocarcinomas (Papaioannou et al. 1975; Stevens 1970). Soon after, in 1981 pluripotent mouse embryonic stem cells, isolated from *in vitro* cultures of mouse blastocysts, were established and propagated *in vitro* cultures by Evans and Kauffman (Evans & Kauffman 1981). The mESC displayed normal karyotypes and proved their pluripotent status *in vivo*, in inoculated mice and *in vitro*; with the capacity to differentiate into tumours consisting of derivatives of all 3 germ layers (ectoderm, mesoderm and endoderm) responsible for giving rise to all cells in the body (Evans & Kauffman 1981). Subsequent advances made in the understanding of mammalian development were made possible by the ability to culture and genetically manipulate mESC derived mouse embryos, as models of mammalian development and tools to study gene expression (Bradley et al. 1984).

## 1.2 Human embryonic stem cells

Murine studies paved the way for the first human embryonic stem cell (hESC) derivation in the 90's. Human embryonic stem cells were first extracted from the inner cell mass of donated *in vitro* fertilization (IVF) embryos cultured to the blastocyst stage (Thomson et al. 1998). The resulting stem cells were co-cultured on mouse embryonic fibroblasts (MEF) and exhibited the same characteristics of pluripotency as their murine counterparts (Thomson et al. 1995). hESC exhibit pluripotency through their ability for prolonged undifferentiated proliferation *in vitro*, the potential to differentiate into all 3 embryonic germ layers in embryoid bodies and through teratoma induction on injection into severe-combined immunodeficient (SCID) beige mice (Thomson et al. 1998).

The clonal derivation of new stem cell lines from H9 stem cells, which were propagated in continuous culture for over 6 months, proved the ability of hESC to maintain pluripotency and their property of self-renewal whilst maintaining normal karyotype over long periods (Amit et al. 2000). The hESC derivative lines showed the same properties of pluripotency as their parental line, demonstrating true potential for scalability. Thus securing the idea that hESC derivatives deserve practical consideration for future clinical applications. In order for hESC research to gain continued support the defining properties of stem cells required detailed characterisation and elucidation of the underlying molecular mechanisms. To this aim, the discovery of key genetic markers for stage specific early differentiation of hESC helped track differentiation from pluripotency to the three germ layers and have been important in enabling research to follow cells at different stages of development (Itskovitz-Eldor et al. 2000).

Attempts to unravel the key factors and pathways responsible for driving self-renewal, pluripotency and differentiation have benefitted from global transcriptional profiling techniques. The key involvement of ligands, receptors and secreted inhibitors of the FGF, TGF $\beta$ /BMP and canonical Wnt pathways for the maintenance of pluripotency were identified by transcriptional profiling studies which found 918 genes enriched in pluripotent hESC, these pathways have subsequently been shown to be responsible for retaining pluripotent states in hESC (Sato et al. 2003; Vallier & Pedersen 2005; Xu et

al. 2009; Vallier et al. 2009). Pharmacological inhibitors has also played an important role in identifying key components of signalling pathways involved in maintaining pluripotency. The potent inhibitor of Glycogen Synthase Kinase (GSK-3), 6-bromoindirubin-3'-oxime (BIO) also demonstrates the importance of the Wnt pathway in maintaining self-renewal and pluripotency for both hESC and mESC; through BIO's ability to control pluripotency by reversible activation of the Wnt pathway (Sato et al. 2004).

With the discovery of chemical inhibitors such as BIO, the removal of animal components from hESC cultures has become a popular concern and goal as research edges toward the goal of clinical application. It is the difficulty in precisely quantifying the effects animal components have on mechanisms governing pluripotency and differentiation, which have spurred research efforts to oust MEFs and other xenogeneic factors from stem cell maintenance and differentiation protocols (Amit et al. 2004). Early attempts to create animal-free hESC cultures succeeded in reducing the risk of exposure to animal pathogens by firstly removing dependency on animal derived serum (Amit et al. 2000). Removal of mouse embryonic fibroblast feeder layers from the hESC cultures followed soon after (Amit et al. 2004). Together developments in removing animal components offer an opportunity for providing more defined micro-environment for stem cell culture, to enable better process control and reproducibility.

There is however a lack of consensus over optimal culture conditions (Table 1.1) and these have prompted efforts to standardise embryonic stem cell culture procedures starting with better characterisation of stem cell lines. 'The International Stem Cell Initiative' was set up to collate data from 17 laboratories across the globe, in an effort to characterize 59 human embryonic stem cell lines (Adewumi et al. 2007). The resulting data allowed researchers to delineate differences in pluripotent cells due to inherent genetic variation as opposed to artefacts from variable culture conditions (Allegrucci & Young 2007). Whether this data was used in the creation of the first truly chemically defined culture mediums (CDM) for hESCs is unknown but the advent of CDMs would surely have helped deduce the key factors responsible for pluripotency (Vallier & Pedersen 2008).

Factor	Pros	Cons
Feeder cell	<ul style="list-style-type: none"> <li>• Supports the maintenance of both human ESCs and iPS cells</li> <li>• Enhances seeding efficiency during both clump and single cell passaging</li> </ul>	<ul style="list-style-type: none"> <li>• A source of xenogeneic contamination</li> <li>• A source for animal-derived pathogens</li> </ul>
Serum	<ul style="list-style-type: none"> <li>• Provides known and unknown factors in supporting the growth and proliferation of human ESCs and iPS cells</li> </ul>	<ul style="list-style-type: none"> <li>• Animal derived</li> <li>• Lot-to-lot variation</li> <li>• Undefined</li> </ul>
Clump passage	<ul style="list-style-type: none"> <li>• Maintains viability during passages</li> <li>• Reduces the potential for genomic aberrations</li> </ul>	<ul style="list-style-type: none"> <li>• Impedes scale-up expansion at manufacturing level</li> <li>• Laborious and time consuming</li> <li>• Prevents single cell cloning strategies such as genetic modifications and disease correction</li> </ul>

*ESC: Embryonic stem cell; iPS: Induced pluripotent stem.*

**Table 1.1** Components of conventional culture highlighting motivating factors for the development of chemically defined medium (Valamehr et al. 2011).

### 1.3 The emergence of induced pluripotent stem cells

Human induced pluripotent stem cells (hiPSC) are human embryonic stem cell-like cells created through reprogramming somatic cells, by driving them to artificially express the key factors responsible for a cell's pluripotent state, as defined by Thomson's seminal work on hESC (Takahashi & Yamanaka 2006; Takahashi et al. 2007; Thomson et al. 1998). The emergence of iPSC has, often and reasonably, been linked to seminal research on nuclear transfer by Briggs and King from 1952. They showed it was possible to use enucleated eggs for re-nucleation with embryonic cell nuclei, to support tadpole development in the amphibian *Rana Pipiens* (Briggs and King, 1952). This early work led to the experiments of Professor John B. Gurdon who subsequently demonstrated the reversible nature of somatic cell specialisation (Gurdon, 1962) in *xenopus*, so laying the foundations for the later establishment of human induced pluripotent stem cells (Takahashi & Yamanaka 2006; Takahashi et al. 2007).

The development of nuclear transfer techniques led to the famously successful nuclear transfer of somatic cells into viable oocytes to create Dolly The Sheep in 1996 (Campbell 1996). Attempts to apply the approach in humans led to the successful production of human totipotent cells through transfer of somatic cell nuclei from human adult thymocytes into enucleated human embryos (Tada et al. 2001). While these cells exhibited great similarities to hESCs, somatic cell nuclear transfer techniques relied on human oocytes and the means of acquiring them by donation were

ethically objectionable in the least and morally unacceptable at worst (Meyer 2008; Tada et al. 2001).

To avoid ethical controversy the scientific community has responded by intensifying research into alternative approaches to achieve pluripotent status from adult somatic cells. The first iPSCs were obtained from adult mouse fibroblasts by overexpressing 4 key transcription factors with DNA integrating retroviral vectors for octamer-binding transcription factor 4 (OCT4), sex determining region Y box 2 (SOX2), myelocytomatosis viral oncogene homologue (c-MYC) and Kruppel-like factor 4 (KLF4) (Takahashi & Yamanaka 2006). In 2007, Shinya Yamanaka showed for the first time that it was also possible to reprogram human somatic cells using DNA integrating retroviral vectors to overexpress the same four reprogramming factors (OCT4, SOX2, c-MYC and KLF4) now referred to as the Yamanaka four factors (Takahashi et al. 2007). The establishment of human induced pluripotent cells won The Nobel Prize in Physiology or Medicine, awarded jointly to Professors John B. Gurdon and Shinya Yamanaka in 2012. By providing an alternate adult source of pluripotent cells, human iPSCs eliminate dependence on the ethically objectionable use of human embryos to derive pluripotent stem cells (Meyer 2008). Human iPSCs promise to provide a potentially infinite source of patient and disease specific cells for disease modelling, drug discovery and cellular therapeutics, without the risks of immune rejection associated with allogeneic ESC derived cells.

#### **1.4 IPS derivation and culture refinement**

The functional equivalence of iPSCs to hESCs was successfully achieved by elucidating the similarities in their mechanisms for maintaining pluripotency and controlling differentiation under defined culture conditions (Vallier et al. 2009). Research promoting standardisation of stem cell culture supported these efforts with the development of a more refined stem cell culture medium in 2011, designed to facilitate clinical application of IPS cells. The commercially available 'E8' medium system (Life Technologies) is free of animal components and is chemically defined, comprising of just 8 essential components (Chen et al. 2011). Such developments play an essential role in the advancement of future therapeutics, especially as international

regulatory guidelines governing cellular therapeutics have begun to merge. Documents for international guidelines such as the PAS 83 and PAS 93 which try to harmonize European and American frameworks together are particularly helpful in facilitating international collaborations to accelerate the translation of stem cell research to clinical scenarios. It is likely that regulations may prohibit the use of xenogeneic materials in the future as they already recommend the use of defined culture mediums where possible (PAS 83 & PAS 93). Since they offer greater visibility over the impact of external factors on the behaviour of stem cells, defined culture mediums are an important consideration for any stem cell based research with potential clinical applicability (Casaroli-marano & Vilarrodona 2014).

#### **1.4.1 Evolution of integration-free iPSC reprogramming methods**

The first iPSC derivation relied on retroviral transduction of somatic cells which required the use of multiple individual viral vectors at high load to deliver the 4 factors and resulted in multiple integrations across the genomes of successfully reprogrammed cells (Sommer 2009). The inherent risk of teratoma formation from retroviral integration into mammalian DNA and low reprogramming efficiency of ( $10^{-4}$ ) encouraged the development of better reprogramming methods to minimise or avoid genomic modifications to the host genome and produce safer, potentially therapeutic cells (Takahashi et al. 2007; Zhou & Freed 2009; Tada et al. 2001; Lai et al. 2011).

The use of lentiviruses to generate iPSCs gained popularity for the ability to transfect proliferating cells in addition to non-dividing cells, which increased their reprogramming efficiency by 10-fold compared to retroviruses (Sommer 2009). The most commonly used lentiviral system is the single cassette reprogramming vector, engineered with a Cre-Lox mediated transgene excision mechanism, to enable clearance of integrated sequences from successfully generated iPSCs (Soldner et al. 2009). The humanised version of the vector 'STEMCCA' has reprogramming efficiencies between 0.1-1.5% (Somers 2010) but as a lentiviral system, still involves the risks of genomic integration and insertional mutagenesis (Walia et al. 2012).

### **1.4.2 Non-integrating virus iPSC reprogramming**

Adenoviral vectors expressing c-Myc, Klf-4, Sox2 and Oct4 have been used to successfully reprogram human somatic cells without transgene integration (Stadtfield et al. 2008). The system has also been used to produce IPS cells which were further differentiated to produce dopaminergic neurons (Zhou & Freed 2009). However, adeno viral vector based reprogramming is less popular, most likely to be due to reportedly very low efficiencies of reprogramming and the requirement for multiple infections (Zhou & Freed 2009).

The Sendai virus, a negative sense single stranded RNA virus, offers an added advantage that it does not enter the nucleus and is therefore unable to integrate into the host genome (Faísca & Desmecht 2007). Sendai virus vectors therefore have become a popular approach to induce expression of exogenous pluripotency genes as RNA transcripts in somatic cells and produce transgene free IPS cells (Fusaki et al. 2009). Since its establishment in 2009, the Sendai virus vector method has been modified to include temperature-sensitive mutations in the virus to facilitate viral clearance post reprogramming by altering culture temperature (39<sup>0</sup>C) (Ban et al. 2011).

### **1.4.3 Non-viral reprogramming**

Non-viral mechanisms for reprogramming include the host factor independent PiggyBac (PB) and Sleeping Beauty (SB) transposition methods. These transposons introduce doxycycline inducible transcription factors in PB or SB transposons that are self-excised post reprogramming, by the inducible expression of transposase enzymes (VandenDriessche et al. 2009; Woltjen 2009). Advances in recombinant transposase design, have also shown modification of PB transposition activity can be used to reduce the risk of damage to the host genome from potential PB transposon re-mobilisation (Meir et al. 2013). Despite efforts to make transposon based techniques safer, they still entail risks of genomic recombination and insertional mutagenesis making them less attractive than integration free methods (Warren et al. 2010).

Direct delivery of reprogramming proteins has also been a successful method of reprogramming as demonstrated in mouse fibroblasts (Kim et al. 2009) and human

fibroblasts (Zhou et al. 2009). Challenges associated with producing sufficient quantities of bioactive proteins with long enough half-lives, able to cross the plasma membrane for efficient reprogramming, make this a troublesome method that requires further development (Lai et al. 2011).

The evolution of non-viral and non-integrating techniques have also given rise to a method of reprogramming by transient overexpression of episomal plasmids encoding the reprogramming factors, but the low efficiency of reprogramming has made this less popular than other techniques (Okita et al. 2011). Similarly, reprogramming by mRNA transfection of the Yamanaka factors has shown great promise as a non-integrating, non-mutagenic method in which synthetic mRNAs complexed with cationic compounds to stimulate uptake by endocytosis are also able to inhibit innate anti-viral immune responses (Warren et al. 2010). Transient overexpression of episomal plasmids has been used to improve reprogramming efficiencies of human fibroblasts from 1.4% in 20 days to 4.4%. This was achieved by culturing the cells at 5% O<sub>2</sub> with medium containing the histone deacetylase inhibitor, valproic acid, the original four reprogramming factors and additional reprogramming factor Lin28 (Warren et al. 2010; Yu et al. 2007). There major different techniques for reprogramming in use have varying degrees of efficiency and inherent risks of integration as summarised in Table 1.2.

Vector	Method	Genomic Integration	Factors <sup>(d)</sup>	Reprogramming efficiency in human fibroblasts <sup>(e)</sup>	Reference
Virus	Retroviral	+	OSKM	++++	Takahashi 2007
	Lentiviral	+	OSKM	+++	Yu 2007
	Adenoviral	- (a)	OSKM	+	Zhou 2009
	Sendai virus	- (b)	OSKM	++++	Fusaki 2009
DNA	Episomal Plasmid	- (a)	OSKMNTL	+	Yu 2009
	Transposon	- (a,c)	OSKM	++	Woltjen 2009 & Kaji 2009
	Minicircle	- (a)	OSNL	+	Jia 2010
RNA	RNA	-	OSKM	+++	Warren 2010
Protein	Cell transparent protein	-	OSKM	+	Kim 2009

**Table 1.2** Comparison of methods for induction of pluripotency to highlight genomic integration risks relative to reprogramming efficiencies. Adapted from (Okita & Yamanaka 2011)

(a) Absence of genomics integration should be experimentally determined.

(b) Absence of virus genome should be experimentally determined.

(c) Transposon vector integration into genome is reversible.

(d) O: OCT3/4; S: SOX2; K: KLF; M: C-MYC; N: NANOG; L: LIN28; T: SV40-large T antigen

(e) + <0.001%; ++ <0.01%; +++ <0.1%; ++++ >0.1%

## 1.5 hiPSC Characterisation

While both hESC and hiPSC cells have the potential for unlimited proliferation and differentiation to produce cells for therapeutic use in vast quantities, only hiPSC can be used for autografts or to mass produce recipient Human Leukocyte Antigen (HLA) matched therapies to minimise the risk of an immune response and reduce the requirement for immunosuppression (Ilic & Stephenson 2013). Considering this potential benefit to medicine and despite a lack of consensus over standards for hiPSC characterization, IPS cell banks are emerging around the world. Most famously, Yamanaka has plans to accrue 75 hiPSC lines to provide sufficiently close-matched-HLA haplotypes for 80% of the Japanese population (Cyranoski 2012).

Without a unified and comprehensive reference for characterisation that each cell bank must adhere to, most researchers seek compliance with guidelines set by local governing bodies such as the Food and Drugs Administration (USA) or the European Medicines Agency. In 2010 the International Stem Cell Banking Initiative (ISCBI) was created to compile and collate a report stating the case and necessity for standardised characterisation of stem cells (Crook et al. 2010). Several stem cell banks were involved in the project globally (Table 1.3) but the success of the ISCBI has yet to be ascertained. The lack of consensus in the methods for characterisation of pluripotent stem cells, has surprisingly not restricted the approval of clinical trials using cell therapeutics derived from hESCs/iPSCs and these are currently required to comply with regulations for clinically compliant biologics (Devito et al. 2014).

•UK Stem Cell Bank	<a href="http://www.ukstemcellbank.org.uk">http://www.ukstemcellbank.org.uk</a>
•Charite Cell Bank–Berlin–Berlin Brandenburg Center for Regenerative Therapies	n/a
•Tel Aviv Sourasky Medical Center Cell Bank	n/a
•National Stem Cell Bank–Banco–Nacional de Lineas Celulares (BNLC)	<a href="http://www.iscii.es/htdocs/terapia/terapia_bancocelular.jsp">http://www.iscii.es/htdocs/terapia/terapia_bancocelular.jsp</a>
•Valencia Stem Cell Bank–BNLC branch	<a href="http://www.iscii.es/htdocs/terapia/terapia_bancocelular.jsp">http://www.iscii.es/htdocs/terapia/terapia_bancocelular.jsp</a>
•National Centre for Cell Science–Cell Repository	<a href="http://www.nccs.res.in">http://www.nccs.res.in</a>
•WiCell International Stem Cell Bank	<a href="http://www.wicell.org">http://www.wicell.org</a>
•Australian Stem Cell Bank	<a href="http://www.ascb.com.au">http://www.ascb.com.au</a>
•Singapore Stem Cell Bank	<a href="http://www.ssc.a-star.edu.sg/stemCellBank.php">http://www.ssc.a-star.edu.sg/stemCellBank.php</a>
•Korean Stem Cell Bank	<a href="http://kscb.co.kr/eng">http://kscb.co.kr/eng</a>
•Taiwan Stem Cell Bank	<a href="http://www.tscb.bcre.firdi.org.tw">http://www.tscb.bcre.firdi.org.tw</a>

*n/a* not available

**Table 1.3** International stem cell banks in the International Stem Cell Banking Initiative (ISCBI) adapted from (Crook et al. 2010).

To date one of the closest practical solutions for harmonizing pluripotent stem cell characterisation attempts is a novel gene expression real time PCR assay, the ‘TaqMan hPSC Scorecard’ (Life Technologies). The scorecard compares 94 qPCR assays per sample to a reference set of functionally validated hESC and iPSC lines to detect genomic signatures of self-renewal and differentiation (Fergus et al. 2014). This approach will push progress towards understanding the genetic changes induced during reprogramming and routine culture. Though it does not detect epigenetic changes. Combining a qPCR approach with DNA methylation analyses and medium-resolution array-comparative genomic hybridization would help bring more resolution to the characterisation of pluripotency at the genetic and epigenetic levels closer to standardisation for hESC and hiPSC (Ilic & Stephenson 2013).

The altered epigenetic or genomic states unique to each hiPS or hES cell line which affect their differentiation propensities and have the potential to impact their safety for clinical application (Osafune et al. 2008).

To help address these concerns the use of genome-wide reference maps of DNA methylation and gene expression derived from comparisons across 20 hES and 12 hiPS cell lines could be used to facilitate better characterisation of pluripotent cells according to their propensities to differentiate into each of the germ layers (Bock et al. 2011). Such an approach would help ensure directed differentiation techniques use the most relevant cell line for their target cell type and reduce cell line specific variability (Pal et al. 2009). Genome-wide reference maps could pave the way for an internationally recognised consensus to aid standardised characterisation of pluripotent stem cells at the genetic and epigenetic levels. Standardisation in this way, may be useful to ensure pluripotent cells intended for directed fate specification toward therapeutic cell types, begin differentiation from a common well characterised start point (Buta et al. 2013).

Genetic reference maps may also help to predictively identify inherent cell line specific differentiation biases to enable the selection of suitable cell lines to ultimately improve reproducibility, reduce risk and increase process and product knowledge in stem cell differentiation dependent bioprocesses. In the absence of a set of genetic reference maps, the first stage of stem cell differentiation, study of the embryoid body stage also provides a method to characterise stem cell lines according to differentiation propensities (Moon et al. 2011)

## **1.6 Stem cell differentiation with embryoid bodies**

Stem cell differentiation processes are susceptible to variability from many sources in addition to that conferred by the individual cell lines selected for expansion and fate specification. A major source of variability in stem cell differentiation protocols comes from the first stage of initiating differentiation, the embryoid body (EB) formation stage (Doetschman et al. 1985; Rungarunlert et al. 2009). Both mouse and human ESC as well as fibroblast derived iPSC undergo spontaneous differentiation

when cultured in suspension without anti-differentiation factors, to form three dimensional aggregates or EBs, that follow patterns of development reminiscent of early embryogenesis (Keller 1995; Thomson et al. 1998; Itskovitz-Eldor et al. 2000; Takahashi et al. 2007; Takahashi & Yamanaka 2006; Doetschman et al. 1985).

The transformation of pluripotent stem cells begins with trophoectoderm formation, followed by primitive endoderm specification progressing to definitive embryonic tissue formation at the later stage of gastrulation, to give rise to each of the three germ layers; the predecessors of all human adult tissues (Keller 2005; Hua & Sidhu 2008). Fine changes in the temporal balance of TGF $\beta$ /Activin/Nodal and BMP within EBs are responsible for orchestrating the transgression from pluripotency through differentiation toward each of three germ layers ectoderm, mesoderm and endoderm (Vallier et al. 2009; Hong et al. 2011; Zhang et al. 2008). The germ layer cell populations are dynamic in their nature as evidenced by their heterogeneous marker expression which has resulted in an alternate nomenclature to encompass these characteristics with the terms ‘primitive ectoderm-like’ cells, ‘mesendoderm-like’ cells and ‘extra-embryonic endoderm-like’ cells (Kopper et al. 2010).

The formation of EBs *in vitro* presents the challenge of identifying the influence of EB formation techniques on differentiation propensity with large discrepancies between EBs cultured in static versus hydrodynamic environments (Yirme et al. 2008). Different EB formation techniques show that the relationship between EB size and differentiation toward specific cell lineages exists albeit cell-line specific (Hwang et al. 2009).

### **1.6.1 EB formation size control**

The techniques available for EB formation have developed greatly since the original method of simply scraping stem cell colonies for suspension culture (Thomson et al. 1998)(Figure 1.1). Early attempts to control EB size include seeding stem cells in micromass culture conditions in 24 well tissue culture plates, hydrophilic petriperm dishes, semisolid mediums such as methylcellulose or hanging drops of medium followed by suspension culture in static or orbital bacterial shaken bacterial grade

cultures dishes (Doetschman et al. 1985; Dang et al. 2002). For human stem cells, using volume controlled drops of medium to culture precise numbers of stem cells for EB formation improved EB size reproducibility at the cost of laborious manual handling and limitations to small EB sizes more suited to mouse EB culture (Dang et al. 2002). EBs have also been formed reproducibly in agarose hydrogel capsules (Dang et al. 2004).

Yirme's work showed expansion of hEBs can be improved using dynamic culture conditions. Compared to 4-fold expansion of hEBs in static culture conditions, fold expansion in Erlenmeyer flasks was reported at ~5-fold, whilst glass boll bulb shaped impeller spinners showed ~6.25 fold hEB expansion levels. In contrast paddle impeller flasks and stirred tank bioreactors had diminished capacities to propagate EBs due to higher percentages of apoptosis which brought their fold expansion levels to below 3-fold (Yirme et al. 2008). Other reports have also showed stirred tank bioreactors to provide 10-fold increases in neural differentiation using hESCs (Serra et al. 2009). Stirred tank lateral vessels (STLV) and high aspect ratio vessels (HARV) have also been reported to improve yields of EBs 3-fold in comparison to static cultures (Gerecht-Nir et al. 2004).

Although improved yields are indeed possible with the use of bioreactors the large volumes required can be prohibitively costly and so research into smaller scale hydrodynamic cultures have yielded important findings. In particular the work Carpenedo et al showed rotary suspension culture on orbital rotary shakers can provide a 20-fold improvement in cell numbers incorporated into EBs compared to static conditions (Carpenedo et al. 2007). Comparing scalable EB production systems considering spinner flasks, stirred tank bioreactors and slow turning lateral culture vessels, seeded with EBs formed as stem cell clumps or single cells in suspension has also demonstrated that adding pre-formed EBs to hydrodynamic environments offers the most homogenous scalable production systems (Kurosawa 2007).

To produce reproducible sized EBs from human pluripotent stem cells it is now possible to utilise cost-effective equipment such as ultra-low attachment V-bottom 96-well plates, seeded with precise numbers of stem cells for size-controlled EBs (Sakai et al. 2011). Though cost-effective, the use of low attachment 96-well plates, confines experiments to 96 EBs per plate and therefore has a relatively large footprint which

can be prohibitive for higher throughput studies. To date the most popular method for EB production builds on this simple technique, by the microfabrication of precisely sized and shaped microwells from cell-repellent, poly (ethylene glycol) (PEG) (Karp et al. 2007). Microwells offer the possibility to produce thousands of uniform sized EBs in a reproducible fashion, to support higher throughput investigations into the initiation of differentiation from EBs in controlled microenvironments (Karp et al. 2007). The technology for producing large numbers of EBs was developed for commercial availability as Aggrewell Plates (Stemcell Technologies) and has been proven using hESCs to form spatially and temporally synchronised EBs (Ungrin et al. 2008) which enable the reproducible production of size-controlled EBs discussed further in Chapter 3.

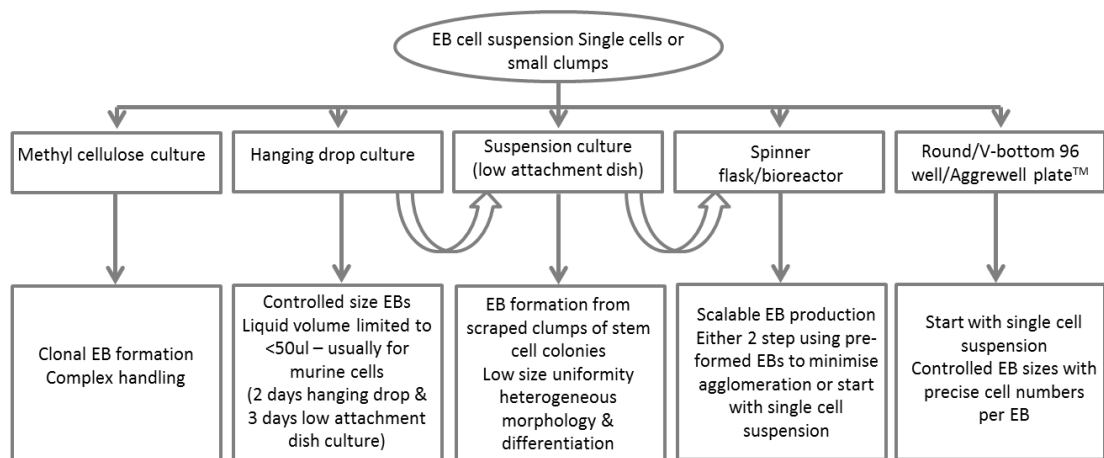


**Figure 1.1** Common methods for EB formation adapted from (Kurosawa 2007).

## 1.6.2 Differentiation biases and the role of size control in EBs

Inherent differences between cell lines for germ layer biases, have also been demonstrated in HUES-9 and HUES-7 cell lines, which show different propensities to develop neuroectodermal tissue and mesoderm/ endodermal specification respectively (Pal et al. 2009). Independently derived pluripotent stem cell lines can also have unique differentiation properties due to hESC cell derivation or iPSC reprogramming

techniques but the mechanisms responsible for these are not yet fully understood. In addition to biases from cell derivation or cell line specific variability, the size of EBs also impacts their differentiation profile and several studies have demonstrated the introduction of developmental biases for specific germ layer lineages through controlled modulation of EB size (Bauwens et al. 2008; Côme et al. 2008a; Choi et al. 2010).

Although EB differentiation can be influenced by modulation of the microenvironment or physical parameters such as EB size, there is no established ideal ratio for EB size to germ layer bias which is independent of cell line variability or the heterogeneity within stem cell culture techniques or colonies of the same cell line (Lim et al. 2011; Bauwens et al. 2008). The influence of EB size on germ layer specification can be dependent on the ratio of endoderm-gene-expressing to neuroectoderm-gene-expressing cells in the parent hESC colonies used to make them (Bauwens et al. 2008).

Nutrient mass transfer rates, availability of soluble factors along concentration gradients and oxygen diffusion to inner cells, are all affected by EB size and are contributing factors in influencing differentiation. The difference in internal oxygen concentrations between EBs of different sizes has been demonstrated by showing, EBs with diameters of 200 $\mu$ m can have 50% higher oxygen concentrations in their centres than EBs with diameters of 400 $\mu$ m (Van Winkle et al. 2012). EB size also influences early fate specification and the ability to form homogenous populations of cells in each of the germ layers (Carpenedo et al. 2007).

By manipulating EB size it has also been possible to accelerate differentiation with one study reporting a 2-fold increase in the yield of target endothelial cells as a result of tight control over EB size (Moon et al. 2014). In the same report EB size control was also used as a tool to counteract inherent cell line specific differentiation propensities; in 2 cell lines (H9 and CHA15) by finding unique optimal EB sizes for the same differentiation protocol for each cell line (Moon et al. 2014). The control of EB size has been shown to be important in helping to establish reproducible and reliable systems for stem cell expansion as well as in differentiation processes to therapeutic cell types such as  $\beta$  cells and retinal cells (Hwang et al. 2008; Yanai et al. 2013; Mfopou et al. 2010).

The potential influence of EB size is therefore an important factor to consider in attempts to influence differentiation (Andres M. Bratt-Leal, Richard L. Carpenedo 2009). Rotary orbital suspension culture methods have been used as a tool for investigating the impact of EB size in murine EBs; altering orbital shaking speeds impacts both EB size and differentiation profiles (Sargent et al. 2010). The ability to control EB size through orbital shaking also facilitated fundamental studies analysing the hydrodynamic environment after removing the influence of EB size by keeping them constant (Kinney et al. 2012). The individual and combined effects of EB size and orbital shaking on differentiation are discussed in more detail in chapters 4 and 5.

## **1.7 The case for orbitally shaking culture systems for retinal differentiation**

Adherent or planar monolayer cultures are still the most commonly used platforms for stem cell differentiation cultures due to the ease of use of 2D tissue culture plastics. Though 2D tissue culture plastics are established well characterised culture systems, cell culture in them lacks mixing and is prone to the accumulation of soluble factor gradients in specific locations within the culture. Extracellular matrices, co-culture techniques and synthetic scaffolds can be used to build stem cell niches able to immobilise exogenous factors, but without mixing the formation of concentration gradients of these and other nutrients is inevitable (Hazeltine et al. 2013).

Suspension protocols for retinal differentiation were first demonstrated by Dutt et al. 2003. Their work differentiated a human retinal progenitor (KGLDMSM) and an epithelium cell line (D407) on Laminin coated Cytodex 3 micocarrier beads (Parnacia) in a NASA developed lateral rotating wall bioreactor to produce photoreceptor-like cells (Dutt et al. 2003). The same group also found retinal progenitor cell lines co-cultured with a retinal progenitor epithelial (RPE) cell line (D407) could be induced to differentiate into Nrl+ photoreceptors in a 3D rotary culture, with conical flasks on a shaker at 90rpm in 10 days demonstrating the feasibility of retinal differentiation in dynamic cultures (Dutt & Cao 2009).

The first report of EB culture on orbital shakers was described by (Carpenedo et al. 2007) who showed orbital shaking of mouse EBs in bacterial grade culture dishes on orbital rotary shakers between at rotational frequencies of 25, 40 and 55 rpm provided a hydrodynamic environment which improved the homogeneity of EB size, shape and gene expression. Improved efficiency of stem cell expansion as well as EB formation compared to hanging drop techniques were also reported. Though the orbital diameter and fluid flow regimes are not reported the authors described a 20-fold increases in numbers of cells incorporated into EBs compared to static cultures and found EB differentiation toward germ layers was accelerated (particularly for endoderm) and more homogeneous (Carpenedo et al. 2007).

A comparison of controlled-size EBs cultured within different hydrodynamic environments has also been demonstrated to produce clinically relevant quantities of mesodermal derived cardiac cells from hESCs (Niebruegge et al. 2009). Comparing EB cultures on static dishes with EBs cultured in dynamic systems (orbitally shaken dishes – with ultra-low attachment plates on a Rotomix shaker at 50rpm, roller bottles on a Barnstead rotisserie system, stirred suspension cultures in DasGip cell-ferm pro spinners systems with a glass bulb spinner and culture within a bellco spinner fitted with a paddle spinner) the authors demonstrated cardiomyocyte generation was higher in dynamic systems. The best improvement was found in glass bulb equipped spinner system (5 fold  $\pm$  2.8) (Niebruegge et al. 2009) but it is unclear how the orbital shaken experiments were optimised and the flow regime within them was not reported.

A more detailed impact of varying the hydrodynamic environment is presented by (Sargent et al. 2010) where rotary orbital suspension culture of mESC derived EBs was demonstrated to influence EB cellular organisation, morphology, kinetic profile of gene expression and derivative cell types from differentiation. The authors formed EBs from single cell suspensions on an orbital shaker (orbital diameter 0.19m, fluid height 1.27mm, vessel diameter 100mm – bacterial grade polystyrene dishes) and varied shaking speeds between 20 and 60rpm for 7 days of culture. The computational fluid dynamics approaches employed allowed characterize the EB distribution patterns with varying shaking speeds and the corresponding shear stresses produced by the hydrodynamic environments created (Sargent et al. 2010). Their analysis of the shear stress by CFD showed these increased with increasing rotary speeds and were highest at the edges ( $< 11\text{dyn/cm}^2$ ) of the vessel but also showed at higher speeds the EBs

tended to occupy regions closer to the centre of the well and didn't experience shear rates above  $2.5 \text{ dyn/cm}^2$  suggesting higher shaking frequencies could have been tolerated (Sargent et al. 2010).

The work of (Sargent et al. 2010) was further developed with a systematic analysis of differentiating forced aggregation formed EBs of uniform size, in different orbitally shaken hydrodynamic environments (25, 45 and 65rpm) over a 14 day culture period. The authors describe the impact of mixing conditions on EB morphogenesis and found morphological biases developed according to the rotary speeds used, namely agglomeration at 25rpm, while 45 and 65rpm cultures maintained EBs as individual entities. However, only subtle variations between their gene expression profiles were observed which could be attributed to the different shaking regimes for example differential temporal expression of mesodermal marker *Nkx2.5* between the 45 and 65rpm peaked at days 7 and 14 respectively (Kinney et al. 2012). These results while conducted in mouse EBs show that different shaking regimes can indeed influence EB differentiation when EB size is removed as a factor.

More recently suspension stem cell culture techniques have developed alongside new differentiation protocols, such as the static suspension culture method used to differentiate mESC into self-forming optic cups, as developed by the Sasai lab (Eiraku et al. 2011). The same approach was also successful in producing hESC derived self-forming optic cups (Nakano et al. 2012) and hiPSC initiated optic cup derived functional photoreceptors (Zhong et al. 2015). Unlike Dutt's protocol the Eiraku, Nakano and Zhong experiments were all carried out under static conditions and may benefit from the introduction of orbital shaken culture to improve scalability and reproducibility. In summary the orbital shaken and retinal cell differentiation experiments discussed above demonstrate the feasibility of introducing dynamic suspension environments to these cultures. In particular with the advent of suspension protocols yielding self-forming optic cup derived photoreceptors there is a need to develop reliable bioprocesses to cater for research in this field and potential therapeutic cell manufacturing processes. It follows then that a demonstration of the feasibility of differentiating retinal cells in a dynamic culture system with potential for scale such as the orbital shaking microwell system, is required and forms the inspiration for the work in this report.

## **1.8 Engineering and flow characteristics of shaken microwell systems**

In order to appreciate the background of the impact of orbital shaking in the cultures discussed in this thesis, an understanding of the behaviour of liquids or flow dynamics within shaken microwell systems as well as an overview of the engineering characterisation of microwell bioreactors used for the culture system would be beneficial. Consequently the following section aims to provide an overview of the fundamental principles involved in terms of the engineering of shaken microwell systems and the flow dynamics within them.

Bioreactors are commonly used for high throughput screening and bioprocess development in mammalian cultures and include shaking tanks, flasks or microtitre plates with nominal volumes from litres to microliters. Of these bioreactors, microwell plates offer multiple uniform wells for parallel experiments at low volumes that can inform process design strategies and are found in formats with 24, 28, 96, 384 and even 1536 wells (Sigma Aldrich). The reduced volumes offered by microwell plates are necessary to lower material and labour costs from conventional scale culture options which are impractical for process development (Girard et al. 2001).

Microwell bioreactors allow for speedier process development times and are commonly used for process optimization and screening with shaking platforms instead of mechanically stirred bioreactors which have comparatively reduced scope for parallelization typically being capable of running between only 4 and 48 experiments together (Puskeiler et al. 2005; Gill et al. 2008). Microwell plates can also be readily incorporated into automation systems to deliver important process design considerations at the lab-scale making them a useful choice for developing new and optimising existing bioprocesses (Lye et al. 2003; Micheletti & Lye 2006). An added advantage for microwell platform cultures is their ability to readily incorporate complex operating strategies including liquid handling and for pH control as described for microwell fermentations of *S. erythraea* CA340 (Elmahdi et al. 2003). The implementation of automation for microwell culture and differentiation of mouse embryonic stem cells also highlights their potential utility for high throughput stem cell process development applications (Hussain et al. 2013).

The fundamental principles underpinning the suitability of shaken microplates for stem cell culture bioprocess development, can be described by engineering characterisation of their environment, which can be used for selecting optimal culture conditions. The engineering characteristics considered below include oxygen transfer, power input, phase of operation, hydromechanical stress and mixing regimes (Klöckner & Büchs 2012).

### Oxygen transfer

Sufficient oxygen mass transfer between the gas and the liquid phase at the surface of the culture medium is required for the cells in culture systems to be supported for cell survival and growth. The oxygen transfer rate OTR ( $\text{mM L}^{-1} \text{h}^{-1}$ ) between the gas and liquid phase is usually defined as:

$$OTR = k_L a (C_L^* - C_L) = k_L a (p_{O_2} \cdot L_{O_2} - C_L) \quad (1)$$

Where  $k_L$  (m/s) is the mass transfer coefficient,  $a$  is the volume specific transfer area (making  $k_L a$  the volumetric gas liquid mass transfer coefficient).  $C_L^*$  and  $C_L$  are the oxygen concentration in the saturated gas-liquid interface and the bulk phase respectively,  $L_{O_2}$  is the oxygen solubility of the culture medium and  $p_{O_2}$  the oxygen partial pressure in the headspace of the culture vessel (Klöckner & Büchs 2012). From the above equation when the  $p_{O_2}$  in the headspace is equal to that of air (0.2095 bar), for maximum OTR,  $C_L$  can be considered as = 0 to give:

$$OTR_{max} = k_L a \cdot p_{O_2} \cdot L_{O_2} \quad (2)$$

In this equation  $k_L a$  is fundamental and changes for different vessel geometries as well as with differing material properties of the vessel and the operating parameters such as fill volumes, shaking diameter and shaking frequency. Using a model sulphite oxidation system (Hermann et al. 2003) were able to characterize oxygen transfer in a single well of a 96-well microwell plate. By studying different shaking frequencies (up to 1000l/min) with different shaking diameters (3-50 mm) and filling volumes (140-200 $\mu$ l) they found that ( $OTR_{max}$ ) is primarily influenced by the specific mass transfer area ( $a$ ) in round-shaped wells. The mass transfer area ( $a$ ) or the liquid surface was also found to be influenced by the surface properties of the vessel material and by

the interfacial tension of the medium which could be modulated by altering the shaking intensity by changing the shaking diameter. The group also demonstrated that for a single well of a standard flat bottom round 96-well plate, in order to improve  $OTR_{max}$  it is first necessary to provide sufficient centrifugal force to the system to break the surface tension of the medium. To cause any liquid movement shaking frequencies must exceed a critical value ( $n_{crit}$ ) which can be determined by equation (3) (Hermann et al. 2003):

$$n_{crit} = \sqrt{\frac{\sigma \cdot D_w}{4 \cdot \pi \cdot V_L \cdot \rho_L \cdot d_O}} \quad (3)$$

where  $n_{crit}$  is the shaking frequency,  $\sigma$  (N/m) is the surface tension,  $D_w$  (m) is the well diameter,  $V_L$  (m<sup>3</sup>) is the vessel fill volume and  $\rho_L$  (Kg/m<sup>3</sup>) is the density of the liquid. The observations of a complete lack of liquid movement below the  $n_{crit}$  is specific to the properties of microwell plates and do not hold true for larger vessels such as shake flasks where the surface properties of the flasks have been shown not to influence power consumption in the system (Buchs et al. 2000). Additionally the reliability of equation 5 was questioned when application of formula (3) to the geometries of 24-well plates provided an  $n_{crit} = 23$ rpm while the experimentally determined range reported was determined to be between 120-300rpm (Barrett et al. 2010).

Alternative approaches for  $k_L a$  calculations for microbial fermentation cultures in 24, 96 and 384 microwell plates were presented by (Doig et al. 2005) which eliminated the requirement for volume specific correlations by utilising Buckingham's  $\pi$  theorem and dimensionless groups to calculate  $k_L a$ . The group also showed that although  $k_L a$  values may be calculated at acceptable values for a given system, insufficient mixing can still lead to oxygen deficient regions at the microwell base highlighting the requirement for mixing after oxygen enters the gas-liquid interface. Though the work described by (Doig et al. 2005) was carried out in a microbial system, similar insights on the development of nutrient gradients within bioreactors described by (Lara et al. 2006) highlighted the potential threat these gradients can cause to cells in culture and emphasized the importance of sufficient mixing.

### **Power input and flow characterisation**

In shaking cultures the power input influences the fluid flow and therefore mass transfer and mixing which make up the hydrodynamic environment (Klößner & Büchs 2012). Power is usually described as the non-dimensional power number and as a function of the Reynolds number which describes whether the fluid flow is in or out-of-phase (ie. when the fluid either does or does not follow the movement of the shaking platform respectively) a description which was first demonstrated by (Buchs et al. 2000). The authors correlated power input and Reynolds number through measurement of power consumption from torque and shaking frequency measurements in Erlenmeyer flasks. Coupled with a visualisation platform, the data showed fluid flow patterns at different operating parameters for vessel size, fill volume, viscosity, shaking frequency and shaking diameter (Buchs et al. 2000). The results produced a method to demonstrate that at a particular rotational frequency  $N$ , the liquid within the vessel is out-of-phase and therefore prone to diminished volumetric power consumption and subsequent gas/liquid mass transfer. A non-dimensional phase number  $Ph$  was also derived by (Buchs et al. 2000) to identify the two phases and is a function of the orbital to flask diameter ratio  $d_o/d$  and the film Reynolds number  $Re_f$ , and the axial Froude number  $Fr_a$  (a dimensionless number describing the ratio of flow inertia to the external field at the axis of rotation):

$$Ph = \frac{d_o}{d} \left( 1 + 3 \log_{10} (Re_f) \right) \quad (4)$$

According to this equation in-phase conditions should occur if  $Ph > 1.26$  but only for high shaking frequencies with  $Fr_a > 0.4$  where only a minority of the liquid would be in contact with the base of the vessel (Buchs et al. 2000). To investigate the power consumption in cylindrical shaken bioreactors (Klößner et al. 2012) showed that using Buckingham  $\pi$  theorem approaches it was possible to calculate the relationship between the Newton number  $Ne$  and Reynolds number  $Re = Nd_i^2/\nu$ , Froude number  $Fr = N^2d_i/g$ , Volume number  $V_l/d^3$  and orbital to cylinder diameter ratio  $d_o/d_i$ :

$$Ne = 9 Re^{-0.17} \left( \frac{N^2d_i}{g} \right)^{0.42} \left( \frac{V_l}{d_i^3} \right)^{0.44} \left( \frac{d_o}{d_i} \right)^{0.42} \quad (5)$$

where  $d_i$  = cylinder inner diameter (m),  $g$  = gravitational acceleration ( $\text{ms}^{-2}$ ) and  $V_l$  = fill volume. The above relationship enabled the conclusion that the power number is

influenced by the orbital to cylinder diameter ratio  $d_o/d_i$  in cylindrical vessels but not Erlenmyer flasks where the conical shape prevents fluid inclination reducing the wetted area while the opposite is true for cylindrical vessels (Klöckner et al. 2012). The authors also determined a new formula for the critical shaking speed  $N_{crit}$ , specific to cylindrical bioreactors (equation 6) to identify when centrifugal acceleration is higher than the inertial forces within the liquid to enable liquid movement.

$$N_c = \frac{1}{d_i^2} \sqrt{0.28V_L g} \quad (6)$$

To address the fact that high Froude numbers used in (Buchs et al. 2000) are not typically associated with mammalian cultures (Weheliye et al. 2012a) performed a pioneering characterisation of fluid flow mechanics at low Froude numbers  $Fr_a < 0.4$  in cylindrical bioreactors to derive a flow scaling law independent of the power law correlations relying instead on dimensionless physical parameters. The effect on flow dynamics was observed when varying shaken cylindrical bioreactors with inner diameter  $d_i = 10\text{cm}$  and  $13\text{cm}$  and fluid heights  $h = 3\text{-}7\text{cm}$ , orbital diameters  $d_o = 1.5\text{-}5\text{cm}$  and shaker speeds  $N = 60\text{-}140$  rpm, by interpreting phase resolved particle image velocimetry (PIV) with free surface measurements (Weheliye et al. 2012a). The authors described in detail how in-phase, out-of-phase and transitional flow can be characterised mostly by observing two counter-rotating vortices near the free surface for  $\Delta h/h < (d_o/d_i)^{0.5}$ . At the critical wave amplitude  $(\Delta h/h_c) = (d_o/d_i)^{0.5}$ , the vortices were observed to increase in size to reach the base of the wells and as rotational speed increases these vortices gradually subside to the walls of the vessel before disappearing, at which point incipient flow transition leads to an out-of-phase flow regime (Weheliye et al. 2012a).

For in-phase flow characterisation, when the Froude number (defined with the characteristic length as the orbital diameter as in equation (7))  $Fr_{d_o} < 0.15$  the report showed in-phase flow can be approximated from the visualisation of a free surface inclined elliptic disc where the longer axis length is in continuously aligned with the direction of the gravitational and centrifugal accelerations due to the moving shaker (Rodriguez et al. 2013; Ducci, A; Weheliye 2014).

$$Fr = \left( \frac{2(\pi N)^2 d}{g} \right) \quad (7)$$

With increasing rotational speeds  $N$  and  $Fr_{d_o}$ , approximation of the free surface is no longer possible as the surface takes on complicated three dimensional shapes which stray from the scaling law derived by the group. The scaling law determined from the in-phase observations using measurements which showed the inclination of the free surface  $\Delta h$  was proportional to the Froude number as seen in equation (8) below:

$$\frac{\Delta h}{d_i} = a_o \left( \frac{2(\pi N)^2 d}{g} \right) \quad (8)$$

where the constant of proportionality  $a_o$  depends on the properties of the fluid and deemed to be 1.4 for water (Weheliye et al. 2012a). This scaling law was further developed to account for deviations from in-phase flow operations, to include situations with increased rotational speeds  $N$  or higher  $Fr$  numbers. Under such conditions the toroidal vortices from in-phase operation transition from horizontal to an extended vertical toroidal vortex, which reaches the bottom of the vessel close to the wall at the shortest side of the free surface and moves around the cylinder axis signalling the end of the transition to out-of-phase operation. (Weheliye et al. 2012a) proposed that the flow transition could be predetermined for when  $h/d_i > (d_o/d_i)^{0.5}$  or  $h/d_i < (d_o/d_i)^{0.5}$  using with the two following equations (9) and (10).

$$\frac{h}{d_i} = a_o \left( \frac{d_i}{d_o} \right)^{0.5} Fr_{d_o} \quad (9)$$

$$a_o Fr_{d_i} = 1 \quad (10)$$

Equation (9) above for predicting flow regimes was implemental in the work of this report, only approximate values were possible due to differences in the inner diameters between the vessels and a  $d_o/d_i > 0.6$  in this report compared to a  $d_o/d_i$  between 0.2 and 0.5 in (Weheliye et al. 2012a) detailed in (Chapter 4.3). Considering the likely flow regimes through theoretical calculations helped select and understand permissive shaking frequencies for orbital shaken EB cultures in this report.

## **1.9 The eye and *in vitro* retinogenesis as a biological model to investigate stem cell differentiation**

Among the multitude of therapeutic cell types under intense research in stem cell labs all over the world, retinal cell generation has been a focal point for several reasons. Apart from the worthy cause and possibility of restoring vision to the blind, research on the ocular environment benefits from the advantage of the eye being an immunologically privileged site due to its immunosuppressive and anti-inflammatory properties (Billingham & Boswell 1952). Ocular immune privilege was discovered by transplanting skin grafts into rabbit corneas; to observe no immune responses were elicited, provided vascularisation did not occur and led to the coining of the term 'immunologically privileged' (Billingham & Boswell 1952). The later discovery of the phenomenon of anterior-chamber-associated-immune-deviation (ACAID), a system of active immune regulation with help from suppressor T cells, provided further support to secure the ocular environments' status as 'immune-privileged'(Waldrep & Kaplan 1983). The eye, is not however a perfect system and is still susceptible to auto-immune diseases such as uveitis and sympathetic ophthalmia, but their rare incidence is evidence for the case of the eye as a model system for intervention (Niederhorn & Wang 2005).

Other factors which contribute to making the eye a particularly suitable organ for study and intervention, include its well characterised and evolutionarily conserved mechanism of development, its relatively simple structure and the availability of cell-specific markers for its constituent cell populations (Gamm & Meyer 2010). Importantly, the eye is non-essential to life has ease of surgical accessibility for graft characterisation and ablation or removal of problematic cells, tissues or grafts making it particularly suitable as a model system for regenerative medicine interventions (Heavner & Pevny 2012).

The majority of inherited retinal disorders and age-related macular degeneration (AMD) (one of the leading causes of blindness in the world), share a key feature - the ultimate loss of photoreceptors preceding impaired vision even though their aetiologies are different (Pearson 2014). The loss of light sensitive photoreceptors in Retinitis Pigmentosa (RP) and Age-Related Macular Degeneration (AMD) cause untreatable blindness in their sufferers (Boucherie et al. 2012). In particular, AMD has been designated a priority eye disease as the third leading cause of visual impairment worldwide, associated with a blindness prevalence of 8.7% it is the leading cause of blindness in industrial countries (WHO Priority Report, 2015).

To date, clinically available treatment options for patients are both limited and unable to restore vision. In contrast, research efforts exploring photoreceptor generation and transplantation as a potentially viable treatment option, provide great hope for all retinal degenerations (Pearson 2014). Pioneering proof of principle studies demonstrating the integration of hESC derived NRL positive photoreceptors into mouse retinæ have paved the way for a growing body of researchers now dedicated to developing cellular therapeutics for retinal disorders (MacLaren et al. 2006; West et al. 2012; Gonzalez-Cordero et al. 2013). The *in vitro* differentiation of retinal cells from pluripotent stem cells recapitulates the *in vivo* biological developmental processes (Meyer et al. 2009). An appreciation of the developmental processes involved in retinogenesis would therefore be beneficial to understand the parallels drawn between the *in vitro* and *in vivo* stages of differentiation in the literature on retinal cell derivation.

### **1.9.1 Retinogenesis and photoreceptor development**

One of the first reports on vertebrate eye development was published in 1885 and localised the beginning of eye development to the anterior medullary grooves in early stages of embryonic development (Sharp 1885). More comprehensive research to describe and illustrate development of the vertebrate eye was reported 110 years ago; from a collection of direct observations made in the developing Chick embryo they provided the first illustrations of the medullary groove and its folds which, over 48 hours, give rise to the bilateral formation of optic cups (Gradon J.T, 1905). Decades later, a report dedicated to understanding the development of the human eye made the first direct observations from the largest collection of human foetuses at the time to provide an analysis correlating eye development with embryo length and gestation period (Mann I.C, 1928).

Thousands of researchers have since contributed to the growing number of publications attempting to elucidate mechanisms underpinning development of the human eye and retinogenesis. A PubMed search for ‘retinal development’ at the time of print returned 22,485 results, making it one of the most studied systems of the

human body. As a result our understanding of eye development has grown rapidly. Although all the mechanisms involved retinogenesis are yet to be fully identified and understood, many key components or factors directing fate along retinal fates have been discovered and are included as exogenous supplements in retinal differentiation protocols (Table 1.5). The current protocols are often complex and efforts to simplify them are already underway. These have led to exciting discoveries using the propensity of stem cells to self-form neural retina and retinal pigment epithelium from PSCs with minimal external inputs (Eiraku et al., 2011 ; Nakano et al., 2012 ; Boucherie et al., 2012 ; Reichman et al., 2014).

To appreciate the advances which led to the accumulation of differentiation protocols directing retinogenesis, a brief description of the main events during retinal development follows. To contextualize *in vitro* retinal differentiation protocols with *in vivo* processes, to help identify some of the underlying mechanisms and provide the rationale for chosen cell markers which feature in the experiments of this report in the following chapters.

Stringent processes of cell discrimination and spatio-temporally defined lineage commitments during early development at the onset of organogenesis, are responsible for the structural organization of cells into tissues and organs (Lancaster & Knoblich 2014). In eye development, finely orchestrated signalling cascades are recruited by the anterior neural ectoderm to initiate formation of the medial anterior neural plate, the primordium of the forebrain and also the location of the eye field or eye primordium (Li et al. 1997). This eye field forms two bilateral depressions which are known as the optic cup primordia (Li et al. 1997; Wilson & Houart 2004).

The anterior neural ectoderm, responsible for beginning the signalling cascades to promote retinal development does so through expression of transcription factors Sex Determining Region Y-Box 2 (Sox2) and Orthodenticle Homeobox 2 (Otx2), which activate other transcription factors: Retina and Anterior Neural Fold Homeobox (Rax) expression and mark the ventral forebrain the prospective eye field; Rax, in turn stimulates expression of the early eye field transcription factors (EFTFs), Sine Oculis Homeobox Homolog 3 (Six3), Paired Box Protein 6 (Pax6) and Lim Homeobox Protein (Lhx2) (Heavner & Pevny 2012). The Rax mediated transcription factors, act as markers for the early eye field, initiate and orchestrate signalling cascades to specify

optic vesicle patterning, during optic vesicle formation from which the optic cup primordia are formed. Retinal progenitor cells here are segregated according to their future morphogenic potentials (Heavner & Pevny 2012; Fuhrmann 2010). Figure 1.2 shows the complexity of the multi-layered transcriptional control mechanisms involved during retinogenesis in normal development (A) and in popularly used retinal differentiation protocols (C).

*In vivo*, ocular development requires the optic vesicles, made up of retinal stem cells, to evaginate and contact the surface ectoderm to begin formation of the lens placode (LP) (Heavner & Pevny 2012). *In vitro*, however it has also been possible for optic vesicles to form the optic cup in the absence of surface ectoderm (Eiraku et al. 2012). In contrast *in vivo*, the optic vesicles begin to invaginate to form optic cups after contact with the surface ectoderm (Jayakody et al. 2015). Before optic cup morphogenesis is complete, retinal stem cells within the optic vesicles are compartmentalised to provide the presumptive neural retina, retinal pigment epithelium and the optic stalk (Heavner & Pevny 2012).

The invagination of the distal portion of the optic cup provides its double walled structure, through simultaneous invagination of the lens placode with the optic vesicle (Eiraku et al. 2011). The resulting optic cup consists of the inner (neurosensory neural retina) and outer (pigmented - early retinal pigmented epithelium) layers of the retina (Heavner & Pevny 2012; Kwan 2014). As an extension of the brain from early morphogenesis, the retina is a part of the central nervous system and is the highly specialized neural tissue responsible for vision (Tian et al. 2015). The retina consists of 6 cell classes, 5 types of neurons and one major glial cell type the Müller cells; arranged into three cellular layers separated by two synaptic layers (inner and outer plexiform) in which visual information is analysed in parallel before leaving the eye (Dowling 2009). Further classification of the cells reveals the 5 neuronal cell types consist of 3 classifications of cone photoreceptors and one rod photoreceptor; 2 types of horizontal cells, 13 bipolar cells, >29 amacrine cells and > 20 types of retinal ganglion cells which project to the brain via the optic nerve (Tian et al. 2015).

In the developed eye, image acquisition from visual cues begin with the rod and cone photoreceptors that first capture photons on their pigmented outer segments to

initiate a series of chemical reactions that result in electrical signals which spread through >20 neural circuits in the retina before transmission to the brain via the retinal ganglion cells (Osakada & Takahashi 2015). Photoreceptors are primary light processing sensory cells essential to vision and are also among the first cells damaged during initial degenerative stages of retinal dystrophies such as retinitis pigmentosa and age-related macular degeneration (Nowak 2006). During the early stages of degeneration, there is selective sacrifice of first order neurons such as photoreceptors, which safeguards the complex neural circuits responsible for higher-order visual processing, but it is ultimately the malfunction and loss of photoreceptors which is responsible for loss of vision (Osakada & Takahashi 2015; Curcio et al. 1996).

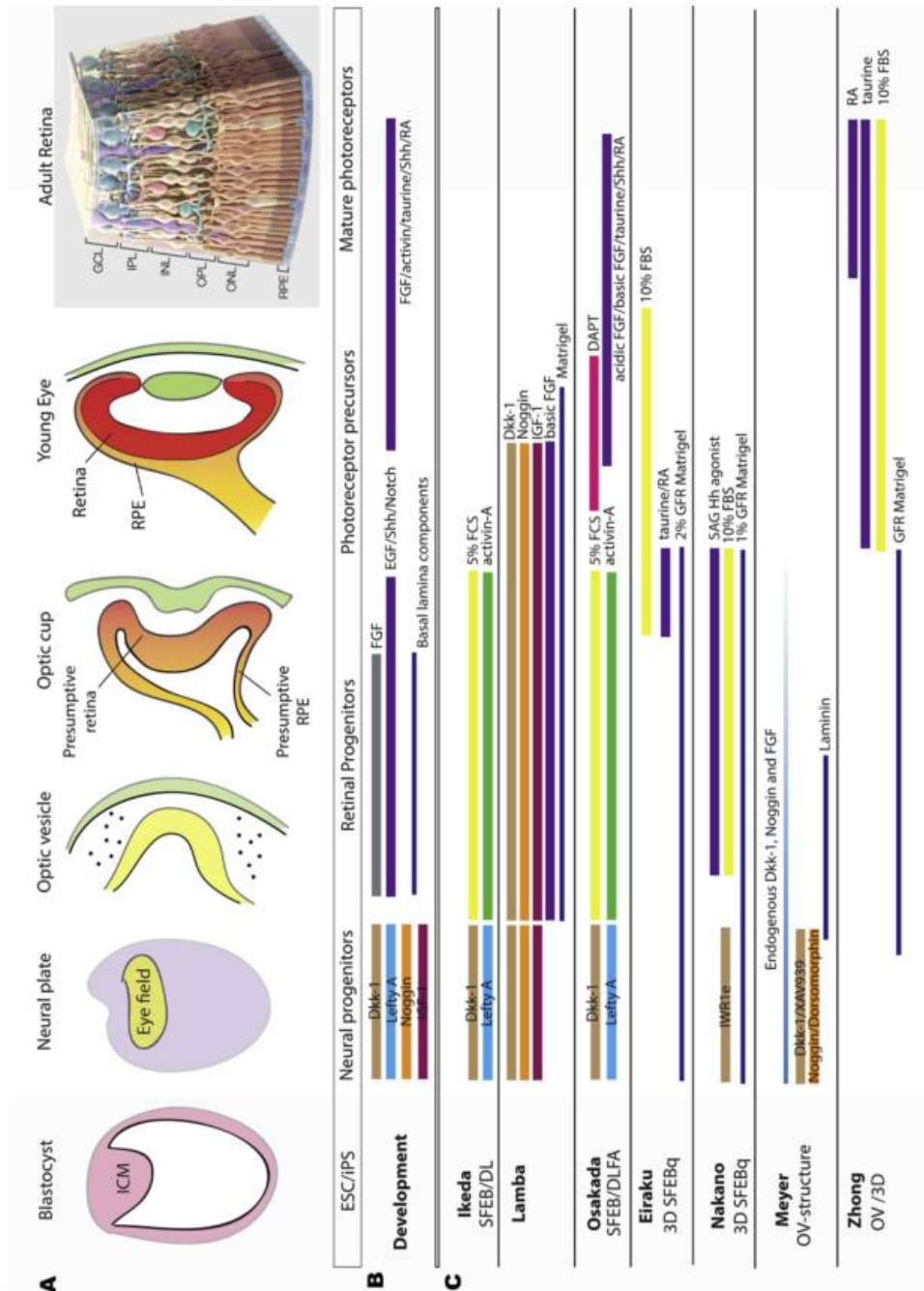


**Figure 1.2** (A) Structural features of the developing retina. (B) Transcriptional control of early eye and photoreceptor development and the developmental cascade of genes involved in early eye and photoreceptor development. (C) Key components of major retinal differentiation protocols, adapted from (Jayakody et al. 2015).

## **1.10 Cues for directed differentiation of pluripotent stem cells into retinal cells**

### **1.10.1 The importance of the extracellular microenvironment**

The evolutionarily conserved mechanisms governing stem cell differentiation are responsive to cues from cytoskeletal and extracellular matrix modelling and remodelling, physical, physiochemical environmental cues such as temperature, pH, oxygen tension and inter and intra-cellular signalling cascades in both paracrine and endocrine mechanisms (Kinney & McDevitt 2013; Serra et al. 2012; Azarin & Palecek 2010). Stem cell researchers targeting therapeutic cell derivation, aim to generate large populations of *in vitro* differentiated cells for humanised disease models or as potential therapeutic transplants. In the case of retinal cell differentiation protocols, evidence for the trend toward research directed at producing larger amounts of cells comes from the increasing number of reports citing differentiation efficiencies and cell yields (Ikeda et al. 2005; Lamba et al. 2006; Hirami et al. 2009; Lamba et al. 2009; Fridley et al. 2010; Meyer et al. 2009; Meyer et al. 2012; Mellough et al. 2012; Nakano et al. 2012; Boucherie et al. 2012; Tucker et al. 2013).

Currently stem cell differentiation protocols use laboratory specific protocols which are subject to operator and cell line specific variabilities. The protocols are further complexed by the unique methods for measuring successful differentiation in each report. Difficulties in measuring differentiated populations, arises from a lack of sufficient unique and comprehensive biomarkers to represent different stages of differentiation effectively and the variability in reported markers. Without definitive markers for referencing various stages of differentiation, protocols are not directly comparable making it difficult for regulatory bodies to create a gold standard for reporting efficiencies of differentiation. As a result comparing individual protocols and their reported efficiencies of differentiation effectively is still a challenge.

Maximising differentiation efficiencies and cell yields from directed differentiation protocols (discussed further in Chapter 1) is nonetheless a key focus of research, as is the study of the roles of the principle components of the microenvironment (depicted in Table 1.5). Academic and industrial interest in the interactions between the

parameters of the microenvironment and their impact on stem cell differentiation have grown into a research field essential to industrialisation of cell therapies (Manuscript et al. 2010; Hazeltine et al. 2013; Hernandez et al. 2011; Christiane & Moens 2013; Kinney & McDevitt 2013; Bae et al. 2011; Veraitch et al. 2008).

For stem cell derived retinal cell generation protocol research, the large number of methods use different cell culture techniques in both planar and/or suspension culture, some with defined culture medium components, others reliant on xenogeneic and undefined materials (Table 1.5). The majority of retinal differentiation protocols use combinations of multiple exogenous factors, at different times, for unique durations and in different concentrations, in order to recapitulate *in vivo* cues for retinogenesis *in vitro* (Table 1.5). The lack of a standardised protocol is likely due to the early stage of research in this field and it represents a key challenge to the development of reproducible strategies, amenable to development for industrial scale production of retinal cells. The challenge will require a multifactorial approach, prompting research into the unique impact of microenvironmental factors.

The microenvironment can be manipulated by changing the culture surface with extracellular matrix or other substrate coatings on tissue culture plastics, to provide mechanical support for differentiating cells and a surface for the attachment of signalling molecules and exogenous factors which create the stem cell niche (Meng et al. 2014). Another strategy to modulate the microenvironment, involves the use of substrates with physiologically relevant Young's Modulus' to influence germ layer specification in differentiating EBs (Earls et al. 2013). In addition, UV/Ozone radiation of tissue culture plastics has also been shown to enhance expansion of pluripotent cells 3-fold in a chemically defined and xeno-free culture system (Saha et al. 2011). Creating hydrophobic culture environments on culture surfaces is also implemented to prevent surface attachment with PDMS coating to promote formation of size specific EBs (100-300µm) (Valamehr et al. 2008).

Investigations into other microenvironmental factors during cell processing in stem cell cultures include inoculation seeding densities (Fridley et al. 2010; Yirme et al. 2008; Veraitch et al. 2008), pH (Wilson & McDevitt 2012; Li & Marbán 2010), temperature (Veraitch et al. 2008; Ban et al. 2011), hydrodynamic forces (Kinney et al.

2012; Fridley et al. 2014; Cimetta et al. 2009) and centrifugal forces (Veraitch et al. 2008; Ungrin et al. 2008). Figure 1.3 illustrates the impact of microenvironmental factors providing a summary of the evidence which supports the requirement to improve control over these parameters. Understanding the influence of these factors on stem cell cultures will facilitates their utility in improving culture conditions for stem differentiation protocols.

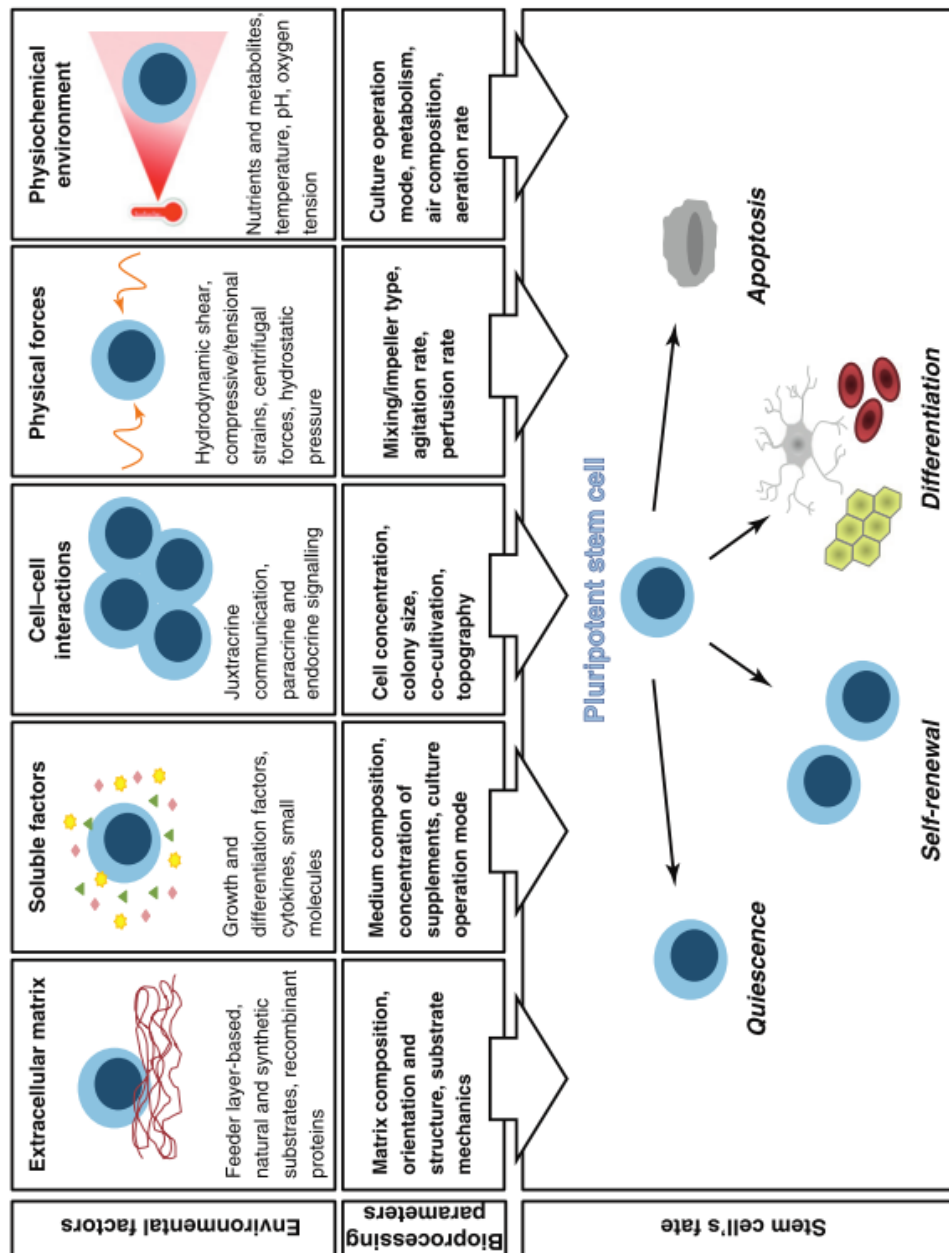


**Figure 1.3** Environmental cues and bioprocessing factors impacting pluripotent stem cell decisions - adapted from (Serra et al. 2012).

### **1.10.2 The role extracellular matrix in protocols for retinogenesis**

The traditional approach for directed differentiation of pluripotent stem cells has been to use exogenous morphogens in 2-dimensional culture systems with the addition of soluble factors and morphogens to the medium as well as a coating on the culture surface to recapitulate endogenous matrices with variable degrees of control. In differentiation protocols reliant on an EB stage for development, the formation of an outer basement membrane layer around the EBs, modulates their microenvironment. The basement membrane limits the diffusive capability of soluble factors such as cytokines, growth factors, vitamins and other small molecules used to induce differentiation and produces extracellular matrix (Sachlos & Auguste 2008).

For retinal development and optic cup morphogenesis, the complex cellular dynamics and molecular mechanisms involved, have been reported in context of the roles extracellular matrix substrates collagen IV, fibronectin and laminin hold to show their functional requirement (Kwan 2014). Using the optically accessible zebra fish model, the functional requirement of laminin has been determined to be necessary at both the early stage of evagination and later again for invagination during optic cup morphogenesis. Similarly the role of fibronectin was deemed functionally required at both lens placode formation and invagination (Figure 1.4)(Kwan 2014).

The affirmed functional requirement of extracellular matrix during morphogenesis has resulted in the widespread use of commercially available Matrigel, an FDA approved but undefined matrix substrate included in many protocols for retinal differentiation to date (Table 1.4). Associated risks of xenogeneic contamination and a lack of knowledge of the concentrations of ingredients within Matrigel, are largely overlooked but have prompted the wider use of defined synthetic and human recombinant protein based alternatives such as collagen IV, laminin and fibronectin, to reduce process variability due to batch differences and risks of contamination with xenogeneic pollutants (Rodin et al. 2010; Heng et al. 2012).

The advantage of removing undefined ingredients, includes conferring the ability to measure the true impact of simple micro-environmental factors by removing the uncertain influence of unquantified factors. This was demonstrated in an interesting

report where two defined alternative substrates to Matrigel, Laminin and Vitronectin were used to investigate the expansion of hESCs in 2-dimensional (2-D) tissue culture plastic versus 3-dimensional (3-D) culture on polystyrene microcarriers (Heng et al., 2012). By removing uncharacterised influences from unknown ingredients in Matrigel they discovered the impact of changing physical parameters, showing 3-D culture performed better than 2-D culture for hESC expansion. In the study, both Laminin and Vitronectin surface coatings promoted an 8.5 fold increase in cell yields for 3-D cultures as compared to planar or 2-D cultures (Heng et al., 2012). Defined substrates such as Laminin and Vitronectin will promote the development of stem cell differentiation protocols with clinical relevance and the advantage of better suitability for translation to scalable, reproducible and standardized culture systems (Serra et al. 2012).

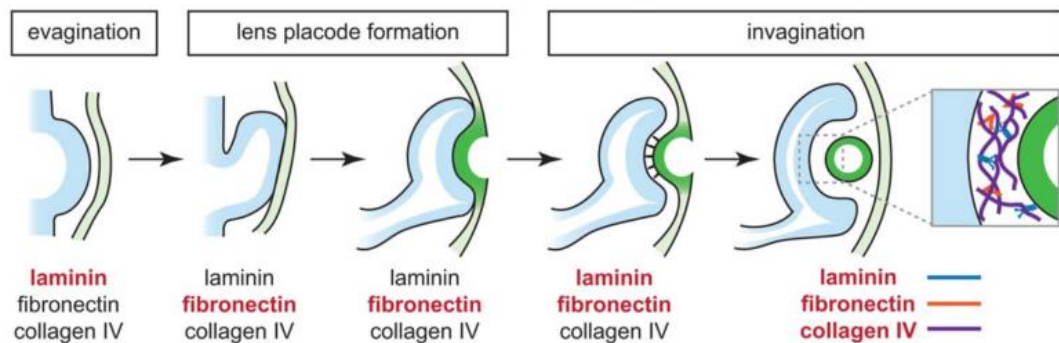


**Figure 1.4** Overview of optic cup morphogenesis and extracellular matrix components. “The optic vesicle undergoes a series of dramatic shape changes to form the optic cup: it first evaginates from the brain neuroepithelium, makes close contact with pre-lens ectoderm as the lens placode forms, then invaginates with the lens to form the optic cup. Laminin, fibronectin, and collagen IV are all present throughout optic cup morphogenesis; when listed in red, it has been demonstrated to be functionally required during that stage of optic cup formation. Inset: Closer view of retina-lens interface at the end of optic cup morphogenesis. Note that ECM is present not just at the retina- lens interface, but also surrounding the eye and lens structures throughout optic cup morphogenesis” (Kwan 2014).

### 1.10.3 The role of growth factors and morphogens in retinogenesis

The framework of our understanding into the role of growth factors during cell specification in embryogenesis stems from fundamental studies in 1924 when Spearman and Goldman showed diffusible substances from salamander embryonic dorsal blastopore cells from one (un-pigmented) Salamander could direct the fate of surrounding tissues, on transplantation to another (pigmented) salamander embryo (Spearman & Goldman 1924). Decades later, mouse embryonic carcinoma cells were found to recapitulate pre-implantation development in simple basal medium, independent of exogenous cues (Heath & Rees 1985). The same group also showed embryonic growth could also be accelerated on increased exposure to insulin-like-growth-factor (IGF), which could regulate both the development of the mouse embryo, as well as its own expression, through feedback loops between germ layer cells and their differentiated derivatives (Heath & Rees 1985).

**IGF-1:** Signalling molecules such as IGF-1 have since been incorporated as key elements of differentiation protocols to generate therapeutic cell types including retinal cells. The role of IGF-1 in retinal morphogenesis has been demonstrated by injecting IGF-1 mRNAs into *Xenopus* embryos, an act which causes the formation of ectopic eyes with neural retinae (Coppola et al. 2009). Experiments in IGF-1<sup>-/-</sup> null mice have shown its essential role in optic nerve development resulting from disruptive structural modifications to the first synapses of the retinal pathway (Rodriguez-de la Rosa et al. 2012). The importance of insulin signalling in photoreceptor development was also shown by disruptions to the IGF-1 signalling pathway; in mice lacking the insulin receptor substrate 2, a 50% reduction in photoreceptor populations is observed by two weeks and near total knockout of photoreceptors by 16 months (Yi et al. 2005). The supplementation of IGF-1 to stem cell differentiation cultures has been demonstrated to improve the yields of retinal progenitor cells (Lund et al. 2006; Lamba et al. 2006).

**FGF family:** Many members of the FGF family of signalling molecules have been implicated for roles in retinal differentiation. The early expression of FGF8 has roles in directing patterning of the embryonic head and can induce optic vesicle regression expression is induced before the developing optic cup makes first contact with the

surface ectoderm and transient expression of FGF 1,2,8 and 9 in the RPE are all able to convert RPE to neural retina (Mellough et al. 2014; Pittack et al. 1997). IGF1 supplementation to the medium has been shown to augment the production of retinal progenitor cells from hESCs and iPSCs (Lamba et al. 2006; Lamba et al. 2010).

**Hedgehog family agonists:** Sonic hedgehog (Shh) agonists act on the evolutionarily conserved hedgehog pathway essential to normal embryonic development. Acting in concentration and time dependent mechanisms they have roles spanning cell survival, proliferation and cell fate determination and also feature in many retinal differentiation protocols (Table 1.4). Shh agonists are used for their ability to influence the formation of separate optic cups, their impact on developing neural retina from ventral RPE and optic stalk and their ability to promote photoreceptor cell production and differentiation (Mellough et al. 2014; Beachy et al. 2010).

**Transforming growth factor  $\beta$  (TGF $\beta$ ) & Bone morphogenic protein (BMP):** The TGF $\beta$ / BMP superfamily of signalling molecules direct cell growth, developmental processes, differentiation and morphogenesis (Horbelt et al. 2012). A key member of the family involved specifically in retinal differentiation Activin A features in many retinal differentiation protocols as it has also been shown to promote photoreceptor formation from progenitor cells by its overexpression in day 18 rat retinal cultures (Davis et al. 2000). For retinal differentiation, BMP4 has a specifically determined role for dorsoventral patterning of the optic cup and its inhibition can prompt initial differentiation from pluripotent cells whilst directing anterior neural specification (Hirami et al. 2009; Mellough et al. 2012).

**Wnt family:** Similar to BMP inhibition Wnt inhibition by molecules such as DKK-1 and Lefty-A helps initiate early stages of hESC differentiation and directs cells toward anterior neural specification (Ikeda et al. 2005; Hiramani et al. 2009; Mellough et al. 2012).

**Notch Signalling:** Notch signalling is also part of the evolutionarily conserved multi signalling-pathway network which regulates cell fate specification during development. Notch signalling operates through contact dependent or juxtacrine signalling in cell to cell or cell to extracellular matrix contact, mediated by transmembrane ligand-receptor crosstalk during development and beyond into adulthood for tissue homeostasis (Andersson & Lendahl 2014). Notch signalling is

inhibited in early retinal differentiation programmes to promote retinal progenitor cell development and later to direct retinal progenitor cells to photoreceptor differentiation (Hirami et al. 2009; Zheng et al. 2010; Eiraku et al. 2011; Nakano et al. 2012).

**Retinoic acid and taurine:** The role of retinoic acid has been described as a powerful morphogen capable of promoting neuronal differentiation (Kumar et al. 2007; Genaro et al. 2013). Its expression during early retinal development at the optic cup formation stage and later during RPE is recapitulated in differentiation protocols for RPE and for later stages of photoreceptor generation protocols to promote the conversion of retinal progenitors into photoreceptors (Kelley et al. 1994). The role of Taurine is similar to that of retinoic acid but more selective by specifically inducing retinal progenitors to develop into rod photoreceptors (Genaro et al. 2013; Hyatt et al. 1996; Militante & Lombardini 2002)

The major retinal differentiation protocols use molecules to modulate the signalling pathways described above but the molecules used vary between protocols as do the timelines required to express retinal cell specific markers and a comparison of the key retinal differentiation protocols is presented in Table 1.4. The amount of variation between retinal differentiation protocols serves as a reminder of the early stage of the field and as evidence for the inherent robust adaptability of retinal differentiation pathways to be able to effect retinal differentiation under so many different conditions.

Our incomplete understanding of the molecular mechanisms governing retinal differentiation is beginning to be addressed using novel tools for single cell transcriptional profiling. In particular the development of a genome-wide single cell transcriptional profiling technique called ‘Dropseq’ has been able to profile the transcriptional variation between single cells from murine retinae to classify them into 39 transcriptionally separate populations in agreement with previously known markers for retinal cell populations (Macosko et al. 2015). Such developments may help investigate subtle differences due to as yet uncharacterised variations in the transcriptome which could lead to the discovery of more complete or novel signalling pathways and molecular mechanisms governing retinal cell function as well as new more specific markers for finer stages of retinal differentiation.

Fortunately, current gaps in our knowledge of molecular control systems in place for retinal differentiation have not hindered our progress toward generating retinal cells

from pluripotent stem cells *in vitro* (Lamba et al. 2006; Meyer et al. 2009; Mellough et al. 2012). It may be the high degree of evolutionary conservation in eye development mechanisms, which has facilitated our progress through extensive experimental research (Zuber et al. 2003). Evolutionary conservation of the major retinal differentiation pathways does not exclude differences in underlying mechanisms, factors involved, timings and pathways induced for cell specialization and development between species (Finlay 2008). Yet despite the many layers of control or maybe because of them, it is possible for optic cup like structures to self-organise from mouse and human stem cell aggregates (Sasai et al. 2012). The demonstration of the ability of hESC and hiPSC cells to ‘self-direct’ differentiation into retinal cells (Eiraku et al. 2008; Nakano et al. 2012) was a landmark achievement and involved EB culture in suspension albeit with the inclusion of Matrigel in the medium combined with relatively few other additional morphogens (see Table 1.4).

The development of finer control over the conditions required for retinal differentiation is dependent on improved understanding of the biological processes involved. Practical improvements over differentiation can be cultivated through operating in a smaller design space with fewer variables. This would promote the development of optimal culture conditions at a faster pace for ultimate translation into reproducible, reliable processes. These are required before standardisation, automation and practical and eventual clinical applicability. Though we have limited understanding of simple factors affecting retinal differentiation such as the influence of light, temperature or pH, stirring or shaking these are being addressed through studies much like this one, with the aims of uncovering mechanisms governing retinal cell differentiation which may be harnessed to improve our chances of creating readily available therapeutic cell types to address errant cells in retinal diseases such as RP and AMD.

The discovery that hESC and hiPSC cells can self-direct their differentiation into retinal cells with minimal external prompts presents an exciting proposition from a bioprocessing perspective (Nakano et al. 2012; Eiraku et al. 2011). With fewer external inputs required for retinal differentiation there is an opportunity to investigate the remaining culture parameters free from avoidable complications arising from unnecessary components in the system. Studying fewer variables to improve understanding of processes governing retinal differentiation may offer

improved understanding of the differentiation process. Discovery and optimisation of new culture techniques able to affect retinal differentiation may also help translate laboratory research protocols into reproducible, reliable processes amenable to standardisation and automation for manufacture of cells as therapies or disease models at scale.



**Table 1.4** A comparison of key retinal differentiation protocols showing exogenous molecules used to induce target retinal cell type and the number of culture days required to express retinal markers where reported.

## **1.11 Project Aims & Objectives**

### **Overall Aims**

This thesis aims to test whether improving process control in a commonly used retinal differentiation protocol can improve the initiation of induced pluripotent stem cell differentiation toward retinal lineages when compared to a standard adherent culture protocol (Lamba et al. 2006). The influence of EB size will be assessed to determine suitable EB sizes with which to initiate retinal differentiation. Furthermore it was hypothesized that the initiation of retinal differentiation with controlled sized hiPSC derived EBs could withstand and benefit from culture in shaken 24-standard round well plates. We tested whether there was an influence of EB size on the initiation of retinal differentiation in orbital shaken cultures compared to static controls. We also tested the hypothesis that orbital shaken culture could be implemental in reducing the requirement for Matrigel, a major source of undefined exogenous factors, from the culture medium. Furthermore, we investigated the impact of orbital shaking on the speed of initiating retinal differentiation for 2 different EB sizes to determine permissive shaking speeds and EB size combinations for the MSU001 iPSC line (see Figure 1.5 for outline of approach).

### **Objectives**

#### **Chapter 3: Stem cell aggregation efficiency and size control**

The objectives of this chapter are to characterize EB formation by traditional scraping techniques as compared to forced aggregation. A fundamental approach of measuring the cell viability and cell losses between the different techniques helps to clarify the impact of each method on the efficiency of EB formation. To assess the impact of each aggregation method on EB formation size, we used the commonly

used and rapidly assessable parameter of EB diameter to measure EB size. The pluripotent nature of early EBs and their initiation of differentiation was assessed using immunostaining and quantitative polymerase chain reaction assay approaches.

#### **Chapter 4: Establishing a potentially scalable, orbital shaken culture protocol to initiate retinal differentiation**

Having established a more reproducible method for uniform EB formation, a range of EB sizes were investigated for their suitability to orbital shaken culture at different shaking speeds, without the addition of any ECM substrates. After identifying suitable EB sizes and shaking speeds for culture in orbital shaken conditions, different size EBs were analysed for their ability to initiate retinal differentiation using a popular differentiation protocol (Lamba et al. 2006). The impact of varying input EB size on the initiation of retinal differentiation in orbital shaken cultures was measured by QPCR and helped identify 2 EB sizes amenable to orbital shaken retinal differentiation culture.

#### **Chapter 5: The impact of controlled size EBs and orbital shaking on the progression of retinal differentiation over 21 days in a Matrigel-free culture**

Having examined the ability of EBs formed by forced aggregation to differentiate toward retinal fates in orbital shaken cultures, in the absence of Matrigel supplementation; the experiments described in this chapter tested whether this culture system was suitable for extended culture periods up to 21 days. In order to characterise the impact of orbital shaking culture on progression through retinal differentiation we used gene expression analyses to illustrate the effects on retinal marker expression for 2 different sized EB cultures over the culture period.

#### **Chapter 6: Orbital shaken culture of a feeder free cell line for retinal differentiation**

In this final chapter the focus turned to testing whether the newly established orbital shaken culture system for retinal differentiation was applicable to another cell line. We tested if the onset of retinal differentiation was replicated using a feeder free hiPSC and gene expression analyses.

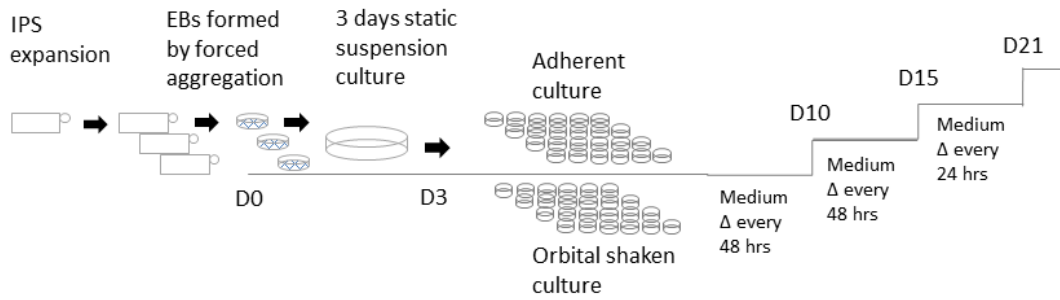


**Figure 1.5** Overview of the experimental approach. HiPSC were cultured and routinely passaged at a ratio of 1:3. Cells for use in experiments were taken from the same passage number and used to form EBs by scraped or forced aggregation. EBs were cultured in pro retinal differentiation medium for 3 days before being split into 2 experiment streams, for either adherent (control) or orbital shaken cultures. Both the control adherent and shaken culture systems were based on the Lamba 2006 protocol for retinal cell generation (see section 2.3). One modification was made to the Lamba 2006 protocol for adherent cultures: the use of uniform size EBs. In shaken cultures, additional modifications were the introduction of orbital shaking culture in 24 standard round well plates and the removal of Matrigel.

## **2.0 Materials and Methods**

### **2.1 Pluripotent stem cell culture and maintenance**

#### **2.1.1 Mouse feeder cell dependent pluripotent stem cell - maintenance**

An induced pluripotent stem (IPS) MSU001 cell line derived from human foetal fibroblasts was used for the majority of the experiments. These IPS cells were routinely co-cultured on mytomycin C (Sigma-Aldrich) inactivated mouse embryonic fibroblasts in culture medium containing KnockOut Dulbecco's modified Eagle's medium (KnockOut DMEM) (Gibco), supplemented with 20% knockout serum replacement (KOSR) (Gibco), 1% minimum essential medium non-essential amino acids (MEM NEAA) (Gibco), 2mM L-Glutamine (Gibco), 0.1mM  $\beta$ -mercaptoethanol (Gibco), and 10 ng/ml bFGF (R&D Systems). IPS medium was replaced daily except the day after passage. Cells were cultured in T25 flasks containing feeder cells at a confluency of 230-250K cells per flask. IPS cells were used between passages 56- 80.

#### **2.1.2 Thawing pluripotent cells from liquid Nitrogen storage**

Vials of pluripotent cells from liquid nitrogen storage were placed in a water bath at 37°C to thaw for up to 2 minutes. On disappearance of ice from the cryovial, the vials were transferred to a tissue culture hood where the cell suspension was aspirated into a 10ml pipette containing 8ml of pre-warmed pluripotent stem cell culture medium. The cells were transferred to a centrifuge tube and centrifuged for 3 minutes at 1200rpm before the supernatant was removed and cells re-suspended in pre-warmed culture medium. The cell suspension was finally transferred to appropriate culture vessels. The mouse feeder dependent pluripotent stem cells (MSU001-IPS) were transferred with 5-7ml of medium to pre-prepared flasks containing feeder cells at a density of 230-250K cells per T25 flask. Feeder free pluripotent stem cells (BJ-IPS) in E8 medium (Invitrogen) were transferred to T25 flasks pre-coated with VTN (Invitrogen) for an hour in advance.

### **2.1.3 Mouse embryonic fibroblast and feeder cell isolation and preparation**

Mouse embryonic fibroblasts (MEFs) from CF1 mouse embryos were isolated at day 13. Heads and internal organs were first removed from the tissue using sterilised tweezers and scissors before washing with PBS and digesting using 0.05% Trypsin/EDTA (Gibco-Invitrogen). The tissue was then finely minced before the addition of more Trypsin/EDTA and transfer to an incubator at 37°C for 5-10 minutes. The digestion reaction was quenched using MEF medium containing Dulbecco's modified Eagle's medium (DMEM) supplemented with 10% (v/v) foetal bovine serum and 1% (v/v) non-essential amino acid (NEAA) (all Gibco-Invitrogen). The mixture was transferred to a centrifuge tube to settle before removal of the supernatant and re-suspension in fresh MEF medium. After centrifugation at 1000rpm for 3-5 minutes the supernatant was discarded and the pellet re-suspended in more MEF medium and transferred to a T75 flask (NUNC, Easy Flasks, Thermo-Fischer Scientific) and returned to the incubator at 37°C. The MEFs were expanded for two population doublings before being designated passage zero (P0). At P0 the cells were harvested using Trypsin/EDTA, and re-suspended in cryopreservation medium (40% MEF medium, 50% FBS and 10% DMSO (Sigma-Aldrich)) before being frozen in liquid nitrogen.

P0 MEFs from liquid Nitrogen were used between P1 and 6 and were maintained in mouse embryonic fibroblast (MEF) medium. The frozen vials were placed in a water bath at 37°C for less than 2 minutes before being re-suspended in MEF medium. The cells were then centrifuged at 1200rpm for 3 minutes before removal of the supernatant and re-suspended in fresh MEF medium before plating into T75 flasks. The MEFs were passaged every 3 days using 0.25% Trypsin/EDTA and split at a ratio of 1:4 – 1:2.

Before MEFs could be used as feeders they were inactivated with mytomycin-C (1 mg/mL) and re-suspended in MEF medium before being seeded on gelatinised T25 flasks (0.1% Porcine gelatine (Sigma-Aldrich) at a confluency of 250K per flask. Inactivated MEFs or Feeders were prepared a day before passaging IPS cells onto them

and were kept in MEF medium until 30 minutes before passaging the following day, when MEF medium was replaced with IPS cell medium. IPS cell medium composed of Dulbecco's modified Eagle's medium (DMEM from Invitrogen) supplemented with 20% knockout serum replacement (KSR), 2mM non-essential amino acids and 2mM L-glutamine (Invitrogen Life Sciences); 0.1mM b-mercapethanol (Sigma) and 10ng/ml human recombinant basic fibroblast growth factor (bFGF - R&D systems).

#### **2.1.4 Mouse feeder cell dependent pluripotent stem cell - passaging**

Confluent flasks of IPS cells were passaged at a ratio of 1:2 or 1:3 on reaching 70-80% confluence. Spent IPS cell culture medium was first replaced with 6mls of fresh medium at least an hour in advance. Undifferentiated IPS colonies were mechanically scraped from the flasks using sterile Pasteur pipettes (Starlabs) under a phase contrast dissecting microscope. Stem cell colony clumps suspended in the medium were pipetted out onto fresh T25 feeder flasks. Feeder flasks were seeded with 230-250K MEF cells 24 hours in advance and were primed for stem cell addition by addition of IPS medium 30 minutes prior to use.

#### **2.1.5 BJ IPS cell line maintenance in fully defined feeder free culture conditions**

The BJ induced pluripotent stem cell (iPSC) line was generated from human foreskin fibroblasts. BJ IPS were created by Sendai virus vector transfection Yamanaka's reprogramming factors in expression cassettes (Takahashi et al. 2007). The transformed cells have a normal male karyotype (National Centre for Global Health, Tokyo). These cells were maintained on Essential 8 Medium (Invitrogen) developed by Jamie Thomson's Lab (Chen et al. 2011) on Vitronectin VTN-N (Invitrogen) coated T25 flasks. Medium was replaced daily except the day after passage.

#### **2.1.6 BJ IPS cell passaging**

Cells were typically passaged every 3-4 days when they reached 70-80% confluency. E8 medium was aspirated from the culture vessel and discarded before washing with

PBS without Calcium or Magnesium. To dislodge the cells 2ml of 0.5mM solution of EDTA in PBS without Calcium or Magnesium was used. Following a 5-8 minutes incubation at room temperature the EDTA was aspirated and E8 medium was added to the flasks and gently titrated. The suspended IPS colony clumps were transferred into new VTN-N coated T25 flasks at a split ratio of 1:4-6 depending on the cell density. For all other assays and differentiation protocols the cells were treated in exactly the same way as the MSU001 cell line.

## **2.2 Aggregation of stem cells and aggregate/EB processing**

### **2.2.1 Manual scraped EB formation**

IPS cells were harvested from their T25 flasks when they reached between 70-80% confluency by manual scraping. Spent medium was replaced with 3mls of EB formation medium (knockout-DMEM, 34, 10% KSR, 2mM L Glutamine, 2mM L nonessential amino acids (all from Invitrogen) supplemented with the appropriate concentrations of retinal induction growth factors (see section on retinal differentiation below). The suspended scraped cell clumps, were transferred to low attachment bacterial grade culture dishes (3cm diameter) and placed in an incubator at 37°C and 5% CO<sub>2</sub> for 3 days. The dishes were shaken once a day to prevent mass clumping of the aggregates.

### **2.2.2 Forced aggregation of pluripotent stem cells using Aggrewells**

To form uniform sized stem cell aggregates, Aggrewell plates (Stemcell Technologies) were used in accordance with the manufacturer's instructions. Briefly, medium from T25 flasks containing IPS cells was discarded and replaced with 3mls of Dulbecco's phosphate buffered saline (PBS) to wash. On removal of the PBS 2mls/T25 of gentle enzymatic dissociation reagent Tryple (Invitrogen) was added to each flask and incubated for 10 minutes at 37°C. At the end of the incubation flasks were tapped on the bench to dislodge cells before 5 ml of IPS medium was used to quench and neutralise the dissociation enzyme. The cell suspension was subsequently passed

through a 40um cell strainer (BD) before being centrifuged at 300G for 2 minutes. Post centrifugation the supernatant was discarded and the cell pellet re-suspended in 2mls of EB formation medium supplemented with 1ng/ml of Rho Kinase Inhibitor (ROKi). In order to count cells in the concentrated suspension with a haemocytometer, the suspension was first diluted by a factor of 10. A sample of 10ul of the cell suspension was mixed in a vial containing 80ul of IPS medium and 10ul of Trypan blue before 10ul of the mixture was introduced to a chamber of the haemocytometer and counted. An average of three cell counts was used for the final measurement of cell concentration. The appropriate volume of cells was finally distributed into Aggrewell plate wells containing 500ul of EBMr and the total volume of each well was made up to 2mls with the addition of an appropriate volume of more EBMr. The Aggrewell plates were placed in an incubator at 37<sup>0</sup>C and 5% CO<sub>2</sub> for 24 hours.

### **2.2.3 Harvesting stem cell aggregate/ EBs from Aggrewells**

After 24 hours stem cell aggregates were dislodged from the Aggrewells by gentle titration using a 5ml pipette. Suspended aggregates were then transferred to a 10ml centrifuge tube and allowed to settle before the medium containing ROKi was replaced with EB formation medium without ROKi. The new suspension was finally transferred to low attachment 3cm bacterial grade dishes and aggregates were returned to an incubator at 37°C for 3 days.

### **2.3 Retinal differentiation**

Whether the stem cell aggregates were formed by manual scraping or by forced aggregation the newly formed stem cell aggregates were harvested by gentle titration using a 5ml pipette and transferred to a 10ml centrifuge tube to settle. The aggregates settled to the bottom of the centrifuge within 5 minutes and the supernatant was aspirated and replaced with phase 1 (P1) retinal induction medium (Lamba et al. 2006) containing DMEM/F12 (Gibco), supplemented with 1ng/ml (R&D Systems), 5ng/ml

IGF-1 (Miltenyi Biotec), 1ng/ml dkk1 (System Biosciences), 10% knockout serum-replacement (KOSR) (Gibco), 1% N2 supplement (Gibco), and 1% L-Glutamine (Gibco). The freshly suspended aggregates were finally transferred to low attachment bacterial grade dishes (ø300mm, Sterilin) and returned to the incubator for 3 days. Aggregate dishes were shaken (twice left to right and twice up and down) daily to avoid mass clumping.

On day 3 the aggregates were harvested from the dishes by aspiration with a 5ml pipette and collected into 10ml centrifuge tubes for settling. The spent medium was replaced with phase 2 (P2) retinal differentiation medium (Osakada et al. 2009) in summary: DMEM/F12 (Gibco), supplemented with 10ng/ml noggin (R&D® Systems), 10ng/ml IGF-1 (Miltenyi Biotec), 10ng/ml dkk1 (System Biosciences®), 1% N2 supplement (Gibco), 5ng/ml B27 supplement (Gibco), 5ng/ml bFGF (R&D Systems), and 1% L-Glutamine (Gibco).

Depending on whether the differentiations were assigned for completion in suspension or in an adherent system (see 4.3.1 and 4.3.2), the aggregates were transferred to the appropriate vessels and medium was replaced every 2 days until day 15 and then as necessary to avoid the medium turning too yellow over the 31 days.

### **2.3.1 Attached differentiation of EBs on Matrigel**

Attached culture of EBs was carried out in 24 well tissue culture plates (Nunc). Plates were first coated with reduced growth factor Matrigel (BD). Coating the wells required the surfaces to be completely submerged in Matrigel for an hour's incubation at room temperature. After incubation the Matrigel was removed and the wells hydrated with 250ul of P2 medium. Finally using sterile Pasteur pipettes 30-40 aggregates were transferred under a dissecting microscope to each well. Tissue culture plates were returned to an incubator at 37°C for the remainder of the culture period with medium changes every day until day 15 and as required thereafter to avoid the medium becoming too yellow.

### **2.3.2 Orbital shaken culture of EBS for retinal differentiation without Matrigel**

Day 3 EBs designated for orbital shaken differentiation culture were transferred to ultra-low attachment 24 well culture plates, dimensions of an individual well were: height=17.40mm, top internal diameter = 16.26mm and bottom internal diameter = 15.62mm (Corning). For each experiment 30-40 aggregates were transferred into each well and additional P2 medium added to make up the total volume to 500ul per well. No Matrigel was added to these plates and they were placed on a shaker with orbital diameter 10mm on an IKA KS 260 Shaker (IKA) set at 120rpm in an incubator at 37°C for the remainder of their differentiation with ~90% medium changes every 2 days until day 15 and then 50% medium changes daily up to day 31.

## **2.4 Analytical techniques for retinal differentiation**

### **2.4.1 Cell counts for suspension cells and cells from EB digests**

Aggregates formed by scraped or forced aggregation after 24 hours, were transferred to a 10ml centrifuge tube and allowed to settle for 5-10 minutes. The supernatants containing unincorporated cells were transferred to fresh centrifuge tubes and kept aside for counting alongside cells from digested EBs at the end of the protocol. The settled EBs were resuspended in 5ml PBS to wash and centrifuged before the PBS was aspirated and replaced with 1ml of Tryple (pre-warmed to 37°C) and the tubes transferred to a water bath at 37°C to activate the Tryple for EB digestion. To aid EB digestion samples were also manually titrated using 200µl Gilson pipettes, for the 3 minutes duration in the water bath. The single cell suspensions from digested EBs containing Tryple were quenched using 3mls of IPS medium before being counted in parallel with the supernatant containing single cells separated at the start of the procedure. The live and dead cell portions of all cell samples were counted using the Trypan Blue exclusion method on a Vi-Cell counter (Beckman Coulter).

For dense aggregates from later time points (10 days+) 100ug/ml DNAase I (Sigma) and 5mM MgCl<sub>2</sub> in PBS were also added to the Tryple for the digestion reaction. In addition the samples needed titration whilst in the water bath at 37°C to obtain break up EBs into suspension.

#### **2.4.2 EB size calculations using Image J software**

Variation in EB size over time (24 hours, day 3, day 10 and day 15) was assessed by calculating the average sizes of EBs (n=100) formed by scraping or forced aggregation. For the 1K EBs analysed at 24 and 48 hours not assigned for EB digestion, the full volumes of the cultures containing the EBs were transferred to 10ml centrifuge tubes as above and the supernatant containing unincorporated cells in suspension transferred to another centrifuge tube for counting separately. The EBs were subsequently resuspended in 3ml of medium and gently titrated using a 5ml pipette to mix before sampling. Samples of 100µl of suspended EBs were taken and distributed into 10 wells of black-walled, flat bottom 96-well plates. EBs were left to settle for 5 mins before being counted or imaged by light microscopy (Nikon epifluorescence Eclipse 2000 inverted microscope) for calculating EB sizes as described below.

For 5K and 10K EBs at days 3, 10 and 15 cultured in suspension, the EBs were allowed to settle to the bottom of their culture wells (5 mins) before being imaged by light microscopy (Nikon epifluorescence Eclipse 2000 inverted microscope). Image J software was used to take 3 pixel length measurements per EB for all EB sizes from the micrographs (transverse, dorsoventral and diagonal). The pixel length measurements were converted to µm lengths in the software using image size parameters to reference known distances (Table 1.5). Finally averages of 3 measurements per EB (n ≥ 100) were calculated to represent the size of each EB.

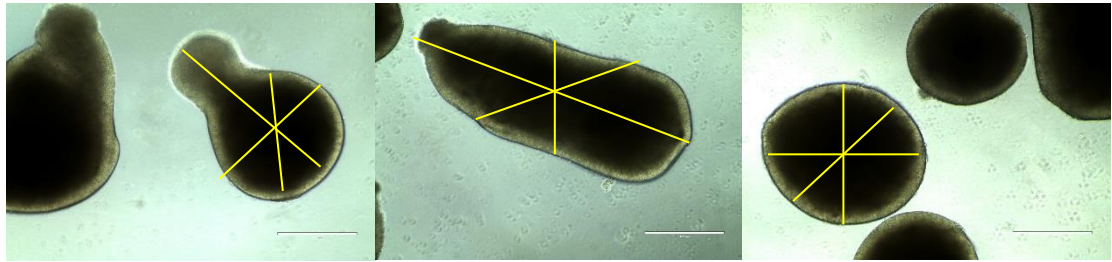


**Figure 2.1** Representative micrographs to show EB size measurement method. The 3 yellow lines per EB illustrate the 3 typical measurements (transverse, dorsoventral and diagonal) taken for each settled EB in the same plane to calculate an average representing the EB's size. Images are of 10K EBs at day 15 of orbital shaken retinal differentiation culture (10x magnification and scale bars = 400  $\mu\text{m}$ ).

Objective used	Image size 2560 x 1920 Known Distance in $\mu\text{m}$ / pixel =	Image size 1280 x 960 Known Distance in $\mu\text{m}$ / pixel =
4x	0.86	1.72
10x	0.34	0.68
20x	0.17	0.34

Table 1.5 Image size  $\mu\text{m}$ /pixel measurements reference table to calculate lengths  $\mu\text{m}$  lengths and average EB sizes.

### 2.4.3 DNA Quantification

DNA quantification was used as an indirect measure of the total cell numbers in adherent and orbital shaken cultures for later cultures which were difficult to digest into live single cell suspensions. The Quant-iT PicoGreen dsDNA assay (Invitrogen) enabled more accurate calculation of the cell numbers by measuring the total quantity of DNA from disrupted cells as an end point assay. Following the manufacturer's instructions, a standard curve for DNA concentration was created using serial dilutions of IPS cells in a range between  $25 \times 10^5$  and  $3 \times 10^6$  cells. Cells were suspended in 1x TE buffer (10 mM Tris-HCl, 1 mM EDTA, pH 7.5) and added to 100  $\mu\text{l}$  of the aqueous working solution of Quant-iT PicoGreen Reagent before making up to a final volume

of 200µl with TE buffer as required. The samples were subsequently incubated at room temperature in the dark for 5 minutes before fluorescence was measured using a Tecan Saffire fluorescence microplate reader (Tecan). Following the same procedure for unknown samples from retinal EBs, the fluorescence readings were analysed against the standard curve to attain relative cell numbers per sample.

#### **2.4.4 Lactate Dehydrogenase (LDH) Colorimetric Assay**

The oxidoreductase lactate dehydrogenase reduces NAD present in the medium to NADH which interacts with a fluorescent probe to emit light ( $\lambda_{\text{max}} = 450 \text{ nm}$ ). LDH content in spent supernatant from culture samples were measured using the LDH Assay (Abcam) according to the manufacturer's instructions. LDH measurements were taken as an indication of the presence of cell damage and toxicity within the differentiating cultures. The stability of the LDH enzyme facilitates its use with frozen sample which were kept from medium changes for retinal differentiation cultures up to 21 days before analysis together on the same day.

Samples (50µl) each were plated into clear bottom 96 well plates (Nunc) in triplicate wells alongside a 1:9 serial dilution of the NADH positive control assay buffer. After addition of 'Reaction Mix' (50µl) per sample, fluorescence readings were taken using a Tecan Saffire fluorescence microplate reader at T0 and after 30 minutes of incubation at 37°C. Following the manufacturer's instructions fluorescence readings were used to create a standard curve from the positive control serial dilutions against which sample measurements were compared for a measurement of LDH Activity with time and plotted for each sample.

#### **2.4.5 Aggregate freezing protocol for cryosectioning**

EBs harvested for cryosectioning were first incubated in 4% paraformaldehyde (PFA) for 20 minutes at room temperature. The 4% PFA solution was replaced with a 30% sucrose PBS buffer solution and incubated overnight at 4°C. The following day the dehydrated cell aggregates had settled to the bottom of the vial. After aspirating and

removing most of the sucrose solution, the final volume was aspirated with low attachment 200ul pipette tips (Starlabs), cut at the middle to allow for larger aggregates to pass and deposited into cryosection moulds. Using absorbent paper excess sucrose solution was removed before adding embedding medium OCT (Tissue-Tek) to cover the aggregates and fill the mould. These OCT blocks were finally frozen at  $-80^{\circ}\text{C}$  and later sectioned using a Thermo Scientific™ Cryotome™ FSE Cryostat into  $10\mu\text{m}$  slices.

#### **2.4.6 Cryosectioning aggregates**

Frozen blocks of aggregates in OCT embedded within their moulds were allowed to thaw for less than a minute in order to facilitate the removal of the mould before placing the blocks within the cooled chamber of the Cryostat ( $-25^{\circ}\text{C}$ ). The blocks were fixed onto a mounting stage using more OCT and finally sectioned into  $10\mu\text{m}$  slices. The slices were picked up using Microslide Superfrost Plus White (VWR) glass slides, allowed to dry at room temperature for at least an hour and then either stored at  $-80^{\circ}\text{C}$  or used immediately for immunohistochemistry.

Cut sections removed from frozen storage are allowed to acclimatise to room temperature before the containers are opened to reduce condensation. The sections were dried for up to two hours under a fan or on the bench overnight before commencing the immunohistochemistry protocol.

### **2.5 Immunocytochemistry**

Cells grown in 24-well tissue culture plates were fixed in 4% PFA for 20min at room temperature. The PFA was removed and cells were washed with PBS. Each well was then treated with blocking buffer (0.3% Triton and 5% goat serum (Invitrogen) in PBS) for 1 hour at room temperature. After incubation in blocking buffer, cells were

incubated overnight at 4<sup>0</sup>C with primary antibody diluted between 1:200 (Table 2.1) and 1:300 for secondary antibodies (Table 2.2) in blocking buffer.

Following incubation with primary antibodies the next day, cells were washed 3 times in PBS for 5mins each on a shaking platform at room temperature. Post washing, cells were incubated at room temperature for up to 1 hour with the appropriate secondary antibodies, pre-diluted in blocking buffer at a ratio of 1:300 – 1:400. Isotype control staining to show the secondary antibodies were specific to their corresponding primary antibody species were carried out alongside each staining process by including wells which were only incubated with secondary antibodies specific for each species of primary antibody used.

After incubation with secondary antibodies cells were washed thrice with PBS as before with 5 minutes per wash, and stained with DAPI before being mounted in PBS and stored at 4<sup>0</sup>C. The Nikon epifluorescence Eclipse 2000 inverted microscope was used to image the cell markers and analysis was performed using the NIS-elements software (version 3.0).

## **2.6 Gene expression analyses**

### **2.6.1 RNA extraction**

RNA samples were harvested from cells using the RNeasy mini-kit (Qiagen) according to the manufacturer's instructions including an in-column DNase step to digest any potentially contaminating genomic DNA. Adherent cells were harvested by scraping and cells in suspension were pelleted before excess medium was aspirated and the samples used or frozen at -80<sup>0</sup>C. Pellets were first re-suspended in RLT Buffer (Qiagen) before being homogenised in Qiashredder Columns (Qiagen) according to the manufacturer's instructions. Harvested RNA samples were eluted in 40µl RNase free water and quantified to ng/µl by measuring 260/280nm absorbance ratios on a spectrophotometer (NanoDrop ND-1000, Thermo Scientific).

## **2.6.2 Reverse transcriptase polymerase chain reaction (RTPCR)**

Synthesis of complementary deoxyribonucleic acid (cDNA) and removal of genomic DNA was performed using the Qiagen RTPCR kit following the manufacturer's instructions. Genomic DNA was eliminated using gDNA Wipeout Buffer (Qiagen) with up to 1µg template RNA and RNase free water in a total reaction volume of 14µl which was incubated at 42°C for 2 minutes in a thermocycler. The entire 14µl reaction volume was subsequently mixed with a mastermix, containing template RNAs, RT Primer Mix Quantiscript RT Buffer and Quantiscript Reverse Transcriptase (all Qiagen) in a total volume of 20µl. The reaction volume was incubated at 42°C for 15 minutes, then 3 minutes at 95°C to inactivate the reverse transcriptase. The synthesised first strand cDNA scripts from the reverse transcription reactions were stored at -20°C and thawed on ice before QPCR analyses.

## **2.6.3 Quantitative (real time) PCR (qPCR)**

The QPCR reactions were performed in Biorad Hard-Shell Low Profile Thin-Wall 96 Well Skirted PCR plates on the Biorad CFX 96 Connect Real-Time PCR System using the Quantitect SYBR Green PCR Kits (Qiagen) according to the manufacturer's instructions. For each reaction Quantitect Mastermix Buffer, Quantitect pre-validated primer assay (Table 2.3), water and cDNA were combined to make final reaction volumes of 25µl. On each 96 well plate samples were analysed in triplicate with 2 internal reference genes GAPDH and  $\beta$ Actin and standard controls NoRT (No reverse transcriptase control) and NTCs (no template control) to check for contaminations which may have occurred during cDNA synthesis or final mastermix preparation.

The real-time PCR results were analysed using the Biorad CFX Manager 3.0 to calculate normalized relative expression ( $\Delta\Delta Cq$ ) of target genes normalized to relative expression levels of the reference genes  $\beta$  Actin and GAPDH, using the Pfaffl method (Pfaffl, 2001). The equations used with the Biorad CFX Manager 3.0 software to measure normalized expression relative to reference target genes (Equation 1) and

standard errors of the mean (Equation 2) are given below. All error bars on QPCR graphs were standard errors of the mean calculated according to equation 2.

$$\text{Normalized Expression}_{\text{sample (GOI)}} = \frac{RQ_{\text{sample (GOI)}}}{\left(RQ_{\text{sample (Ref1)}} \times RQ_{\text{sample (Ref1)}} \times \dots \times RQ_{\text{sample (Refn)}}\right)^{\frac{1}{n}}}$$

- RQ = Relative Quantity of a sample
- Ref = Reference target in a run that includes one or more reference targets in each sample
- GOI = Gene of interest (one target)

**Equation 1:** Formula for normalized expression used to calculate gene expression comparisons across multiple plates for QPCR (Biorad CFX Manager 3.0).

$$SE_{GOIn} = GOIn \times \sqrt{\left(\frac{SE_{NF_n}}{NF_n}\right)^2 + \left(\frac{SE_{GOI}}{GOI}\right)^2}$$

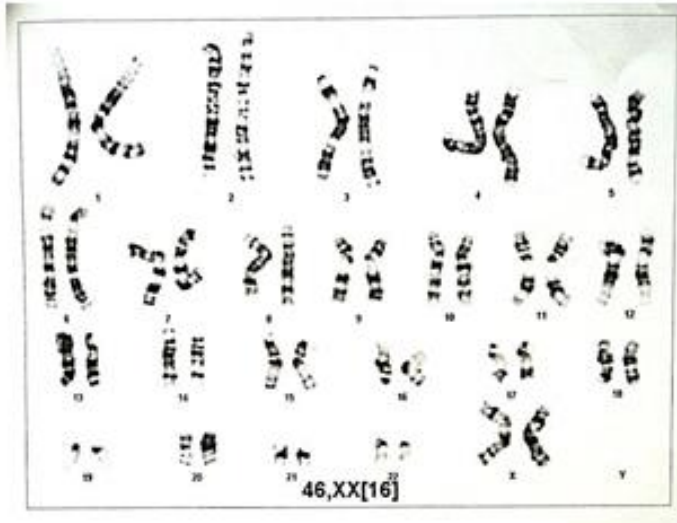
- SE = Standard error
- GOI = Gene of interest (one target)
- NF = Normalization factor
- n = Number of reference targets

**Equation 2:** Formula used to calculate standard errors for normalized expression of genes of interest (Biorad CFX Manager 3.0).

## 2.7 Mycoplasma Testing and Karyotyping

Both the MSU001 and the BJ IPS cell lines were tested for mycoplasma (Surrey Diagnostics, Cranleigh, UK) and for karyotypic abnormalities after extensive passaging by The Doctor's Laboratory (TDL 60 Whitfield Street, London). The samples sent for testing were subjected to G banding and up to 20 cells were used in the analyses (Figure 2.2).

**A. MSU001 (XX)**



**B. BJ IPS (XY)**



**Figure 2.2** Karyotypic Analysis of MSU001 and BJ hiPSC lines. Standard G banding karyotypic analyses were routinely performed on hiPSC lines (TDL Genetics, Whitfield Street, London). (A) Typical G banded chromosomes for MSU001 at passage 62. The majority of analyses for MSU001 resulted in normal 46 XX karyotype. (B) Typical G banded BJ IPS chromosomes at passage 51. The majority of BJ IPS cells showed a modal karyotype 46 XX. In an anomalous result one cell showed a chromosome loss 45, XY.

<b>Primary Antibody</b>	<b>Source</b>	<b>Host</b>	<b>Isotype</b>	<b>Dilution</b>
<b><i>Pluripotency Markers</i></b>				
Oct3/4	Santa Cruz	Mouse	IgG2b	1:200
Tra-160	Millipore	Mouse	IgG	1:200
SSEA4: Mab4304	Millipore	Mouse	IgG3	1:200
Tra-181	P. Andrews, Sheffield University	Mouse	IgM	1:200
SSEA 1	P. Andrews, Sheffield University	Mouse	IgM	1:200
SSEA3	P. Andrews, Sheffield University	Mouse	IgG	1:200
<b><i>Retinal Differentiation Markers</i></b>				
Rax: WH0030062M1	Sigma	Mouse	IgG	1:200
Rax: Ab3729	Millipore	Rabbit	Poly	1:200
Pax6: Mab5552	Millipore	Mouse	IgG	1:200
Otx2: AJ1560a	Abgent	Rabbit	IgG	1:200
Otx2: Ab9566	Millipore	Rabbit	Poly	1:200
Crx: Sc377207	Santa Cruz	Mouse	IgG2	1:200
Crx: WH0001406M1	Sigma	Mouse	IgG1a	1:200
Rhodopsin: R5403	Sigma	Mouse	1D4	1:200
Opsin: 04886/051m597	Sigma	Mouse	IgG1	1:200
Six3: AT3893a	Abgent	Mouse	IgG2ak	1:200
Chx10(N): Ab9016	Millipore	Sheep	Poly	1:200

**Table 2.1** Primary antibodies used for immunocytochemistry to assess pluripotency and retinal differentiation.

Secondary Antibody	Source	Dilution
Alexa Fluor 488 Goat Anti-Mouse IgG	Invitrogen	1:300
Alexa Fluor 488 Goat Anti-Rabbit IgG	Invitrogen	1:300
Alexa Fluor 555 Goat Anti-Mouse IgG	Invitrogen	1:300
Alexa Fluor 555 Goat Anti-Rabbit IgG	Invitrogen	1:300
Alexa Fluor 488 Goat Anti-Mouse IgM	Invitrogen	1:300
Alexa Fluor 555 Goat Anti-Mouse IgM	Invitrogen	1:300

**Table 2.2** Secondary antibodies used against the primary antibodies in assessing pluripotency and differentiation marker expression.

Description	Quantitect Primer Assay	Qiagen Reference
Reference	Beta Actin	QT01680476
	GAPDH	QT01192646
Pluripotency	POU5F1	QT00210840
Early eye field	PAX6 (Paired box 6)	QT00071169
	RAX (Retina and anterior neural fold homeobox)	QT00212667
	OTX2 (Orthodenticle homeobox 2)	QT00213129
	SIX3 (Six homeobox 3)	QT00211897
Photoreceptor specific	CRX (Cone-rod homeobox)	QT01192632
	NRL (Neural retina leucine zipper)	QT01005165
	RHO (Rhodopsin)	QT00035700

**Table 2.3** List of primers used to quantify the level of expression of key markers of retinal differentiation.

## **3. Stem Cell Aggregation Efficiency and EB Size Control**

### **3.1 Introduction**

Manual scraping produces heterogeneous EB sizes and results in large cell losses, yet is still a frequently used technique for their production, despite the availability of more controlled methods for EB formation (Heng et al. 2007). The ability to efficiently aggregate stem cells to form uniform sized EBs is important for maximising the yield of desired cell types from differentiation protocols dependent on EB stage transgression (Bauwens et al. 2008). When considering the potential of differentiation protocols for scale up into industrial manufacturing production bioprocesses; the efficiency of EB formation and consistency in size will affect production costs and the ability to direct differentiation in to desired cell types reproducibly (Ungrin et al. 2008). In this chapter two EB production techniques are characterised to assess the efficiency of aggregation and reproducibility of EB sizes in each. The first method evaluated is the conventional manual scraping technique as used in the Lamba 2006 protocol for retinal differentiation. The efficiency of aggregation and uniformity of EBs produced from manual scraping will be compared to the same outputs from a popular, commercially available method for forming EBs by forced aggregation (Aggrewell plates from StemCell Technologies) selected for its reputed ability to produce uniform sized EBs. Comparing the efficiency of aggregation and EB size uniformity for scraped and forced aggregation will allow an assessment of the suitability of the Aggrewell technique for reproducible and scalable production of EBs for retinal differentiation.

EB formation by manual scraping and spontaneous differentiation is both labour intensive and inefficient. Manual scraping requires highly trained operators to first identify good quality compact and undifferentiated stem cell colonies. Second, these colonies need to be manually excised by scraping into as uniform sized clumps as possible, with a sterile plastic Pasteur pipet. These stem cell clumps are subsequently cultured in suspension in low attachment culture dishes, where they spontaneously differentiate into EBs. Following EB formation, the micro-environment must provide appropriate nutrients in the medium and specific signalling cues from soluble factors to

support differentiation along the retinal developmental pathway, a topic discussed in more detail in chapter 4.

Manual scraping can cause cell death through mechanical force but also leaves many cells attached to the tissue culture plastic surface which are not subjected to the differentiation protocol (Heng et al. 2007). Manual scraping aims to dislodge stem cells from colonies as clumps, but a population of cells which are not scraped off as clumps are dissociated into single cell suspension. Without the addition of Rho Kinase Inhibitor (Y-27638) the stem cells in suspension are more likely to undergo apoptosis causing another source of waste in the differentiation protocol (Watanabe et al. 2007).

Cells not incorporated into EBs due to apoptosis or due to being suspended as single cells are responsible for the inefficiencies in the aggregation process and are characterized in this chapter. We report higher cell deaths, lower aggregation levels and higher numbers of unincorporated cells left to float away in the medium from manual scraping methods for EB production compared to forced aggregation.

The exclusion of large populations of stem cells from incorporation into EBs and therefore the differentiation process will necessarily impact negatively on the production yields of therapeutic cell types dependent on EB stage facilitated differentiation. The efficiency of the aggregation technique is therefore of interest to all EB stage dependent differentiation protocol developers, aiming for robust and consistent cell therapy manufacturing techniques.

The variable reproducibility of reported cell derivation and differentiation efficiencies from published protocols using scraped EBs, requires an analysis based on fundamental principles. Consequently in this chapter, mass balance calculations were employed to investigate the efficiency of the process of stem cell aggregation into EBs. The total number of initial cells available for aggregation, versus the numbers of cells left in suspension or dead following aggregation after 24 hours were calculated to illustrate advantages and disadvantages of both scraped and forced aggregation systems. Comparing the total number of cells available from the beginning with the total number of differentiated cells at the end of a given differentiation protocol should provide an indication of the efficiency of the method used and therefore provide a more robust and detailed depiction of the impact of aggregation efficiency on the bioprocesses in manufacturing therapeutic cells from pluripotent stem cells. Knowing

the efficiencies of the differentiation protocol should have valuable implications for development of leaner bioprocesses at industrial manufacturing scales.

### **3.1.1 Chapter aims and objectives**

The aim of this section was to characterise different EB formation techniques and determine the most efficient EB formation platform. This is an important first step in establishing a scalable differentiation protocol for stem cell derived products which need to differentiate through an EB like stage such as retinal photoreceptor precursor cells, the example differentiation protocol throughout this thesis. The specific objectives were:

- To compare the traditional scraped EB formation technique with forced aggregation using the Aggrewell technology.
- To measure the levels of cell losses and determine the cell yields associated with each technique.
- To calculate the impact of the aggregation technique on aggregation efficiency.
- To characterise both techniques in terms of their impact on EB size variability, pluripotency and differentiation.

## **3.2 Characterisation of EB Formation**

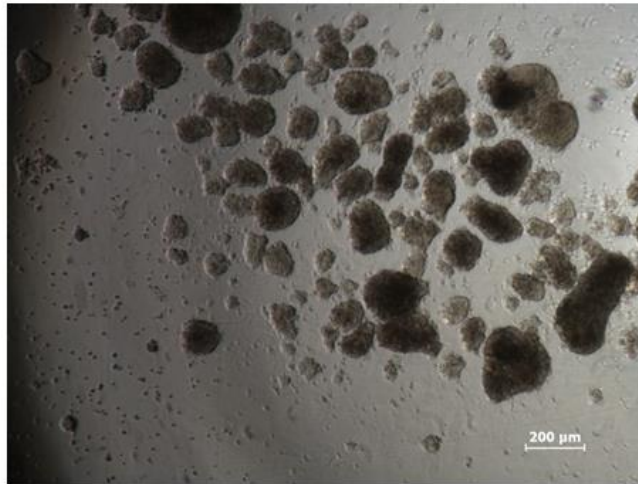
### **3.2.1 Forced aggregation is more efficient than scraped spontaneous aggregation.**

Forming EBs by manually scraping stem cell colonies led to the evaluation of Aggrewell plates (StemCell Technologies) a recent commercially available innovation for scalable aggregation of precise numbers of stem cells into EBs. The Aggrewell plates formed of PDMS microwells can be either 400µm or 800µm in diameter depending on the desired EB sizes to be manufactured. The company claims higher

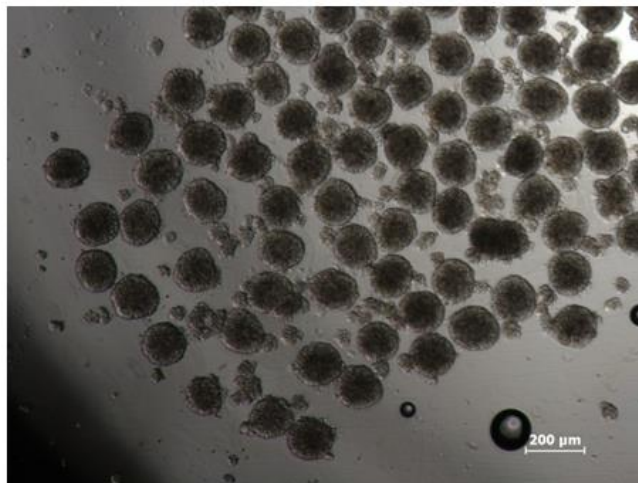
reproducibility of EB sizes but at the time of print they made no claims as the impact of this aggregation technique on cell viability or on the efficiency of the process. When comparing EBs made by manual scraping or using forced aggregation in Aggrewell plates, there is a stark difference in the resultant EBs.

By visual inspection EBs formed by manual scraping appear more heterogeneous in size and shape whilst those formed by forced aggregation are more homogenous as shown in the micrographs of EBs at 24 hours post aggregation in Figure 3.1a & b. In addition to the observed differences in EB uniformity between techniques there also appeared to be more single cells or visible cell debris in scraped EB cultures compared to their forced aggregate counterparts. Quantification of these visually observed initial findings for both methods involved calculating numbers of whole EBs produced from equal numbers of input cells in each technique to appreciate the yield of EBs from each technique. Cell numbers from digested EBs as well as live and dead cell counts from suspended cells in the medium surrounding EBs 24 hours post formation were also measured to calculate the efficiencies of each aggregation technique.

**A** Scraped



**B** Forced



**C**

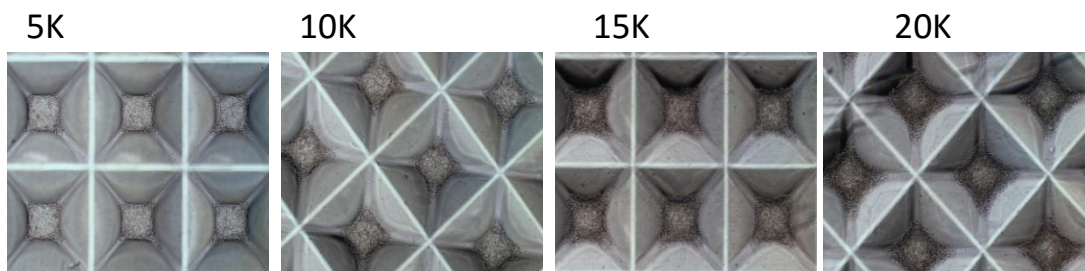


**Figure 3.1** Micrographs show stem cell aggregates at 24 hours. (A) Shows the aggregates formed by scraping or (B) by forced aggregation. (C) Shows how similar different numbers of stem cells appear in Aggrewwells of 800um diameters at day 0, for 5K cells/ well, 10K cells/ well, 15K cells/ well and 20K cells/ well.

### **3.2.2 The impact of aggregation technique on cell yield**

The efficiency of aggregation is usually calculated solely from the percentage of live cells incorporated into EBs. This measure does not take into account the number of cells available for aggregation at the beginning or the cells which are lost during the process of aggregation. In order to account for these losses, cell yields after 24 hours for both techniques were used to calculate the level of cell death and therefore waste associated with either spontaneous aggregation by manual scraping or forced aggregation. Figure 3.2 shows calculating the total percentage of live cells incorporated into EBs after 24 hours as a percentage of the number of cells available for EB formation at the start of the protocol provided a measure of viable cells available to continue differentiating within EBs. Figure 3.2 also shows more viable cells were found within aggregates from forced aggregation. In terms of cell yields alone, forced aggregation was found to be significantly more efficient than scraping by an order of over 3-fold ( $p < 0.05$ ).

### **3.2.3 Aggregation efficiency**

Samples of EBs in suspension at  $t=24$  hrs from the start of the aggregation stage and unincorporated single cells leftover from the aggregation process were analysed using a ViCell cell counter (Beckman Coulter) to determine numbers of live and dead cells per sample by the trypan blue dye exclusion method (see section 2.4.1). In order to calculate aggregation efficiency, the numbers of live and dead cells from samples of digested EBs and suspended unincorporated cells leftover after EB formation, were calculated as percentages of the starting population of input pluripotent stem cells.

To determine aggregate formation efficiency, aggregate formation protocols for scraped and forced aggregation were initiated with all iPSCs harvested from a single T25 flask of the same passage number each per experiment. The T25 flasks of each passage were derived from a single confluent T25 flask of hiPSCs split 1:3 every 4 days on reaching 70% confluency and cultured in parallel. In these experiments, this consistent passaging ratio allowed an assumption that differences in starting hiPSC cell

numbers were negligible between T25 flasks of the same passage number. This assumption was necessary because it was not possible to dissociate the hiPSC colonies required for scraped aggregation before scraping them into EBs.

A motivating factor for investigating aggregation efficiency and the use of forced aggregation to control aggregate size, was to try to reduce the variability introduced in stem cell differentiation cultures by the unknown numbers of cells per EB in scraped EB formation. To illustrate, if cell numbers making up individual EBs are ignored and only population level cell numbers are used, figure 3.2 A shows that average total numbers of cells making up EBs then appears misleadingly similar across techniques (Scraped: 313 cells/EB Standard deviation SD=72.63; Forced: 357 cells/EB SD=4253 with no statistically significant differences observed between the average number of cells per EB).

In order to investigate the efficiency of EB formation analysis of the constituent cell populations, similar numbers of input hiPSCs per T25 flask in each aggregation experiment were assumed to permit an evaluation of the aggregation efficiency between scraped and forced aggregation. Figure 3.3 shows the percentage of unincorporated live and dead cells within the medium surrounding EBs and those obtained by digesting EBs. Figure 3.3 shows aggregation efficiency varied significantly between techniques in both the MSU001 and BJIPS cell lines (Figure 3.3A & B). For example, in the MSU001 cell line, scraping resulted in significantly fewer cells incorporated into EBs and many more cells left dead in the medium at 24 hours. From forced aggregation the corresponding unincorporated, consisted of almost equal numbers of live and dead cells. Overall for the MSU001 hiPSCs, compared to scraping forced aggregation resulted in 5 fold ( $p < 0.05$ ) fewer unincorporated dead cells in the medium at 24 hours and 3 fold ( $p < 0.05$ ) more live cells within EBs (Figure 3.3A).

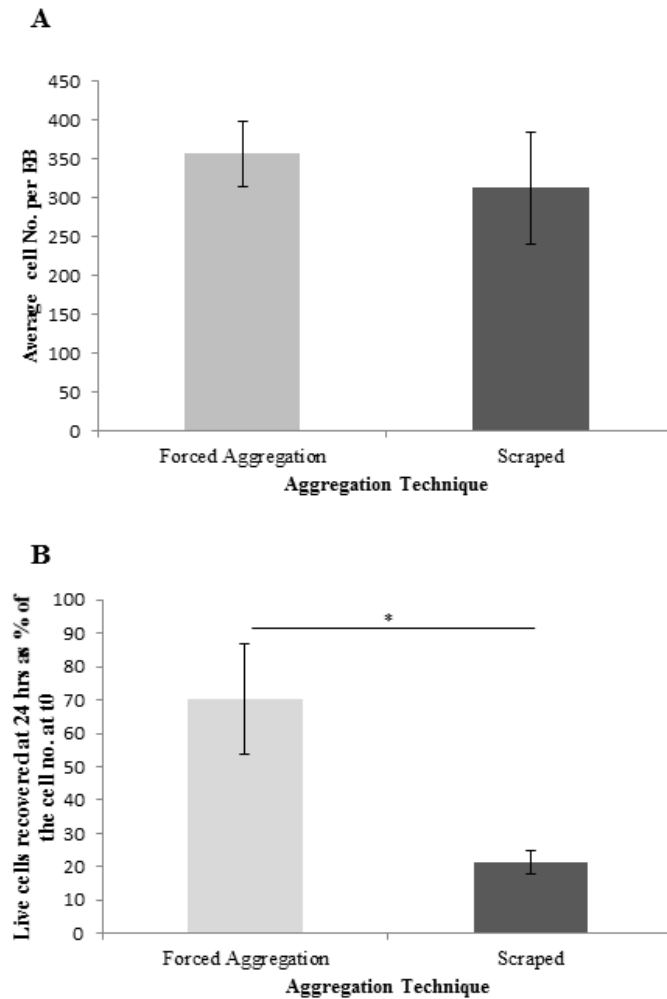


**Figure 3.2 (A)** Average numbers of cells per EB calculated from total numbers EBs and total numbers of cells from digested EBs from scraped or forced aggregation without considering input cell population counts. Average numbers of cells per EB between aggregation techniques appear insignificant as a result. Total number of cells from EB digests / number of EBs after 24 hours. Data are means  $\pm$  Standard deviation, n=3. **(B)** Graph shows the percentage of live cells after 24 hours as a portion of the input number of pre-aggregation IPS cells for scraped and forced aggregation. Data are from means  $\pm$  Standard deviation, n=3. Students 2 paired T-test  $p < 0.005$ .

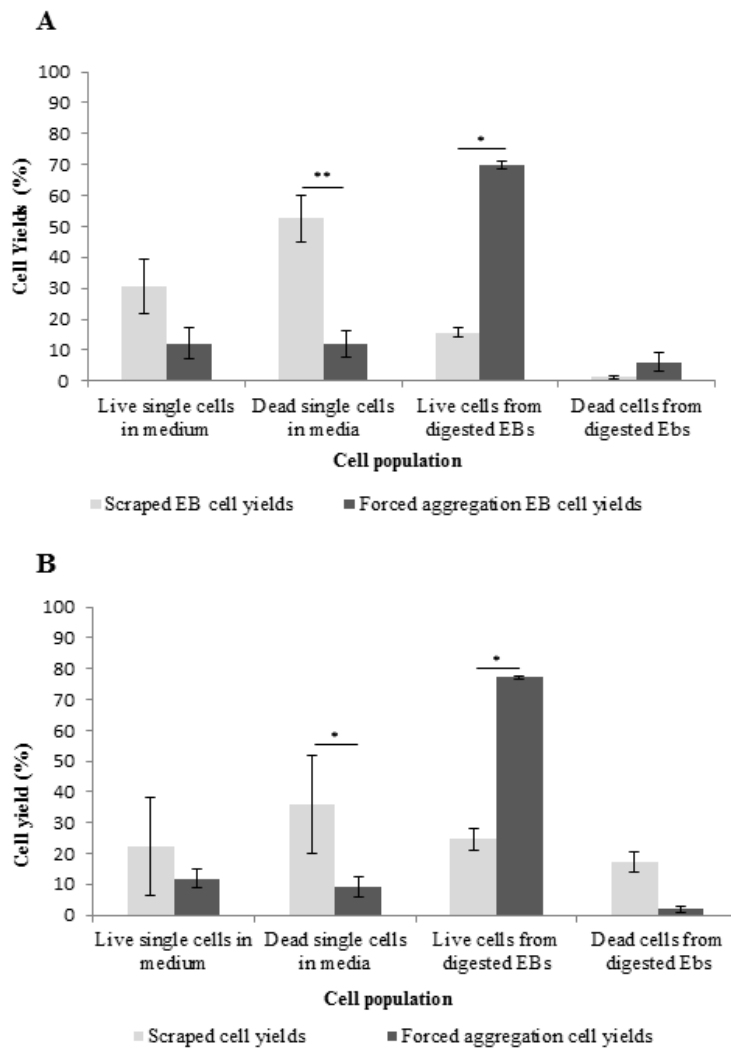


**Figure 3.3** Live and dead cell counts from aggregation by scraping or by forced aggregation for MSU001 IPS (**A**) and BJ IPS (**B**) cells. 24 hours post aggregation cell numbers of live and dead cells from unincorporated cells in the medium and digested EBs were counted using a Vi-cell counter (Beckman Coulter). Values are reported as mean  $\pm$  SD and ANOVA single factor analysis performed on data for significant values of \* $p < 0.05$  and \*\* $p < 0.001$ .

### 3.3 The impact of aggregation technique on EB size

The impact of EB size on differentiation trajectories has been previously investigated to size controlled EBs promote biases in development towards specific cell lineages (Bauwens et al. 2008; Niebruegge et al. 2009). To measure the impact of EB formation technique on the size of the resulting aggregates, EBs were imaged by light microscopy after 3 days in suspension culture. Average EB diameters were measured for both scraped and forced aggregation EBs from the images by taking three length measurements as described in section 2.4.2. The triplicate measurements from each EB were averaged to obtain average EB size measurements. Figure 3.4 shows that as expected and in agreement with the manufacturers claims, EBs formed by forced aggregation in Aggrewell plates displayed greater control over EB size than those formed by the scraping and spontaneous differentiation technique (Figures 3.4 and 3.5).

Figures 3.4 and 3.5 show forced aggregation demonstrated consistent control over EB size in stark contrast to highly heterogeneous scraped EBs. EBs formed by manual scraping varied greatly in diameter with a broad range between 25- 150 $\mu\text{m}$  (mean= 77.65 $\mu\text{m}$  standard deviation (SD) = 48.33) (Figure 1B). In contrast mean diameters for EBs formed by forced aggregation were slightly larger (101.43  $\mu\text{m}$ ) and far more consistent as reflected by the lower SD of 24.94. The improved regulation of EB size can be directly attributed to the precise starting number of cells in each microwell ready to form each EB (Dang et al. 2002).

After 48 hours EB diameter measurements were taken again for both scraped EBs and forced aggregation EBs. As expected the average EB diameters were larger for both techniques scraped EBs had average diameters of 112.45  $\mu\text{m}$  SD=15.57 and forced aggregation EBs averaged diameters of 124.06  $\mu\text{m}$  SD=14.31. The changes in EB sizes between t=24hrs and t=48hrs in this experiment can be attributed to growing EBs as well as aggregation of smaller sized EBs. The EB volumes were also calculated for both the 24 and 48 hr EB populations. Using the average EB sizes as a proxy for EB diameter and assuming EBs to be spherical the average EB volumes for scraped EBs at 24 hrs was 245,145  $\mu\text{m}^3$  whilst the average volume of forced aggregation EBs was 546,383  $\mu\text{m}^3$  representing forced aggregate EBs to have larger volumes by 301,239

$\mu\text{m}^3$  on average. The same calculations performed for the 48 hour time points shows the average scraped EB volume was  $744,520 \mu\text{m}^3$  against  $999,755 \mu\text{m}^3$  for forced aggregation EBs, representing a difference of  $255,234 \mu\text{m}^3$ . The reduced difference in EB volumes between 24 and 48 hrs for scraped versus forced aggregation EBs ( $301,239 \mu\text{m}^3$  vs  $255,234 \mu\text{m}^3$ ) may indicate differences in growth rates for EBs with different starting sizes. This hypothesis is supported by the greater delta EB volumes calculated for scraped EBs between 24 and 48 hours against forced aggregation EBs ( $499,376 \mu\text{m}^3$  vs  $453,372 \mu\text{m}^3$ ) however; the assumption that all EBs are spherical is a caveat which must be taken into account in drawing any strong conclusions from these calculations (Table 3.1).

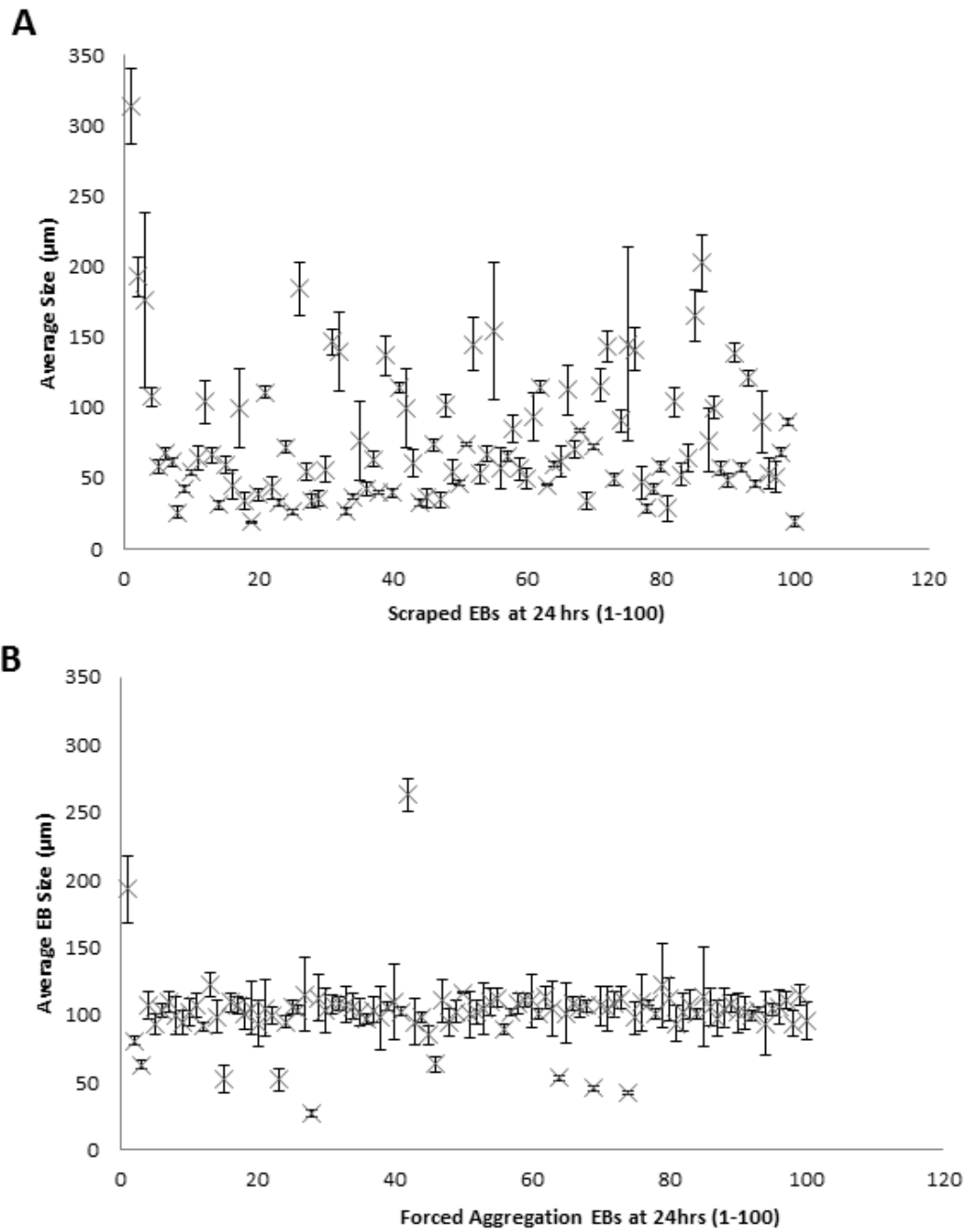


**Figure 3.4** Size distribution plots show the variation in size per EB between techniques (A) scraped and (B) forced aggregation. Sizes are taken as averages of 3 length measurements per EB (transverse, dorso-ventral and diagonal) at 24 hours post aggregation. EBs were cultured from MSU001 IPS cells.

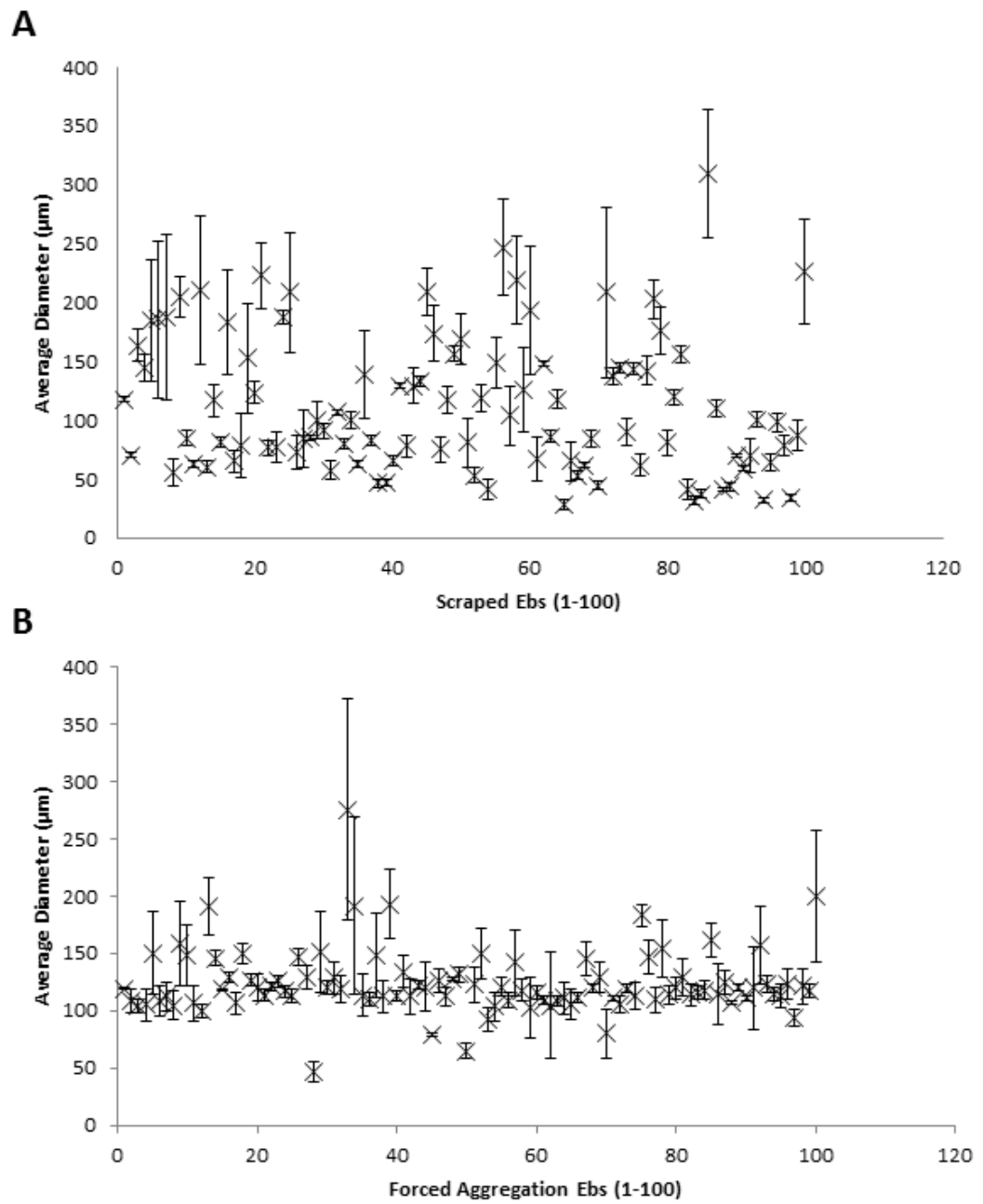


**Figure 3.5** Size distribution plots show the variation in size per EB between techniques (A) scraped and (B) forced aggregation. Sizes are taken as averages of 3 length measurements per EB (transverse, dorso-ventral and diagonal) taken at 48 hours post aggregation. EBs were cultured from MSU001 IPS cells.

	Scraped		Forced Aggregation	
	24 hrs	48 hrs	24 hrs	48 hrs
EB diameter ( $\mu\text{m}$ )	77.65	112.45	101.43	124.06
Volume $V=4/3\pi r^3$ (ml)	$2.5 \times 10^{-8}$	$7.4 \times 10^{-8}$	$5.5 \times 10^{-8}$	$10.0 \times 10^{-7}$
Delta V (ml) 24-48 hrs	$5.0 \times 10^{-8}$		$4.5 \times 10^{-8}$	
Delta V (ml) Scraped vs Forced Aggregation at 24 hrs	$3.0 \times 10^{-8}$			
Delta V (ml) Scraped vs Forced Aggregation at 48 hrs	$2.6 \times 10^{-8}$			

**Table 3.1** EB volume calculations at 24 hrs and 48 hrs. Calculated using measurements for average EB size as a proxy for EB diameter, EBs are assumed to be spherical for the calculations.

### 3.4 Pluripotency and differentiation capacity of EBs

The EBs formed of pluripotent stem cell colonies (Figures 3.6 and 3.7) remain pluripotent for longer than the first 24 hours post aggregation. Newly formed EBs at 24 hours are not expected to have differentiated and should express pluripotency markers (Pekkanen-Mattila et al. 2010). In order to determine whether the formed EBs were still normally pluripotent, 24 hours old EBs were dehydrated in sucrose before cryopreservation in cryo-preservant OCT at  $-80^{\circ}\text{C}$ . The EBs were cryosectioned using a cryotome before immunochemical labelling to show expression of pluripotency markers SSEA4 and Oct4 (Figures 3.8).

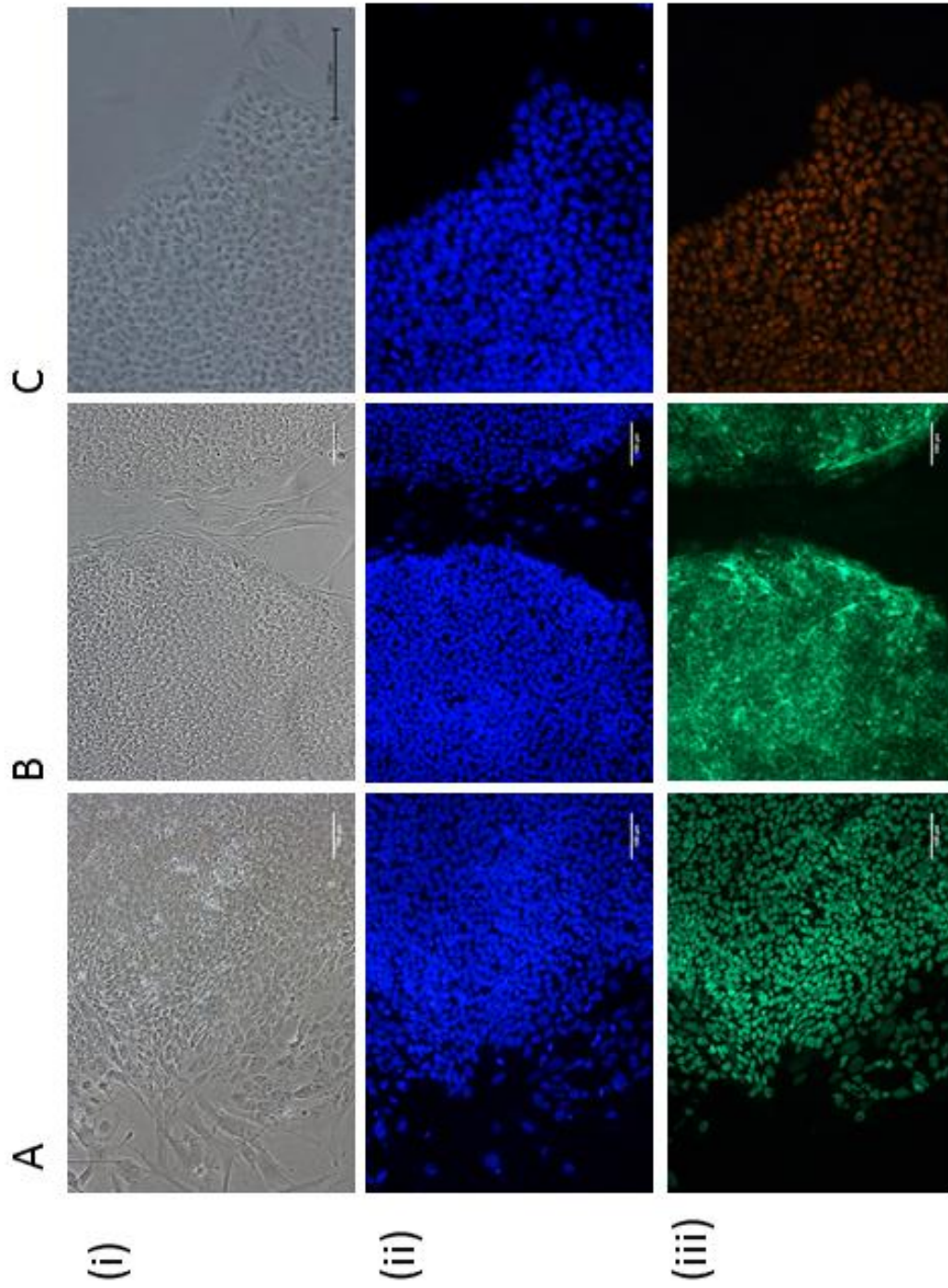
### 3.5 Differentiation capacity of EBs

To assess the differentiation potential of the resulting EBs from each formation technique, they were differentiated in pro-retinal conditioned medium for 3 days and

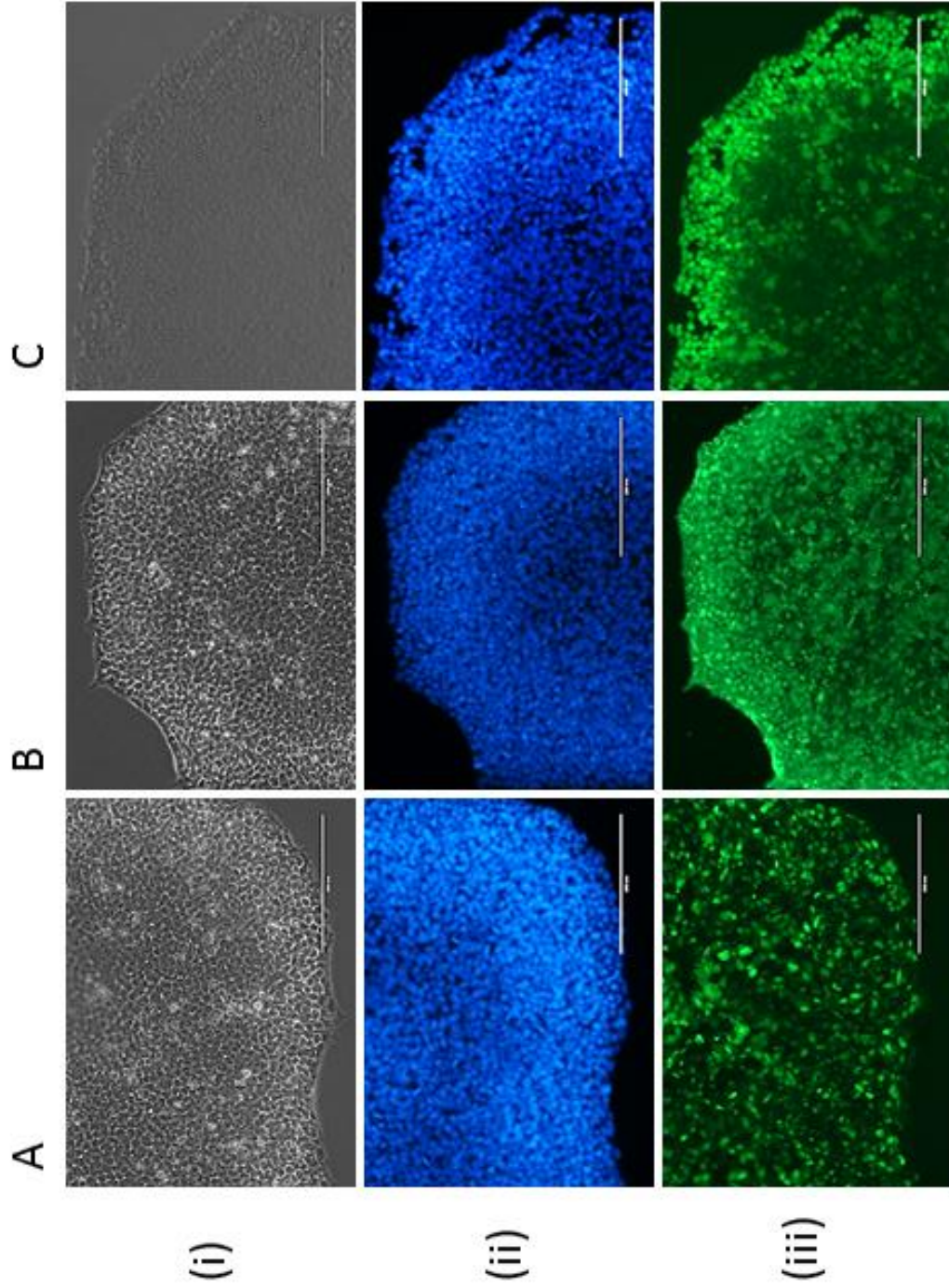
analysed for retinal gene expression by QPCR analysis. Differentiation was carried out under typical cell culture conditions (5% CO<sub>2</sub> (v/v) incubator at 37 °C and 90% humidity) EBs were left to grow in low attachment dishes (Nunc) with a full medium change at day 2. Figure 3.9 shows that at day 3 of differentiation the EBs were harvested and QPCR analysis showed that EBs from both conditions had comparable expression profiles of each of the retinal markers investigated. Consistent with the work of Mellough et al both scraped and Aggrewell EBs co-expressed POU5F1 with retinal markers at this early stage (Mellough et al. 2012). Interestingly we found the scraped EBs only out-performed the controlled size EBs for Pax 6 expression (a master transcription factor for retinal development) when compared to the smallest sized 1K cells/ EBs (Hsieh & Yang 2009; Larsen et al. 2009).

### **3.6 Summary**

In summary, using Aggrewell plates for forming controlled size EBs made it possible to increase the efficiency of aggregation and improve the yield of cells incorporated into EBs by >3 fold. Using forced aggregation also afforded greater control over EB size. The increased homogeneity in EB size will be of particular use in attempts to synchronize EB development towards retinal cell lineages as discussed in chapter 4. We found that the use of forced aggregation did not adversely affect the cells in terms of viability nor did it impair their ability to differentiate towards retinal lineages. The finding that scraped EBs displayed higher expression of Pax 6 was particularly interesting and prompted investigation into the impact of EB size on retinal differentiation, which was the major difference between the scraped and forced aggregation EBs. Together these findings show that using scraped EB formation is wasteful and therefore inefficient as a system for future scale-up. The use of forced aggregation addressed the issues of low yields and poor size control associated with scraped EB formation but appropriate sizes of EBs need to be selected to improve retinal differentiation propensity.

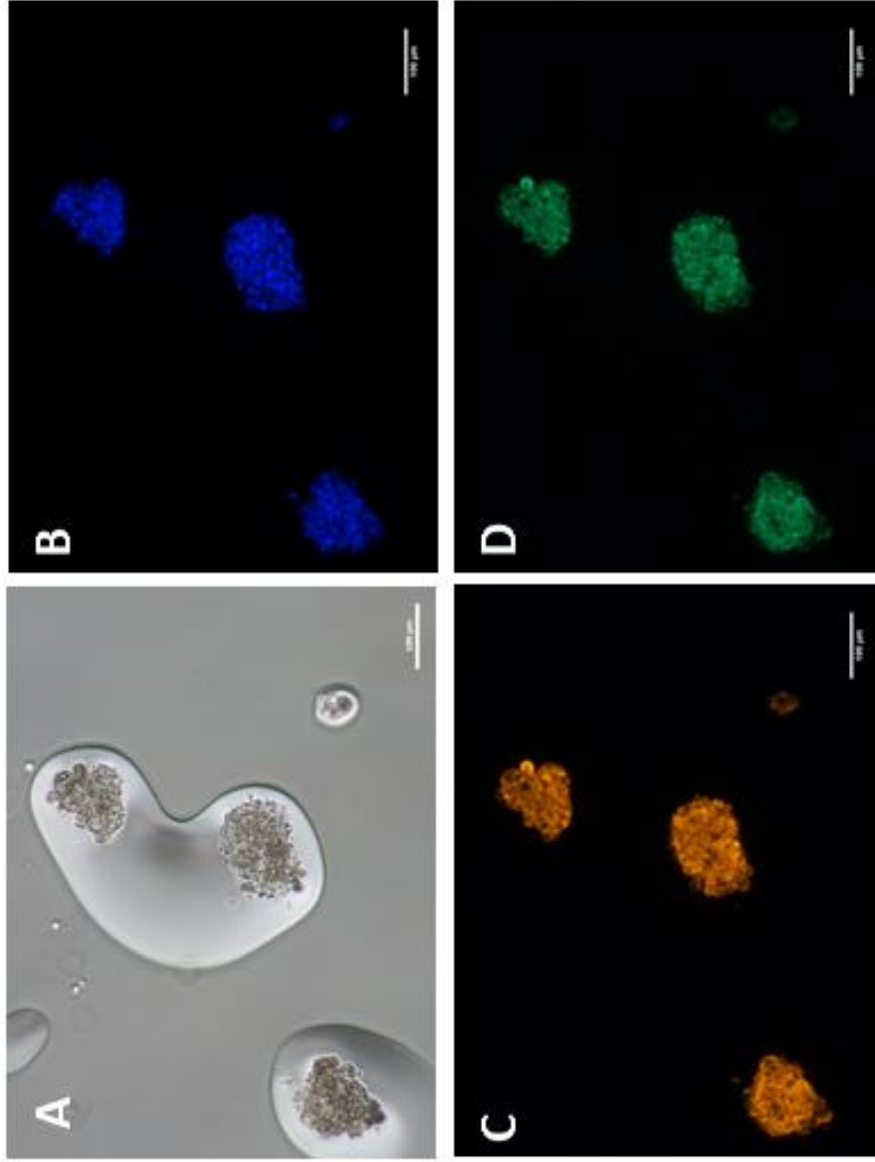


**Figure 3.6** Immunocytochemistry of MSU001 IPS cell colonies stained for the expression of (A) Tra160, (B) SSEA4 & (C) Oct4, (i) Phase contrast images (ii) nuclear marker for DAPI and pluripotency markers (iii). Images were taken at 20X magnification using a Nikon Phase and Fluorescence Microscope. Scale bars = 100µm.



**Figure 3.7** Immunocytochemistry of BJ IPS cell colonies stained for the expression of (A) Tra160, (B) SSEA4 & (C) Oct4, (i) Phase contrast images (ii) nuclear marker for DAPI and pluripotency markers (iii). Images were taken at 20X magnification using an EvosPhase and Fluorescence Microscope (Life Technologies). Scale bars = 200µm.

**Figure 3.8** Fluorescent micrographs of stem cell aggregates at 24 hours. Immunocytochemical labelling shows small stem cell aggregate cryosections (~100cells/EB) 12µm per section. Images show (A) phase contrast, (B) DAPI (blue), (C) P0u5F1 (orange) and (D) SSEA4 (green). Images were taken at 20x magnification with a Nikon fluorescent microscope. Scale bar=100µm.



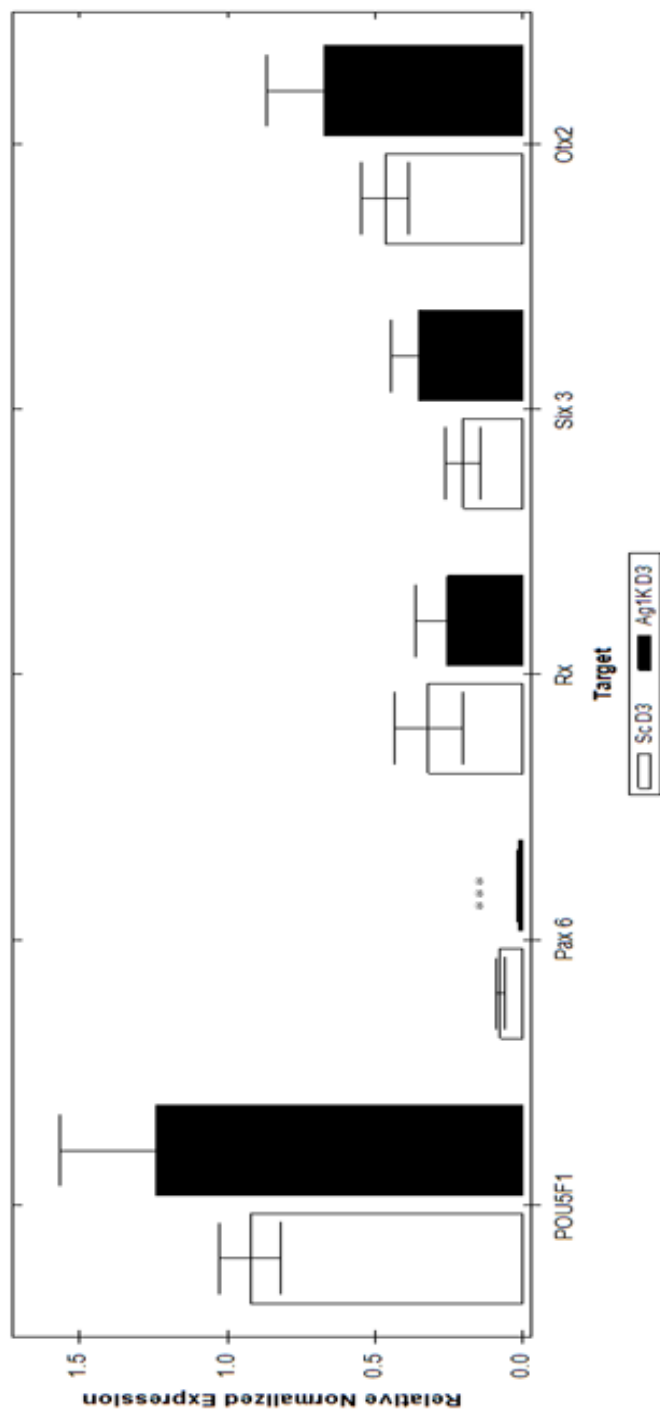


**Figure 3.9** Relative expression of pluripotency marker POU5F1 and early retinal transcription factor genes Pax 6, Rx, Otx2 and Six3 at day 3 in MSU001 EBs formed by scraped (ScD3) or forced aggregation (Ag1KD3) with 1000 cells/EB at day 3. One way ANOVA analyses of gene expression levels in scraped EBs against forced aggregation EBs are shown. (\* $p < 0.05$ , \*\* $p < 0.01$ , \*\*\* $p < 0.001$ ).

## **Chapter 4 – Establishing an orbitally shaken culture protocol to initiate retinal differentiation**

### **4.1 Introduction & Aims**

In this chapter an attempt was made to introduce the potential for scalability to the retinal differentiation protocol. This was done by introducing orbital shaking to the suspension cultures of EBs whilst excluding the impact of a potential source of variability due to undefined quantities of xenogeneic ingredients found in Matrigel, commonly used in standard protocols for retinal differentiation (Table 1.4).

**The need for future-proof manufacturing strategies:** Standard techniques for retinal differentiation use 2D adherent culture protocols reliant on open and manual processing techniques. Manual processing techniques such as scraping stem cell colonies from tissue culture for EB formation are particularly labour-intensive and are therefore less amenable to scale up. The commonly used protocols for retinal differentiation frequently include the use of undefined components (Table 1.4). Xenogeneic ingredients such as serum and the undefined matrix substrate Matrigel incorporated in these protocols leave the systems prone to contamination as well as batch quality variability arising from the numerous unquantified components they are comprised of (Davie et al. 2012). As a result such protocols are less suitable to manufacturing scales beyond the laboratory research setting.

Future therapeutic cell production strategies for allogeneic or autologous cell therapies will require closed, controlled, scalable and industrialized processes to deliver on the promise of the cell therapy industry. Cell manufacturing processes will need to be agile as requirements will vary greatly according to optimal cell dose requirements. Annual production requirements could easily reach into trillions as current clinical trials explore doses of 100s of millions of cells and above per patient (van den Bos et al. 2013). Translating variable 2D adherent and labour intensive protocols for cell differentiation into more controlled 3D suspension culture systems, presents an opportunity to improve the potential scalability of laboratory research and provide flexibility for future development of manufacturing processes.

**Practical considerations before setting up orbital shaking experiments:** The retinal differentiation protocol used throughout our work already involves a suspension phase during the first 3 days post EB formation so, adapting the whole culture protocol to a suspension system in light of the work of others seemed plausible. Orbital shaking culture in 24-well microwell plates was expected to provide better mixing of the costly nutrients, growth factors, signalling molecules and morphogens supplemented to the system and those produced by differentiating EBs within, than static conditions.

Adaptation from an adherent to a suspension system together with the improved mixing expected from orbital shaking could eliminate dependency on the undefined matrix substrate Matrigel. By adapting the process from 2D to a 3D culture, the EBs in suspension may no longer require Matrigel as a substrate to adhere to. Removing Matrigel would reduce the impact of many unknown and unquantified factors, since its composition is proprietary with over 600 ingredients at undisclosed concentrations (Polykandriotis et al. 2008).

To test the hypothesis that retinal differentiation is possible in an orbital shaken culture system we first needed to shortlist potential EB sizes for their capacity to differentiate along a retinal trajectory. Secondly these EBs were ranked according to size and their ability to survive and endure orbital shaking culture as intact aggregates for 7 days. To find suitable, controlled size EBs for retinal differentiation we assessed their ability to up-regulate expression of early eye field transcription factor genes, after 3 days of suspension culture in retinal differentiation medium. EBs of varying sizes formed by forced or scraped aggregation techniques were treated equally and analysed for changes in retinal gene expression in parallel by QPCR at the end of the 3 day culture period.

### **4.1.1 Chapter Aims and Objectives**

In this chapter the aims are to:

- Establish a range of EB sizes able to withstand orbital shaking conditions without being dispersed into the medium as single cells or clumping together to be able to establish orbital shaking cultures.
- Test the hypothesis that retinal differentiation can be initiated with IPS cell derived EBs in an orbital shaken culture system without the use of Matrigel.
- To characterize the impact of EB size on the onset of retinal differentiation in suspension culture.
- To determine and characterize a suitable orbital shaking frequency for EB cultures

### **4.2 Establishing a range of viable EB sizes permissive to retinal differentiation in suspension culture**

In order to identify ideal EB sizes suitable for higher throughput studies, they were ranked according to practical considerations. Ease of EB handling was considered important to ensure EBs did not spend too long outside normal tissue culture conditions, during transfer from culture plates or whilst medium was changed. Consequently, it was important that EBs could easily be seen by eye for rapid counting and simple manipulation in assessing their suitability for the higher throughput experiments. Forced aggregation as characterised in chapter 3 provided control over input EB size compared to scraped aggregation. Consequently forced aggregation was adopted for subsequent experiments to form uniform sized EBs reproducibly. Uniform sized EBs allow a comparison of different sized EBs for their suitability to tissue culture, before being assessed for potential retinal differentiation experiments and higher throughput studies to investigate a suitable orbital shaking frequency for retinal differentiation.

The ideal system for EB manufacture is required to be both practical in an academic laboratory setting and efficient, to produce enough EBs for future optimisation experiments (discussed in chapter 5) routinely and with minimal waste. The first EBs to be excluded from further experiments were EBs formed of 1000 cells each. These small sized EBs (~100µm diameters) were difficult to see by eye for quick counting and therefore not easy to manipulate for higher throughput experiments. Taking into consideration the recent work of Sasai's group, in which successful suspension culture for retinal differentiation was possible with larger EBs made of 9K cells/EB helped provide support for focusing experiments on larger EBs (Eiraku et al. 2011). Consequently a range of EB sizes: 5K, 10K, 15K and 20K cells/EB is assessed for amenability to scalable tissue culture techniques.

In agreement with the reproducible EB sizes formed by forced aggregation as characterised in chapter 3, Figure 4.1 shows IPS cells seeded into Aggrewells at day 0, before the 24 hours of incubation required to form EBs after 24 hours (shown alongside them) for the selected sizes. The representative images in the micrographs illustrate the expected uniformity of EB shape and diameters as assured by the manufacturers and characterised in chapter 3. The suitability of different sized EBs as screened by eye for rapid assessment of EB uniformity and size, suggested any of these EB sizes could have been appropriate for further experiments. Another key factor for consideration in addition to EB size however, was the practical feasibility of using larger EBs, which require more input hiPSC to form.

The numbers of hiPS cells required to produce different sized EBs were used to calculate theoretical cell number requirements per experiment are represented in Tables 4.1 and 4.2. The average number for hiPS cells harvested per T25 flask was derived from routine cell number calculations described in chapter 3 which showed an average cell yield of  $6 \times 10^6$  cells/T25 flask. Using the cell number requirements provided in the Aggrewell protocol, it was possible to calculate numbers of hiPSC required to produce each EB size and use these to calculate total cell numbers required to complete one full experiment. Each experiment required sufficient material for 3 analytical assays (immunohistochemistry, QPCR and an extra well for contingency repeat experiments) for 4 time points (days 3,10,15 and 21) as discussed in Chapter 5.

The theoretical calculations helped exclude the 15K and 20K EB sizes from shaking speed selection studies due to the impractically large numbers of cells ( $6.4 \times 10^7$  and  $8.6 \times 10^7$  cells) required to complete a full experiment. The 5K and 10K sized EBs require  $1.5 \times 10^6$  and  $3 \times 10^6$  cells per Aggrewell respectively, numbers sufficient for triplicate experiments to be performed from the cells produced by 2 to 3 T25 flasks ( $< 18 \times 10^6$  cells in total). Consequently the 5K and 10K EB sizes were found to be the most practical candidates for further experiments to determine the feasible shaking speeds for orbital shaken culture. Furthermore the numbers of cells produced and required to complete experiments using 5K and 10K cells/EB ensured it was possible to produce sufficiently powered data from further differentiation experiments in order to assess the influence of size on retinal differentiation in triplicate for 3 time points over 21 days of culture.

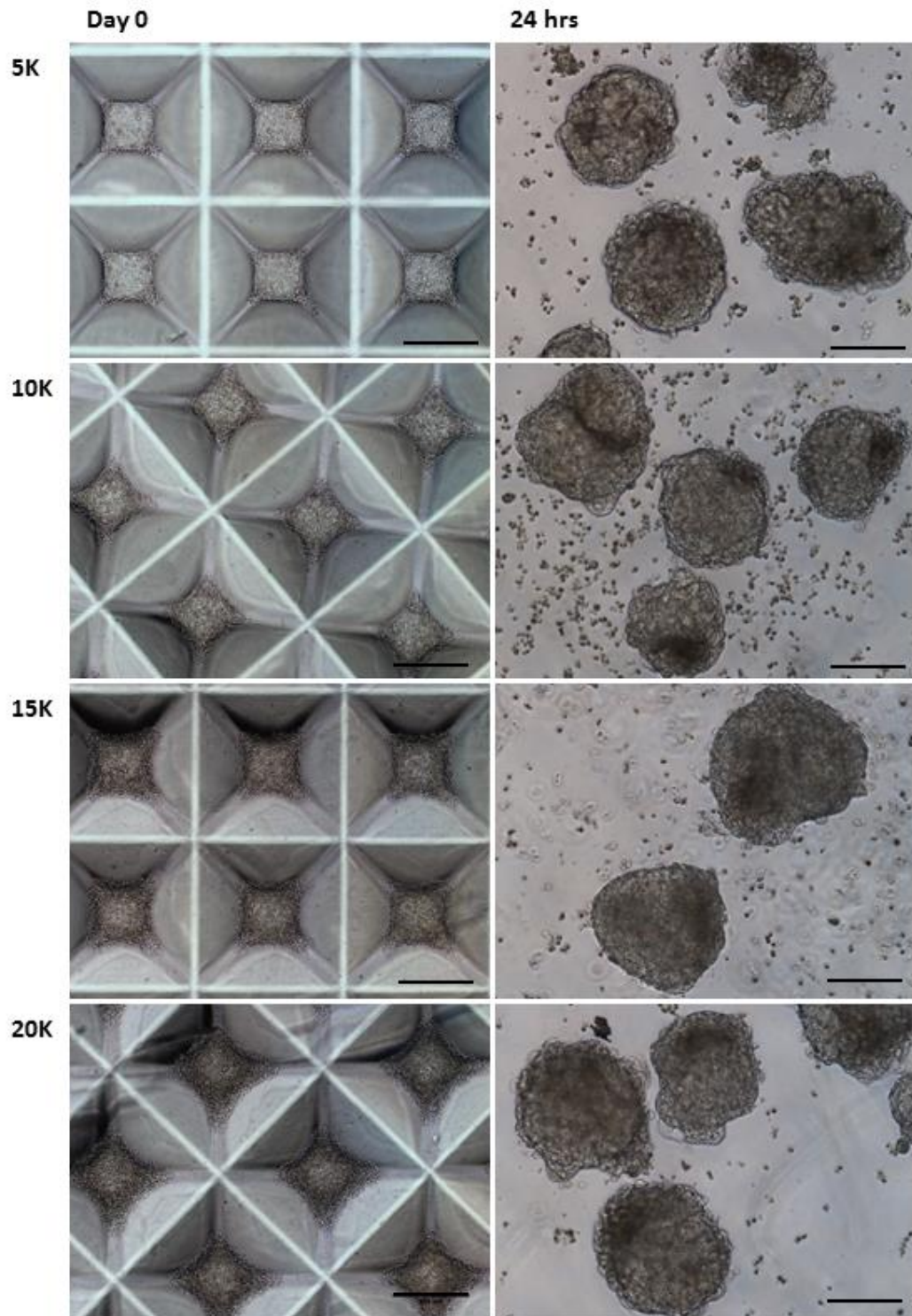


**Figure 4.1** Micrographs of IPS cells seeded into Aggrewells at day 0 to form EBs made from 5,000, 10,000, 15,000 and 20,000 cells shown beside them to the right after 24 hours. A Nikon phase and fluorescence microscope was used to create all images with 4x magnification at day 0 and 10x at 24 hours. Scale bars = 400 $\mu$ m

EB Size (no. cells per EB)	Required no. cells per well	Required no. T25 IPS flasks yielding $6 \times 10^6$	Resulting number of EBs
1000	1.E+06	0.2	1200
5000	2.E+06	0.25	300
10000	3.E+06	0.5	300
15000	5.E+06	0.75	300
20000	6.E+06	1	300

**Table 4.1** Total cell numbers required to form different sized EBs using the Aggrewell protocol.

No. Cells per EB	EBs per well (24 well plate)	No. EBs per time point (n=3)	Total no. EBs for 4 time points	Total no. EBs for 3 assays per expt.	Total Aggrewells per expt.	Total no. cells per expt.	Total no. T25 flasks yielding $6 \times 10^6$ cells per expt.
1000	40	120	1440	4320	14.4	1.73E+07	2.88
5000	40	120	1440	4320	14.4	2.16E+07	3.6
10000	40	120	1440	4320	14.4	4.32E+07	7.2
15000	40	120	1440	4320	14.4	6.48E+07	10.8
20000	40	120	1440	4320	14.4	8.64E+07	14.4

**Table 4.2** Total cell numbers required per EB size calculated for numbers of experiments taking into account material required for analysis in triplicate at 4 different time points with 3 assays (QPCR, immunohistochemistry and cell quantification. One experiment

### **4.3 Selection of orbital shaking frequencies for EB culture**

To determine orbital shaking speeds which may support EB survival as separate entities for longer term cultures, EBs formed of 5K and 10K cells were cultured in orbital shaking suspension for up to 7 days. EBs were assessed daily depending on how long it took for them to dissolve into the medium or clump into large aggregates. Daily assessment for survival or disaggregation of EBs into the medium was carried out rapidly by visual inspection.

No previous reports describe retinal differentiation from human induced pluripotent stem cell derived EBs in orbital shaken cultures. Consequently there was no directly relevant precedent for optimal shaking speeds with our cell culture system. Therefore in order to find a range of shaking speeds for empirical testing, a combination of speeds from reports for orbital shaking cultures of murine stem cell cultures were used albeit from different vessel geometries. Sargent et al.2010, reported that between orbital shaking speeds of 20 and 60 rpm in 100mm bacterial grade polystyrene Petri dishes, average EB area distributions decreased with increasing speed, indicating improved homogeneity of the EB sizes at higher speeds in their cultures. Additionally Sargent et al., 2010 report increased cell yields from EBs shaken between 40 and 60 rpm, providing the rationale to start testing for permissive shaking speeds beyond 50 rpm the midpoint between 40 and 60 rpm. In our experiments the search for a permissive shaking speed to support hiPSC derived EBs in shaking culture to an upper shaking speed of 240 rpm. This speed selected with reference to another murine stem cell differentiation culture using this shaking speed for neural stem cell differentiation to oligonendrocytes in T75cm<sup>2</sup> tissue culture flasks (Sher et al. 2012).

The impact of different shaking frequencies on EB morphology were assessed over 7 days of orbital shaken culture to provide an indication of the potential longevity of the EBs in orbital shaking culture. Slower speeds, such as 50rpm resulted in agglomeration of EBs into large clumps while faster speeds, such as 150rpm resulted in their dissolution into the medium. At a speed of 120rpm EBs were able to survive as individual entities over the 7 day culture period without showing signs of deterioration. Representative images in Figures 4.2A and 4.2B show variation in EB morphology with orbital shaking speed.

Alongside the empirical determination of suitable shaking speeds able to support EB cultures by iterative experiments, the influence of shaking speeds on the liquid mixing was also theoretically investigated. Predicted mixing speeds were calculated to determine the likely critical shaking speeds which define the transition between laminar and turbulent flow regimes under our culture conditions using the previously reported formula in (Weheliye et al. 2012b):

$$\frac{h}{d_i} = a_o \left( \frac{d_i}{d_o} \right)^{0.5} Fr_{d_o} \quad (1)$$

and culture parameters in Table 4.2. While the calculations supported a narrowing of the potential shaking frequencies to between N=115 and 140 rpm, finding the suitable shaking speed of 120rpm remained a mostly iterative empirical process.

### 4.3.1 Determination of the critical shaking speed and flow regime

It was possible to derive a critical Froude number and a range of critical shaking speeds ( $N_{Cr}$ ) where flow transition occur at 115rpm and 140rpm for the minimal and maximal working volumes respectively (see Table 4.3 for details of dimensions, volumes, constants and determined values). Theoretical calculations using the vessel dimensions, shaker diameter, working volume (table 4.3) with equation (1) above from (Weheliye et al. 2012a) suggested the empirically determined permissible rotational frequency of 120rpm, falls into a turbulent flow regime which should be evidenced by visible waves at the surface of the medium in each well (Weheliye et al. 2012a). However, it should be noted that it was only possible to calculate approximate values due to differences in the inner diameters between the vessels and a  $d_o/d_i > 0.6$  in this report compared to a  $d_o/d_i$  between 0.2 and 0.5 in (Weheliye et al. 2012a).

In the absence phase resolved image velocimetry (PIV) application, the lack of clearly visible waves at the medium surface under these conditions suggested that the medium and EBs may have been in a transitional flow regime. During the calculations for deriving critical Froude numbers and critical shaking speeds, the constant value for viscosity ( $a_o$ ) was the value determined for water 1.4 as recommended in (Weheliye et al. 2012a). Though retinal differentiation medium appears to be very similar to water

in its viscosity, the exact viscosity was not determined here and actual differences may help account for some of the variation observed. Additionally the most obvious variation would be the addition of EBs in the present system whose volumes may be considered insignificant from the values calculated in Table 3.1.

Differences in the well geometry parameters between our culture vessels and the two bioreactors vessels (inner diameters of 10cm and 13cm) used for the calculations in Weheliye et al. 2012 could also help explain the variation between the expected and observed flow regimes in this report. In this report observations lacked waves and though a flat liquid surface with an elliptical shape during orbital rotation at 120rpm may be subjectively visible it is slight and would need confirmation using PIV (Appendix1). Though the images in Appendix 1 are not definitive enough to claim the presence of an elliptical shape the result of a 3 minute mixing time and the lack of complex waves suggest that the fluid flow was in-phase under these operating conditions (Weheliye et al. 2012a).

To investigate the potential influence of the introduction the additional volume of the EBs into the system, expected EB volumes were calculated for EBs made of 5K and 10K cells per EB by forced aggregation at day 3 of culture. Day 3 EBs were selected as this is the time point shaking is initiated in the retinal differentiation protocol for the experiments in this report. Average EB sizes were used as a proxy for EB diameters to calculate EB volumes and surprisingly by day 3 the EB diameters were very similar for both the 5K (297.82  $\mu\text{m}$  SD 60.8) and 10K (295.23  $\mu\text{m}$  SD 64.54) EBs as depicted in the similar profiles of the size distributions of both 5K and 10K EBs at day 3 in Figure 4.3. Consequently expected average volumes calculated according to the formula:  $\text{Volume } V = \frac{4}{3}\pi r^3$  using the average EB diameters also showed great similarity ( $V = 13.8 \times 10^{-6}$  ml for 5K EBs and  $V = 13.4 \times 10^{-6}$  ml for 10K EBs). Importantly the relatively small volumes of the EBs are unlikely to account for the absence of expected wave forms at the liquid surface from the theoretical calculations and further investigations to understand the changes in the liquid viscosity which can alter the power required to break the surface tension of the fluid in the wells during the culture period would form potential future work (Buchs et al. 2001).

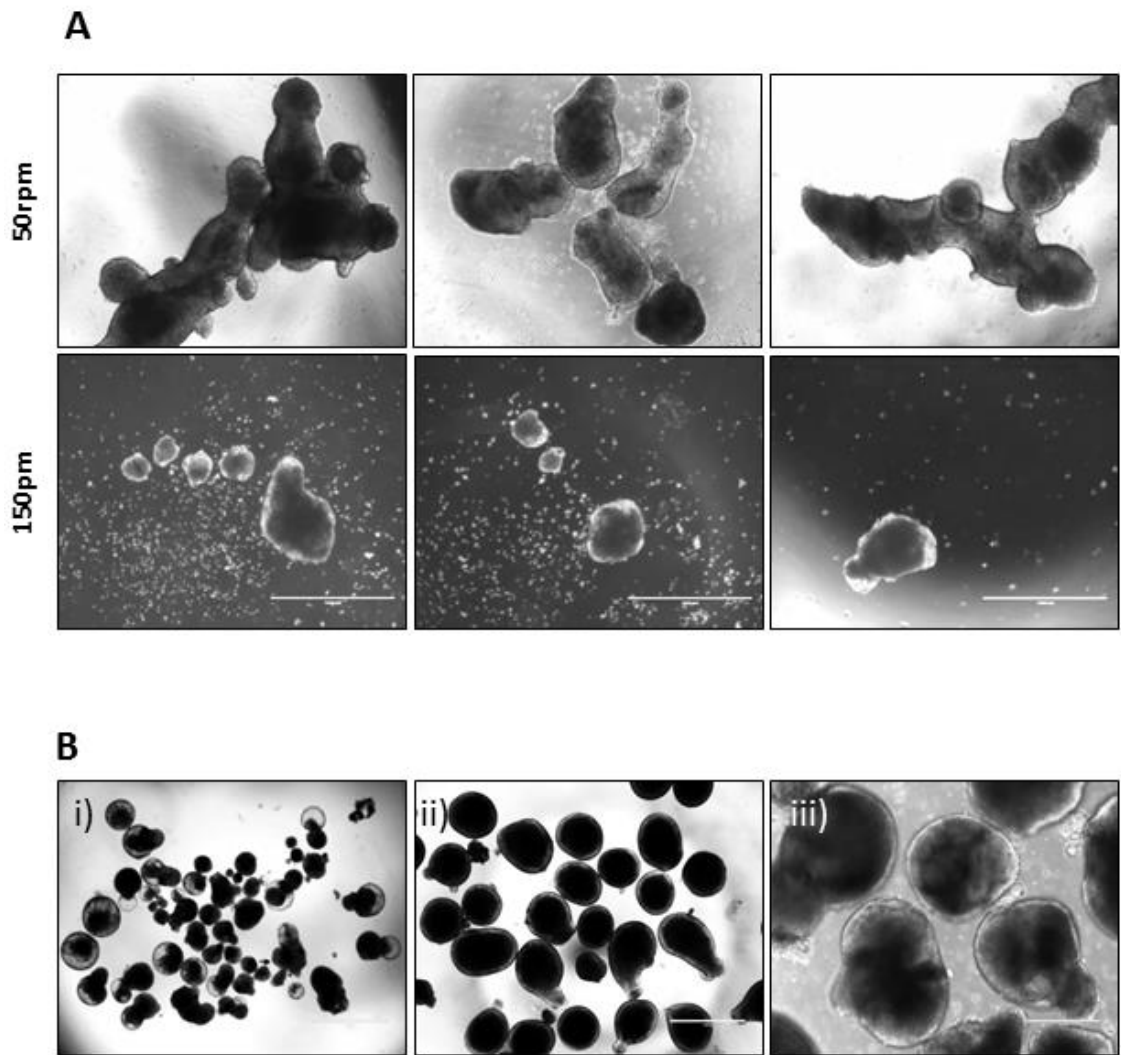


**Figure 4.2** Micrographs of 7 day old stem cell aggregates cultured in retinal differentiation medium in orbitally shaken cultures at different speeds: (A: 50rpm) and (A: 150rpm) At speeds above 150 rpm there were no EBs to image after the first imaging time point of 24 hours. (B) shows the improved survival rate of EBs made from 10,000 cells at the orbitally shaken speed of 120rpm at different magnifications 4x (Bi), 10x (Bii) and 20x (Biii). All images were taken using a Nikon Phase and Fluorescence Microscope. Scale bars = 100µm.

Well Geometry and operating conditions			Units
Well inner diameter	$d_i$	0.0156	m
Orbital diameter	$d_o$	0.01	m
Fluid height	$h_{min}$	0.00198914	m
Fluid height	$h_{max}$	0.00298371	m
Liquid volume (min)	$Vl_{min}$	0.00000038	$m^3$
Liquid volume (max)	$Vl_{max}$	0.00000057	$m^3$
Shaking speed range	N	10-500	$min^{-1}$
Critical dimensionless ratios			
$h_{min}/d_i$	0.127509	$< (d_o/d_i)^{0.5}$	
$h_{max}/d_i$	0.191263	$< (d_o/d_i)^{0.5}$	
$a_o$	1.4	Water-like viscosities	
$d_o/d_i$	0.641026		
$(d_o/d_i)^{0.5}$	0.800641	$= \square h/h_{cr}$	
Derivation of $Fr_{cr}$ from:			
$h/d_i = a_o (h/\square h)_{cr} Fr_{cr}$	$h_{min}/d_i$	$h_{max}/d_i$	Units
$Fr_{cr}$	0.072921	0.10938079	
$N_{cr}$	1.903677	2.33151883	$s^{-1}$
$N_{cr}$	114.2206	139.89113	$min^{-1}$

**Table 4.3** Parameters used to determine the critical shaking speed  $N_{Cr}$  for the minimal and maximal working volumes of 24 well microwells used for EB culture according to equation 6 in Weheliye et al., 2012.

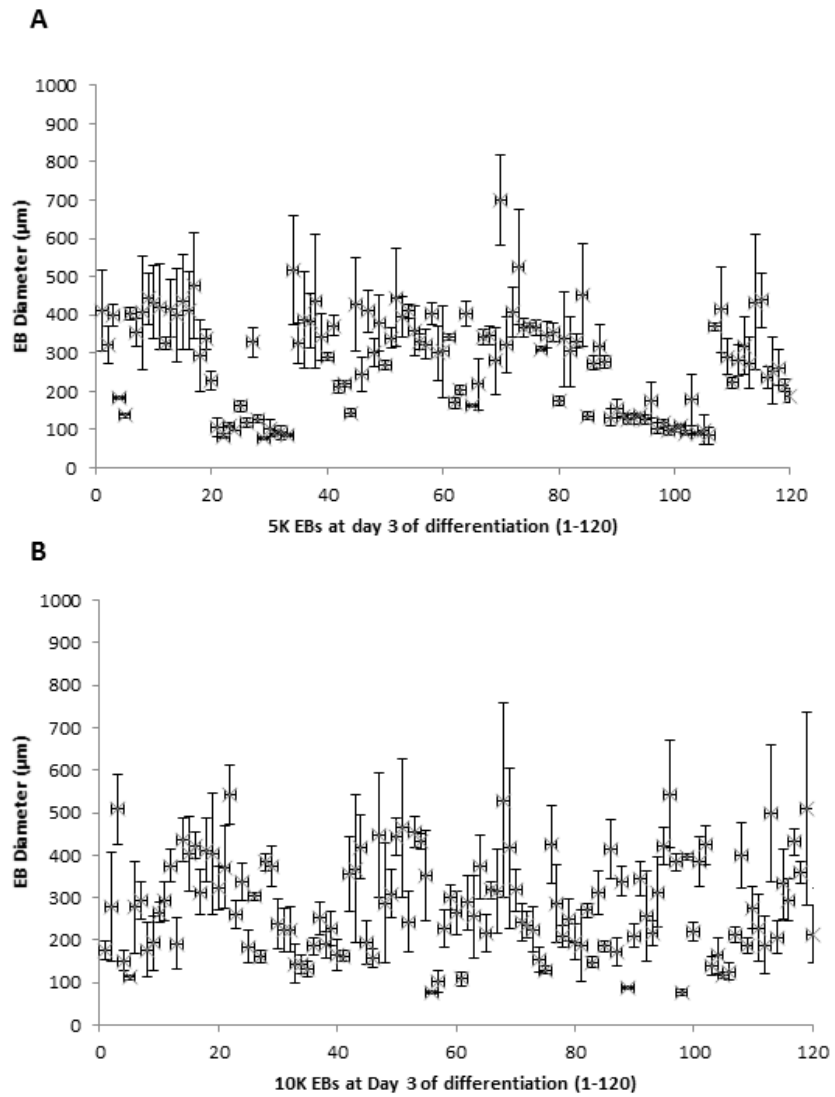


**Figure 4.3** EB size distribution pots for 5K (A) and 10K (B) EBs formed by forced aggregation at day 3 of differentiation. EB diameters are taken as averages of 3 measurements per EB (dorso-ventral, horizontal and diagonal). EBs were cultured with MSU001 IPS cells.

## **4.4 Characterizing the impact of EB size on initiation of retinal differentiation in suspension culture**

In order to assess the impact of EB size on the onset of retinal differentiation, EBs were cultured in retinal induction medium in suspension for 3 days post-formation. The EBs were not shaken for the first 3 days of culture to remain consistent with the standard protocol and EBs formed by manual scraping were designated as control experiments. Gene expression profiles from all EBs were normalised against internal reference genes  $\beta$  Actin and GAPDH before comparison against control scraped EBs using one way ANOVA analyses to investigate relative changes in gene expression for 1K, 5K and 10K cell EBs.

### **4.4.1 Pluripotency and retinal differentiation marker expression at day 3 (Figure 4.4)**

#### Expression of pluripotency marker POU5F1

A reduction in pluripotency within cell populations is evidenced by down-regulation of master regulators of pluripotency such as POU5F1 (Oct4) (Hough et al. 2009). A day 3 comparison of the relative normalised expression of POU5F1 with scraped EBs as the control showed the smaller 1K cell EBs did not present a statistically significant change in POU5F1 expression ( $p > 0.05$ ), indicating similar levels of pluripotent cells persist in both scraped and smaller 1K EBs. In contrast medium (5K) EBs showed a 16.55 fold ( $p < 0.05$ ) reduction in POU5F1 expression and the larger (10K) EBs displayed a 6.31 fold reduction ( $p < 0.05$ ) of the same marker. Reduced POU5F1 expression in the 5K and 10K populations may indicate a transgression of pluripotent cells to differentiated states as they begin to specify into desired early eye field marker expressing cells.

#### Expression of early eye field transcription factors: Pax6, Rx, Six3 and Otx2

Activation of the early eye field transcription factors Pax6, Rx, Six 3 and Otx2 characterises specification of the anterior neural plate which goes on to form the

retinae of developing vertebrate embryos (Bailey et al. 2004). The smaller 1K forced aggregation EBs displayed a 5 fold decreased expression of Pax6 ( $p < 0.0005$ ) and no significant changes in gene expression of the other retinal markers compared to the scraped controls, eliminating them from consideration as suitable for retinal differentiation. In contrast the larger EBs did show increased expression of Pax6, Rx, Six3 and Otx2 indicating initiation of retinal differentiation. The 5K EBs displayed a 3.52 fold increase in expression of Rx ( $P < 0.01$ ) and a 2 fold up-regulation of Six3 ( $P < 0.05$ ) compared to scraped controls. EBs composed of 10K cells also showed significant up-regulation of Rx (3.12 fold,  $p < 0.05$ ) and Six3 (5 fold,  $p < 0.001$ ) compared to the scraped controls. The data presents a convincing argument for a favourable impact of EB size on retinal differentiation which is discussed further in Chapter 5.

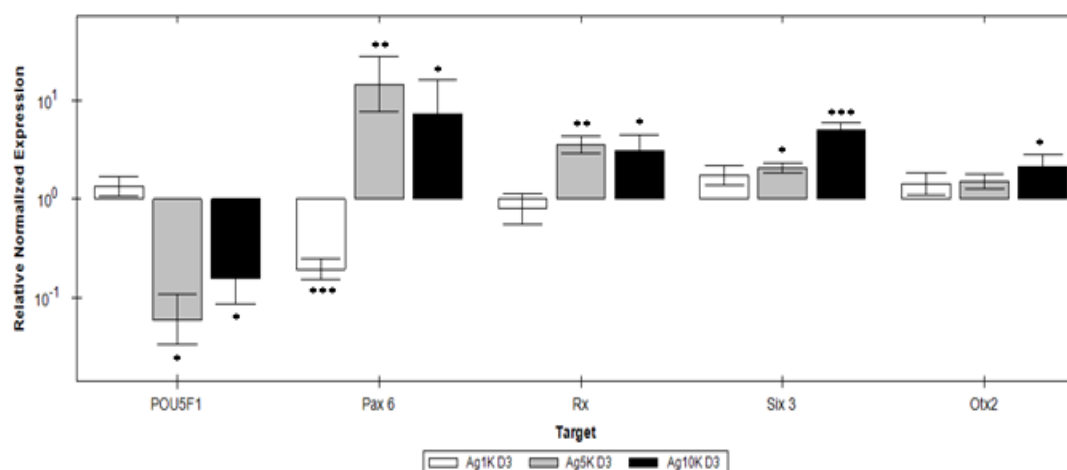


**Figure 4.4** Relative normalized expression of early retinal transcription factor genes, Pax6, Rx, Six 3 and Otx2 and pluripotency marker POU5F1 in differentiated EBs at day 3. Samples of EBs made from forced aggregation with 1K (Ag1KD3), 5K (Ag5K D3) or 10K (Ag10K D3) cells/EB were normalized against expression profiles from scraped EBs. All EBs were produced with MSU001 cells. One way ANOVA of gene expression levels were performed against EBs made by scraping (\*p<0.05, \*\*p<0.01, \*\*\*p<0.001).

## 4.5 Summary

In this chapter we found 2 EB sizes (5K and 10K cells/EB) which were suitable for investigating orbital shaking cultures and appropriate shaking speeds to support EBs to initiate retinal differentiation. EBs composed of 5K and 10K cells each were found to be suitable for experiments to test EB survival under different shaking speeds due to their ease of manufacture, handling and practically feasible cell number requirements. Additionally the impact of EB size variation on the ability to express early markers of retinal differentiation Rx, Six3 and Otx2 after 3 days of suspension culture in retinal differentiation medium showed 5K and 10K EBs were more suitable for initiating retinal differentiation than smaller 1K EBs. All of the early eye field transcription factors were expressed at day 3 for all EB sizes but more pronounced expression of retinal markers observed in the larger EBs coincided with their down-regulation of pluripotency marker POU5F1 expression. The coinciding up-regulation of early eye field markers with down-regulation of POU5F1 suggested that the larger EB populations were advancing into retinal differentiation faster than both smaller 1K EBs and the scraped EB controls.

As a result the 5K and 10K EBs were taken forward in experiments to determine the suitable shaking speed of 120rpm. At this orbital shaken speed EBs survived 7 days in culture as single entities, without showing signs of deterioration observed at higher speeds and the EB agglomeration detected at lower shaking speeds (Figure 4.2). This specified the suitability of EBs formed by forced aggregation from 5K and 10K cells/EB, for further studies to investigate progression of retinal differentiation discussed in chapter 5.

## **5.0 The impact of size controlled EBs and orbital shaking on the progression of retinal differentiation over 21 days in a Matrigel-free culture**

### **5.1 Introduction**

Current methods to produce retinal photoreceptor-like cells from pluripotent stem cells in adherent or static suspension protocols typically involve culture timeframes between 10 and 126 days with an average culture period of 58 days (Ramsden et al. 2014). In order to assess the suitability of orbital shaking for the differentiation over long culture periods, we determined a period of 21 days to measure the impact of orbital shaking and initial EB size on the progression of differentiation towards retinal cell fates, as evidenced by key retinal gene expression profiles detected by QPCR and immunohistochemical analyses. The 21 day timeframe allowed enough time to detect expression of later retinal markers which were also detected in preliminary experiments by day 15.

Within the human retina photoreceptors make up >70% of the final cell population (Curcio et al. 1990; Hendrickson et al. 2008). Consequently up-regulation in the expression of markers for retinal differentiation followed by photoreceptor specific genes expression in differentiating EB cultures can indicate their level of progression through retinal fate specification. In order to track retinal differentiation the early eye field transcription factor *Otx2* and the photoreceptor precursor and homeodomain transcription factor protein cone-rod homeobox (*Crx*) indicate earlier retinal differentiation states. The presence of more mature cell types within the differentiating EBs are indicated by upregulated expression of the basic motif-leucine Neural Retinal Leucine Zipper transcription factor (*Nrl*) a regulator of photoreceptor development/function and another photoreceptor specific gene for the visual pigment Rhodopsin (*Rho*) (Bailey et al. 2004; Hendrickson et al. 2008; Pan et al. 2011).

Previous reports have shown that larger EBs can contain neural enriched cells and an EB size of 9K cells/EB has also been found to be optimal for the efficient generation of retinal progenitor cells from hESC in another report (Nakano et al. 2012; Bauwens et al. 2008). To our knowledge there is no report yet, which combines the impact of EB size variation on differentiation towards a retinal lineage with orbital shaking culture. To investigate the influence of changing EB size in adherent and orbital shaken cultures during differentiation experiments two EB sizes, 5K and 10K EBs were chosen. The 5K and 10K EBs were picked in favour of smaller 1K or scraped uncontrolled EBs from chapter 4 (initiation of retinal differentiation) as they showed the highest expression of early retinal differentiation markers compared to static adherent controls at day 3 and survived 7 days of orbital shaken culture. In this chapter in order to allow separate analyses of the effects of orbital shaking and those of varying EB size, the input EBs used in adherent control samples were also size matched to their paralleled orbital shaken cultures.

The aim of the work in this chapter is firstly to test whether orbital shaking can continue to support progression of retinal differentiation beyond 3 days in culture (as observed in chapter 4). We investigate whether the resulting micro-environment is conducive to the production of later retinal cell types such as photoreceptor cells, in the absence of supplementation with Matrigel through the measurement of total cell yields, cell health and the expression of retinal markers. The influence of EB size on retinal differentiation is considered in both the adherent and orbital shaken systems, firstly by controlling the input EB sizes and secondly by tracking changes in EB diameters over the 21 day culture period.

### **5.1.1 Aims and Objectives**

- To test the hypothesis that progression of retinal differentiation is possible in orbital shaken cultures without Matrigel supplementation up to 21 days.
- Investigate changes in EB size with time, in orbital shaken cultures with for 2 different EB sizes (5K and 10K cells/EB).

- Assess the impact of orbital shaking during retinal differentiation on cell health and yields.
- Characterize the effect of EB size variation and orbital shaking on progression through retinal differentiation by gene expression analyses.

## **5.2 Characterising the impact of orbital shaking culture on retinal differentiation**

### **5.2.1 EB morphology and size variability**

Over the of 21 days of orbital shaking culture, light microscopy images of the differentiating EBs enables us to observe a close relationship in morphology between the 5K and 10K EBs. The images taken were mostly indistinguishable between the 2 sizes showing similar responses to orbital shaking throughout the culture period. Figure 5.1 shows the 5K and 10K EB cultures as they appeared under a light microscope at days 3, 10, 15 and 21 the key sampling time points chosen over the duration of the experimental period. Morphologies were similar in both EB size cultures showing a rise in the number of dense, dark centred EBs and hollow bubbly EBs, as they progressed along the 21 days of culture. The edges of EBs also frequently appeared to possess secondary structures such as phase dark rings around the EB perimeters, occasional invaginations along the edges of EBs as well as optic cup like shapes (Figure 5.1 D15), similar to previously reported observations in protocols for neural epithelial induction (Nakano et al. 2012; Eiraku et al. 2011; Heavner & Pevny 2012).

The larger 10K EB were sometimes distinguishable from the smaller 5K EBs when they appeared denser and larger at later time points. The densest cores were suspected of being necrotic centres which prompted investigation into the cell health with LDH assays and assessment of cell yields between the 2 EB size cultures (section 5.2.4). Although we did not directly test whether the centres of dense EBs were necrotic there

was often an absence of nuclear marker DAPI staining at the centres of EBs. The immunocytochemistry assays of cryosectioned EBs in Figure 5.10(A) together with the observed increase in LDH release over time seen in Figure 5.4 (B) may provide evidence to support the hypothesis that some larger EBs had necrotic cores. An assessment of the changes in EB sizes over the culture duration was also performed to investigate how different EB starting sizes correlated with different EB sizes observed throughout the culture period.

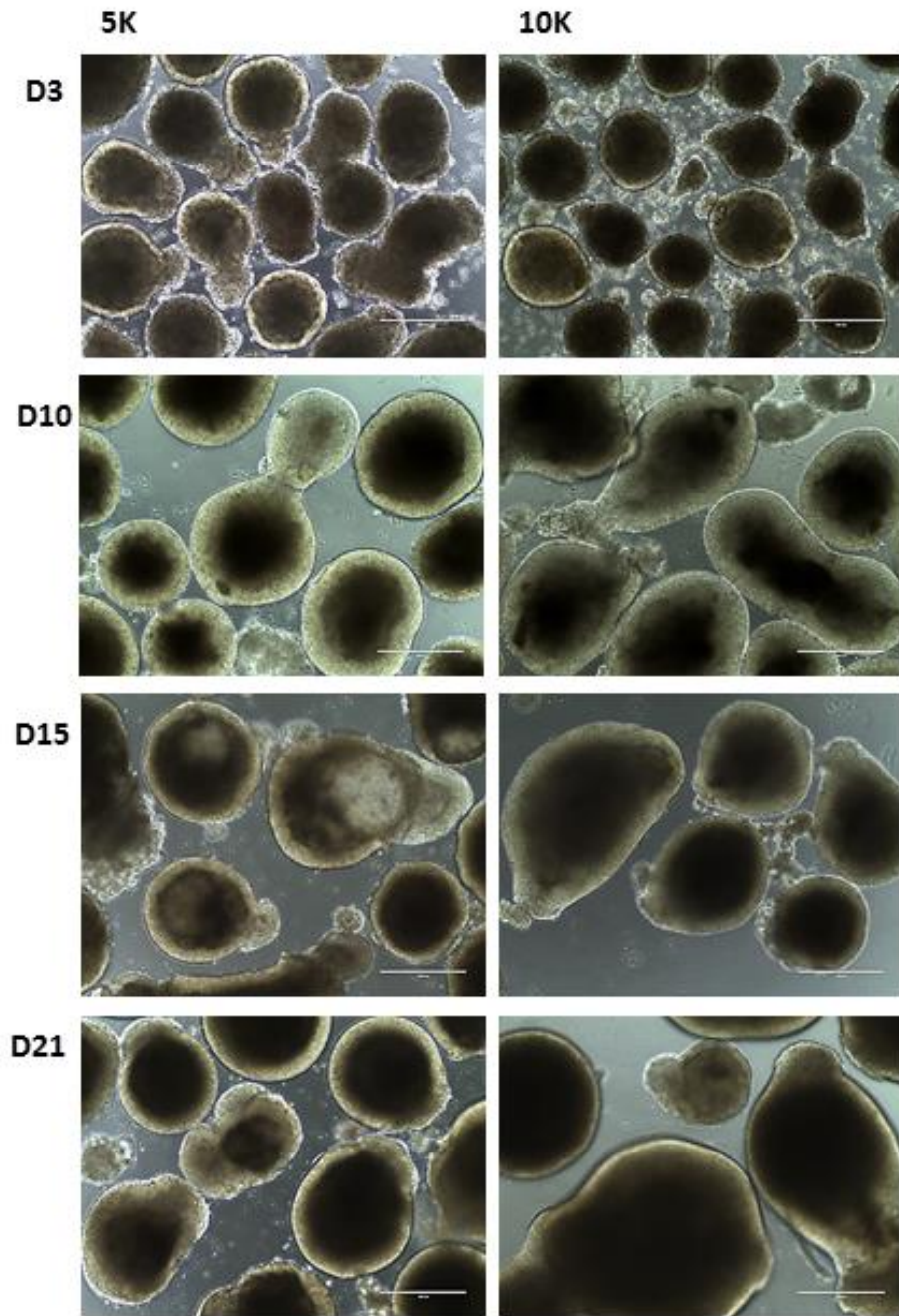


**Figure 5.1** Representative micrographs of MSU001 retinal EBs made from 5000 or 10,000 cells at days 3, 10, and 21 of retinal differentiation. Scale bar = 400 $\mu$ m

### **5.2.2 EB size variation during retinal differentiation**

Aggregate size was specified at EB formation by using forced aggregation as demonstrated in chapter 3 but the EBs varied greatly in size over the culture period. Creating uniform EB sizes to initiate cultures firstly helped assess the impact of input EB size on the onset of retinal differentiation. Secondly, uniform EB sizes facilitated the selection of 2 EB sizes which were subsequently used to investigate the feasibility of orbital shaking retinal differentiation culture and the removal of Matrigel from the system. Reducing the impact of initial EB size as a culture variable aimed to facilitate the investigation of the impact of the introduction of orbital shaking as a factor, on both the onset of and progression through retinal differentiation up to 21 days.

Instead of observing uniform sized EBs throughout the culture period, EBs varied greatly in size. The EB size variations were characterised by performing EB diameter measurements throughout the culture period to create cumulative frequency plots for a visual representation of the size distribution of EB populations over the culture period. The data show similar patterns in EB size variation over time were observed in EBs made from 5K or 10K cells (Figure 5.1A and B).

### **5.2.3 Characterising size variation over 21 days of retinal differentiation**

By day 3 of retinal differentiation culture (white bars on Figure 5.2 (A) and (B)) most EBs from both 5K and 10K populations measured between 200-600 $\mu\text{m}$  in diameter with fewer than 20% measuring  $\leq 200\mu\text{m}$ . At day 10 the majority of EBs remained categorized between 200-600  $\mu\text{m}$  for both 5K and 10K EBs which may indicate the existence of a potential optimal size for this stage of retinal development in orbital shaken culture (Figure 5.2). By day 15 (dark grey bars on Figure 5.2) a similar pattern is again observed for both the 5K and 10K EBs, which by this time in culture span the full range of EB diameters in an almost normal distribution (Figure 5.3). Between days 3 and 15 however we observe the majority of EBs (~80%) were split almost evenly between the 3 specific size categories. 200-400 $\mu\text{m}$ , 401-600  $\mu\text{m}$  and 601-

800 $\mu$ m (Figure 5.2). No significant variation was observed in the spread of EBs categorised into each of the size ranges in either the 5K or 10K EBs suggesting that between days 3 and 15 both cultures behaved similarly in their progression through differentiation in terms of EB size.

The first signs of variation between the EB size distributions of cultures initiated with either 5K or 10K EBs was observed at day 21. By day 21 in orbital shaken culture, ~40% of the larger 10K EBs measured between 800-1000  $\mu$ m in diameter, while the majority of 5K EBs (~80%) were categorised into a smaller size range between 600-800  $\mu$ m, with less than 20% of them achieving EB diameters above 800 $\mu$ m.

More detailed analyses of these cell populations to provide insight into the nature of the differences observed in different EB sizes over time during retinal differentiation would be possible with FACS analysis approaches. FACS analysis would facilitate an investigation into the relationship between EB size and retinal differentiation at the cellular level to provide constituent retinal cell populations within EBs. While this would form interesting future work, time restraints and challenges with resolving EBs into single cell populations made this an unfeasible option for this report. Instead here, we present a correlation between variation in EB size distribution throughout the culture period with culture oxygen saturation and culture pH as illustrated in Figures 5.5 and 5.6.

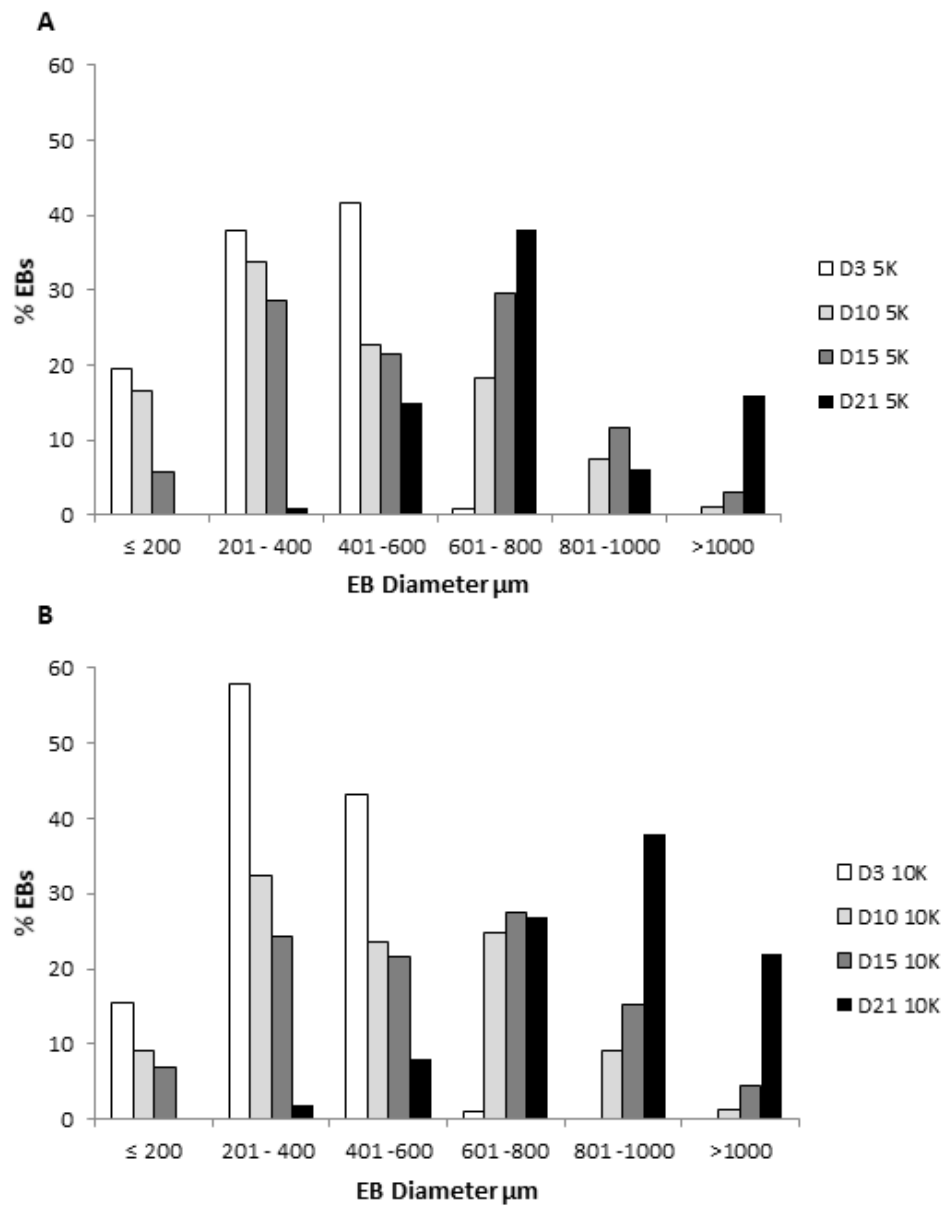


**Figure 5.2** Size distribution of retinal EBs formed of (A) 5000 or (B) 10,000 cells per EB between days 3 and 21 of culture. MSU001 retinal EB diameters were measured to determine the spread of EB size with time in differentiating EB cultures. EB diameters were measured at each time point (n=100) and average diameters used to determine size distribution from absolute percentage frequencies of EBs in each size bracket between  $\leq 200\mu\text{m}$  and  $> 1000\mu\text{m}$  in diameter. The percentages of EBs populating each size bracket are presented above. EBs were imaged using a phase contrast microscope and images were analysed to measure average diameters using Image J software.

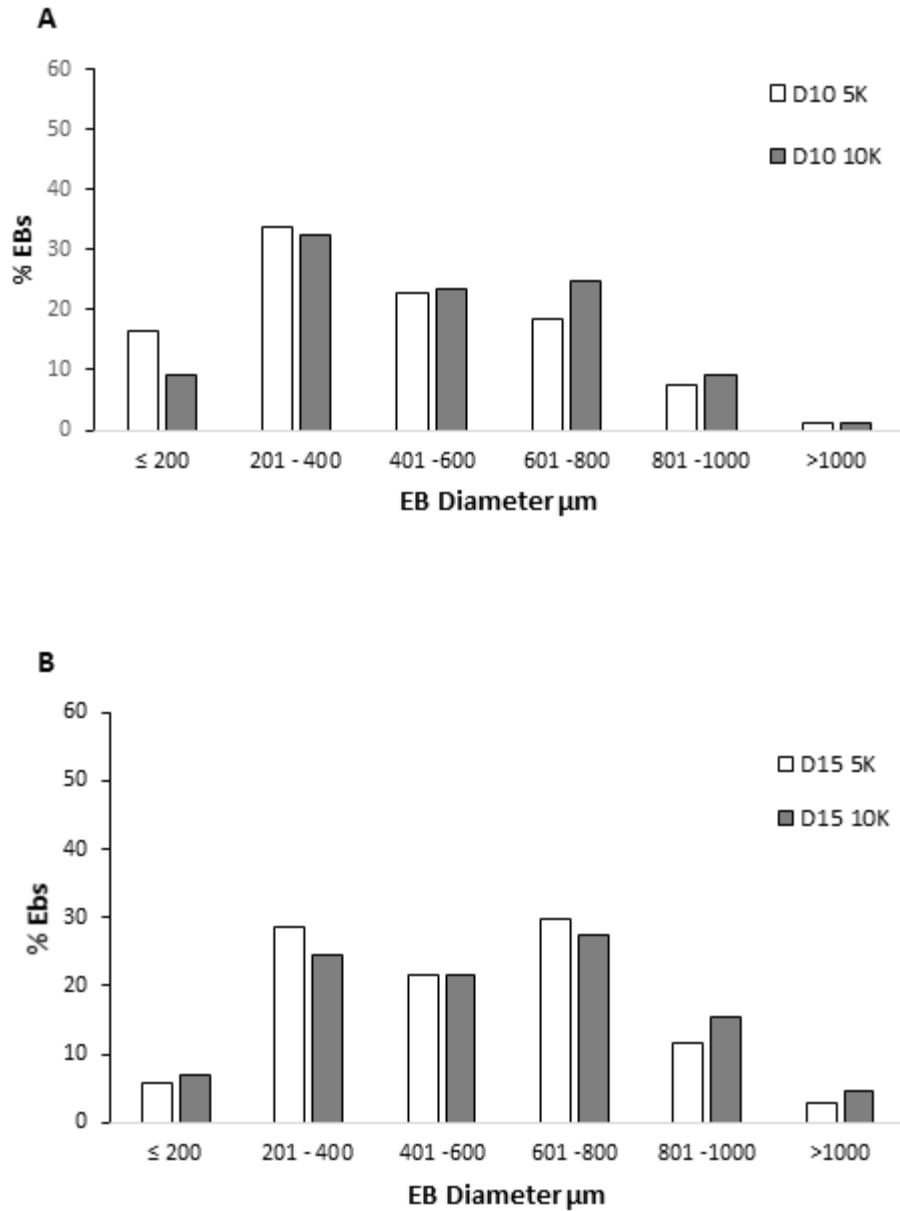


**Figure 5.3** A comparison of the size distribution of MSU001 EBs with different starting sizes through differentiation at day 10 (**A**) and day 15 (**B**). Cumulative frequency distribution plot was calculated using 3 measurements of diameter per EB (n=100) to determine average sizes, which have been allocated to different size bands according to frequency. MSU001 EBs were formed with 5,000 or 10,000 cells and cultured in retinal differentiation medium for 10 or 15 days.

## 5.2.4 Cell quantification and cytotoxicity analyses

### Pico Green Assay for cell quantification from absolute DNA

The Pico Green absolute DNA quantification assay (Life technologies) helped to assess the impact of orbital shaking culture on cell yields. By plotting a standard curve using absolute DNA quantification measurements from known quantities of pluripotent cells, it was possible to estimate total cell numbers present in samples of EBs in adherent and orbital shaken cultures using a linear regression approach. A further comparison of DNA quantified from cell samples of orbital shaken cultures with absolute DNA quantified from control adherent cultures helped measure the impact of orbital shaking on cell numbers (Figure 5.4(A)). For each experiment, in both adherent and orbital cultures, 40-50 EBs were plated per well of a 24 well plate and medium was changed as necessary (every 2 days up to day 15 then daily up to day 21). Interestingly, the relative quantities of cells remained similar across culture techniques and between different starting size EB populations under the same culture conditions. The striking similarity between the different culture systems poses the question, whether nutrient availability may have become a limiting factor for continued growth of cells and the possibility that available nutrients could only support a maximum of around  $2 \times 10^6$  cells per well for both adherent and orbital shaken systems.

### LDH Colorimetric Assay for quantification of cell death

To investigate whether the similarity between total cell quantities observed between different cultures was due to an increase in levels of cell death or cell lysis; we measured the Lactate Dehydrogenase (LDH) released into the medium using an LDH colorimetric assay (Abcam). The results indicated that LDH release increased over the culture period for both EB sizes in orbital shaken cultures. Figure 5.4(B) shows the increase in LDH activity measured from the spent medium of cultures over 21 days with 5K and 10K EBs. The graph in Figure 5.4B shows a rise in levels of LDH up to day 16 and then a gradual decrease for the remainder of the culture period. The apparent decrease in LDH activity measured from day 16 to 21 is actually an artefact

of the experiment, wherein the medium exchange regime was changed from every 48 hours to every 24 hours from day 15 onwards as indicated on graph 5.4(B).

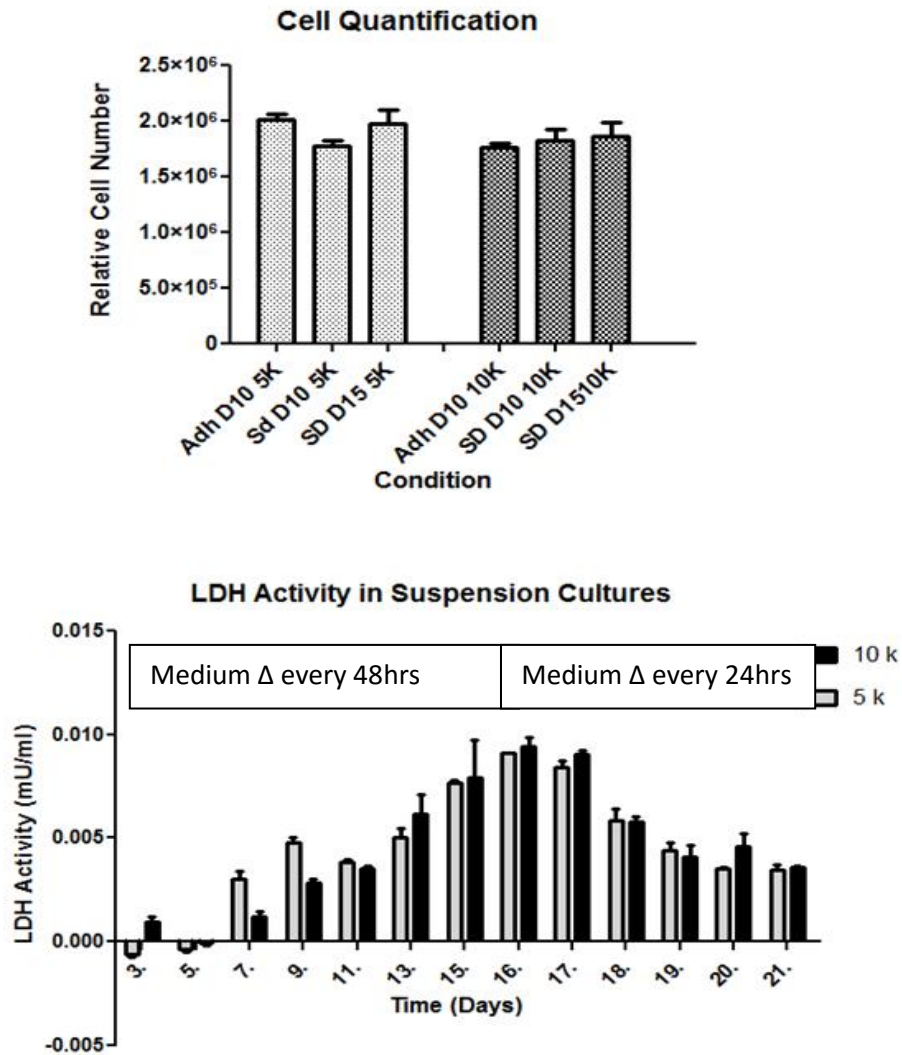


**Figure 5.4 (A) Cell quantification of retinal EBs** Relative cell numbers were obtained using the Quant-iT Pico-Green (Invitrogen) DNA quantification method. Samples of 5K and 10K adherent EBs at day 10 (Adh D10 5K, Adh D10 10K) and for orbital shaken cultured EBs at days 10 and 15 (SD D10 5K, SD D15 5K and SD D10 10K and SD D15 10K). Cell numbers were calculated by reference to an IPS cell DNA standard curve. **(B) LDH activity in suspension cultures.** LDH activity of LDH released into the supernatant of retinal differentiation cultures from 5K and 10K EBs over 21 days of differentiation in orbital shaken culture.

### **5.3 Immunocytochemistry analyses show retinal marker expression in orbital shaken cultures is comparable to that of static culture**

To determine whether EBs in orbital shaken culture were able to differentiate along a retinal trajectory, immunocytochemical analyses were performed to test for protein level expression of early eye field marker orthodenticle homeobox 2 (Otx2) and the later expressed photoreceptor specific transcription factor, the cone-rod homeobox (Crx). The presence of octamer-binding transcription factor 4 (Oct4 or POU5F1) was also detected indicating the persistence of cells maintaining a pluripotent state within the cultures.

Both adherent control (Figures 5.5, 5.6 and 5.7) and orbital shaken (Figures 5.8 and 5.9) cultures expressed markers for retinal differentiation in the 5K and 10K size EB populations (5K and 10K EBs). Representative immunocytochemistry images showed comparable protein level expression of the early field transcription factor Otx2 and the later expressed photoreceptor precursor marker Crx in adherent and orbital shaken culture systems. Interestingly, with no major differences in retinal marker expression were observed from the immunostain micrographs between the culture systems, or amongst different sized EBs, at each time point investigated. Additionally there seemed to be no visibly detectable difference in immunostain intensity between the markers of retinal differentiation and POU5F1 (Figure 5.5) at day 10. The apparent similarity in pluripotency marker POU5F1 and retinal marker expression may indicate that, for day 10 at least, EB size variation between 5k and 10K may not have been sufficient to affect the rate of loss of pluripotency or the rate of acquisition of retinal marker expression. Without observable differences in marker expression between the 2 EB sizes further investigations to measure the differences were performed using a QPCR approach.

Evidence for the protein level expression of early and later retinal markers by immunohistochemistry presented in Figures 5.5 – 5.9 was an important step in demonstrating that eye field cells, including photoreceptor precursor cells were likely to be present in both the adherent and orbital shaking cultures. More detailed analyses were however necessary to quantify changes in the constituent cell populations between systems and over time at the genetic level using QPCR. Real-time

quantitative polymerase chain reaction analyses were performed on samples throughout the culture period at days 10, 15 and 21. The QPCR approach enabled measurements to be taken to represent changes in the level of expression of eye-field transcription factors over the course of the differentiation, in response to differing input EB sizes and culture techniques (adherent vs orbital shaken).

### D10 Adherent MSU001 Ebs 5K cells/EB

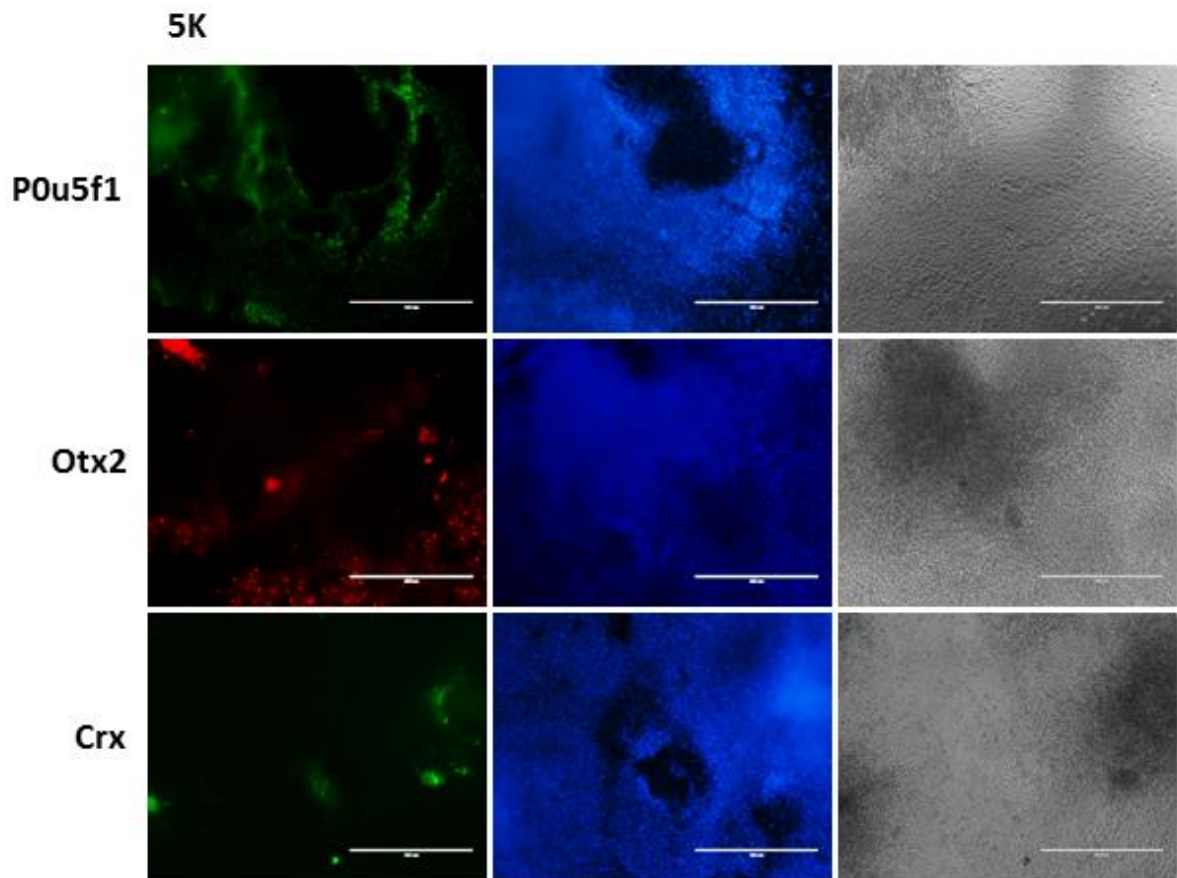


**Figure 5.5** Immunocytochemistry of adherent retinal EBs made from 5K cells at day 10, for pluripotency marker POU5F1, early retinal transcription marker Otx2 and photoreceptor precursor marker Crx. Scale bars = 400 $\mu$ m.

## D10 Adh MSU001 EBs 10K cells/EB

10K

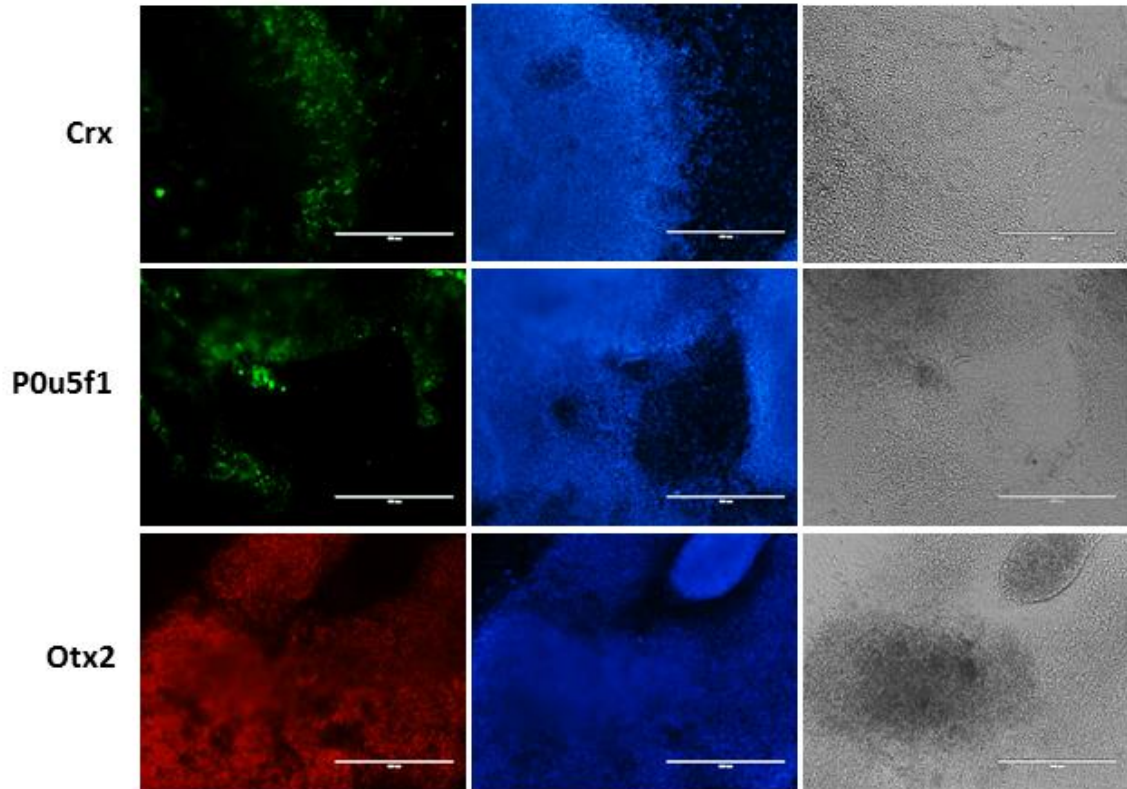


**Figure 5.6** Immunocytochemistry of adherent retinal EBs made from 10K cells at day 10, for pluripotency marker POU5F1, early retinal transcription marker Otx2 and photoreceptor precursor marker Crx. Scale bars = 400μm.

## D15 MSU001 Adherent EBs

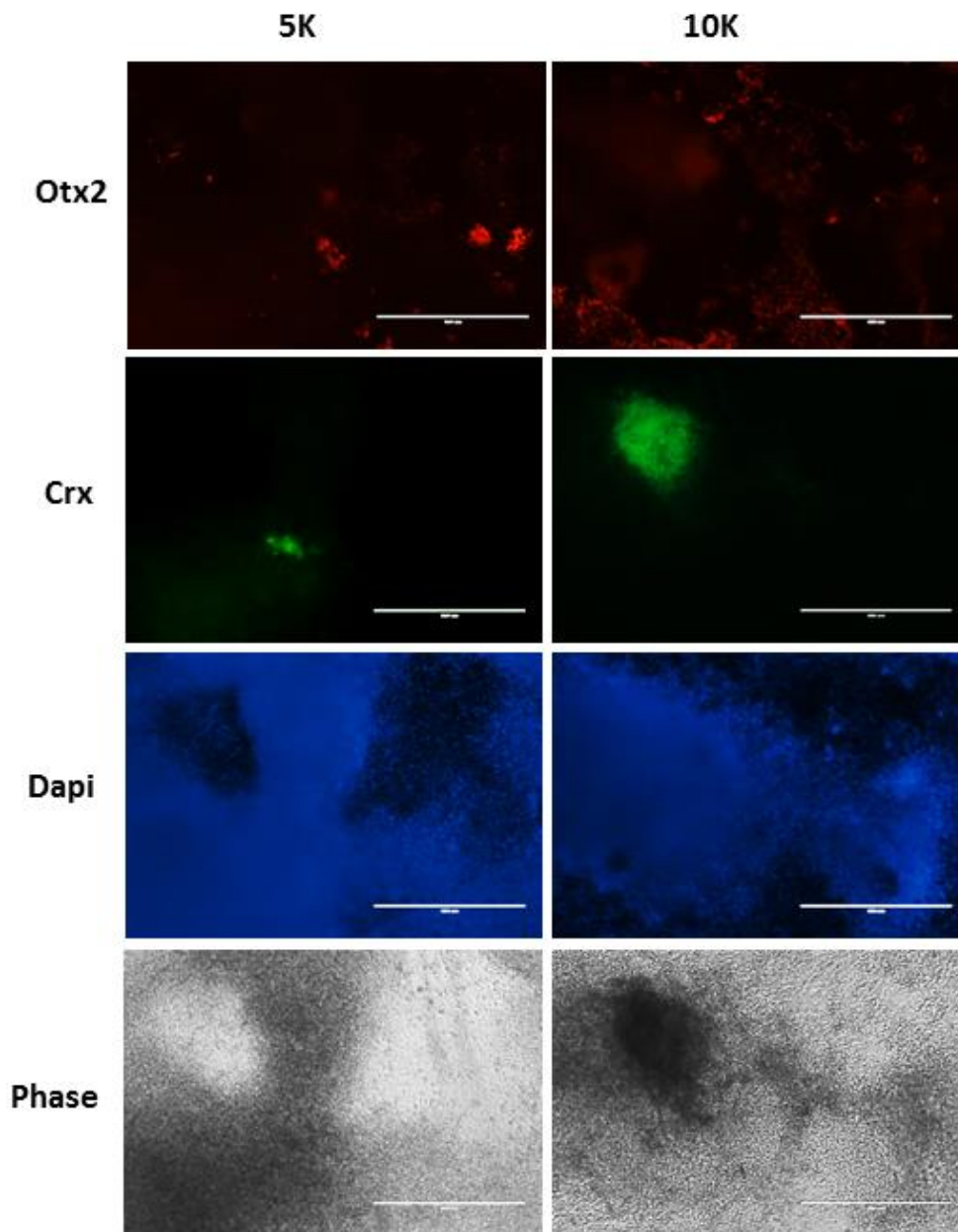


**Figure 5.7** Immunocytochemistry of adherent retinal EBs made from 5K or 10K cells at day 15, for early eye field transcription factor Otx2, photoreceptor precursor marker Crx, nuclear stain DAPI and corresponding phase images. Scale bars = 400 $\mu$ m.

### A) MSU EB Cryosections (5K cells/ EB)

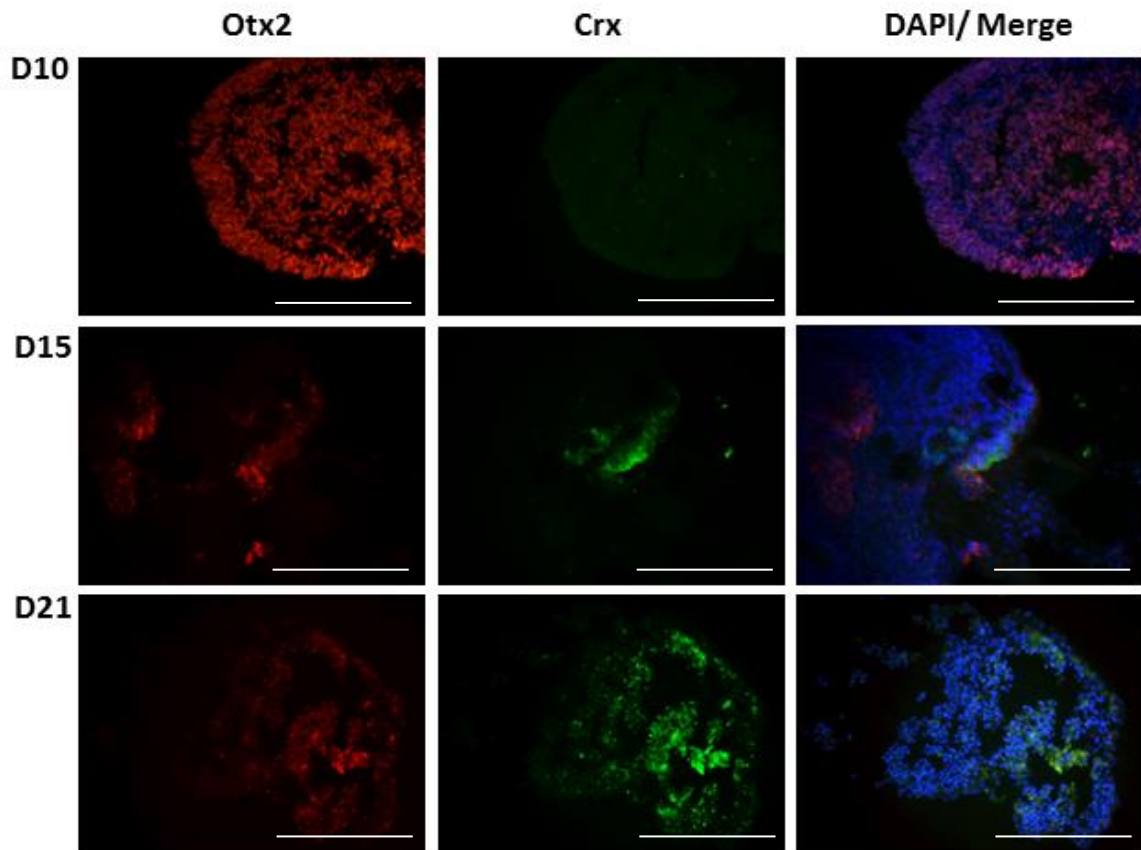


**Figure 5.8** Immunocytochemistry of cross-sections of orbital shaken retinal EBs made from 5K cells/EB at days 10, 15 and 21 of retinal differentiation culture. Images show early eye field transcription factor Otx2, photoreceptor precursor marker Crx and nuclear stain DAPI. Scale bars = 400 $\mu$ m.

**B) Crx and Otx2 MSU001 EB Cryosections (10K cells/EB)**

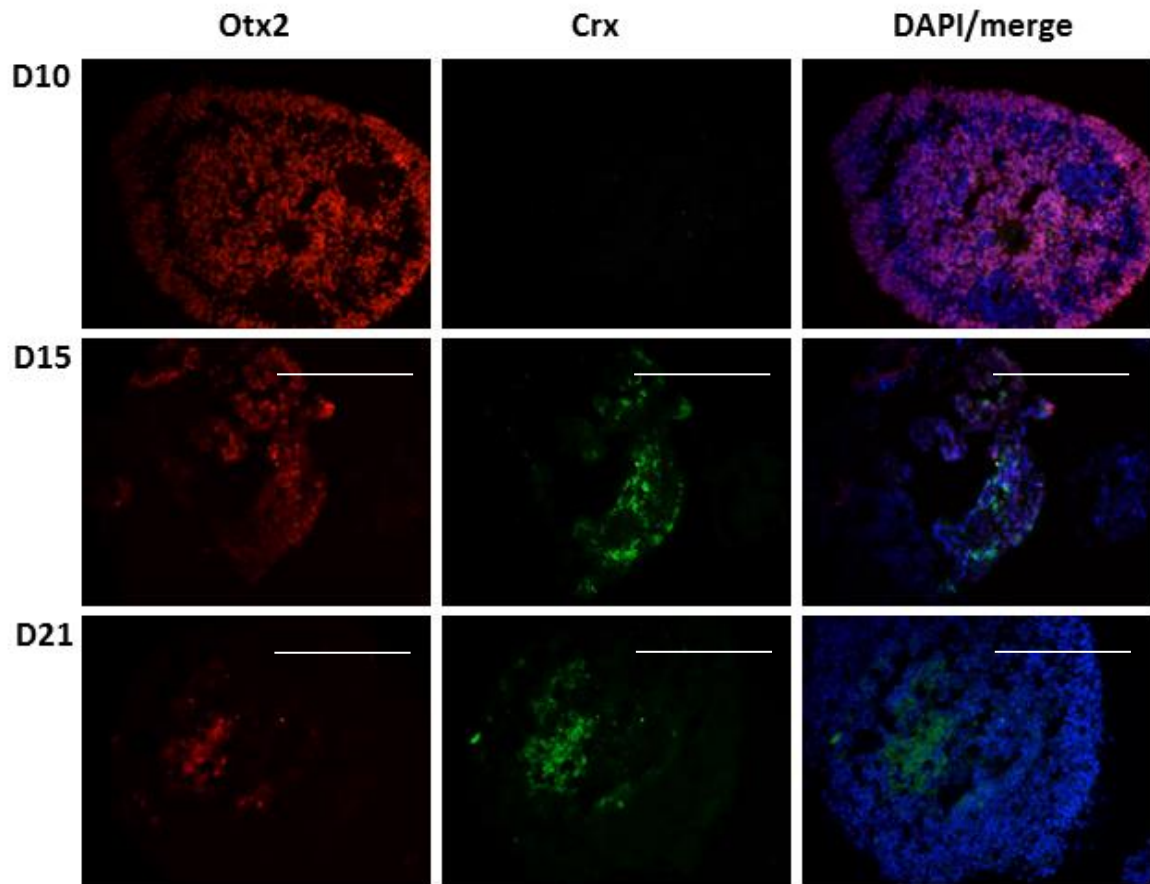


**Figure 5.9** Immunocytochemistry of cross-sections of orbital shaken retinal EBs made from 10K cells/EB at days 10, 15 and 21 of retinal differentiation culture. Images show early eye field transcription factor Otx2, photoreceptor precursor marker Crx and nuclear stain DAPI. Scale bars = 400 $\mu$ m.

## **5.4 QPCR Analyses of retinal differentiation in adherent and orbital shaken cultures**

Progression through retinal differentiation was quantitatively assessed by QPCR analyses of the transcriptomes extracted from samples of EBs cultured in retinal differentiation medium in adherent or orbital shaken cultures. Triplicate samples of EBs formed from 3 different hiPSC passages, cultured in both adherent and orbital shaken systems were frozen at  $-80^{\circ}\text{C}$  for QPCR analyses at days 10, 15 and 21 of differentiation. Data for the relative expression of eye-field transcription factors and pluripotency marker POU5F1 are presented in graphs in Figures 5.10 to 5.15. Over the course of the differentiation protocol, changes in gene expression for eye-field transcription factors Otx2, Crx, Nrl and Rho were compared between adherent and orbital shaken cultures.

The aim was to compare expression levels between each EB size and across culture techniques separately for each time point. Firstly, relative marker expression is compared according to EB size, keeping the culture techniques constant so as to observe the impact of the culture technique on retinal differentiation at each EB size. The second part of each QPCR data set presented, allows a comparison of the changes in gene expression arising from modifying the culture technique from adherent to orbital shaken culture for both EB sizes. This approach was used to simply highlight differences in gene expression arising specifically as a result of changing either EB size from 5K to 10K cells/EB or the culture technique from adherent to the orbital shaking system.

### **5.4.1 Day 10 QPCR Analyses of EFTFs and POU5F1 expression**

At day 10 all of the eye field transcription factor genes investigated were expressed at low levels. At day 10 no statistically significant variations were observed between different sized EBs whether they were cultured in adherent or orbital shaken protocols (Figure 5.10A and B). ANOVA analyses comparing gene expression profiles of POU5F1, Otx2, Crx, Nrl and Rho between size-matched adherent and orbital shaken

samples also showed no statistically significant differences ( $p>0.05$ ) (Figure 5.11). Together the QPCR data at day 10 show adherent and orbital shaken cultures to be equivalent in their expression of the selected markers of differentiation towards retinal cell lineages.

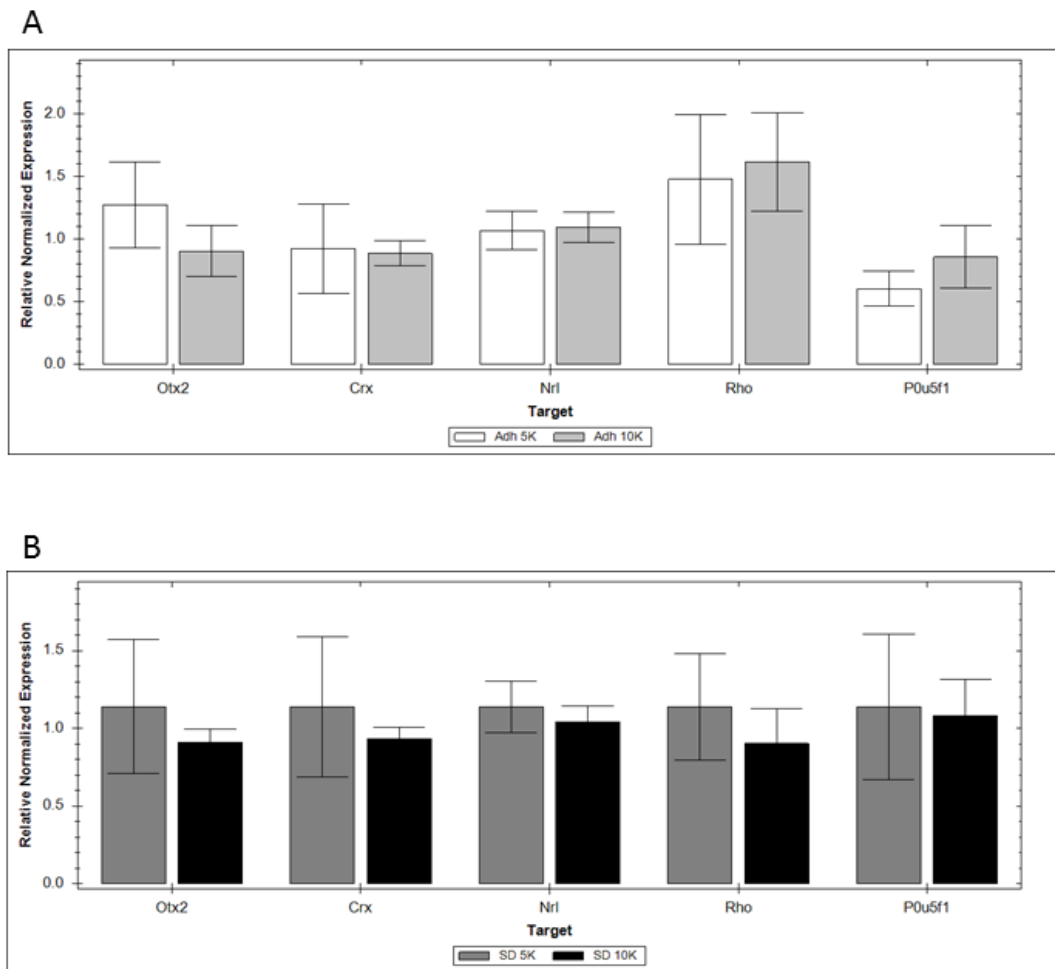


**Figure 5.10** The impact of EB size on differentiation in adherent and orbital shaken culture at day 10. Relative expression of eye field transcription factor genes Otx2, Crx, Nr1, Rho and pluripotency marker POU5F1 in EBs at day 10 for (A) adherent (Adh 5K & Adh 10K) and (B) orbital shaken cultures (SD 5K & SD 10K). Retinal EBs with formation sizes of 5K or 10K cells/EB were produced using MSU001 cells.

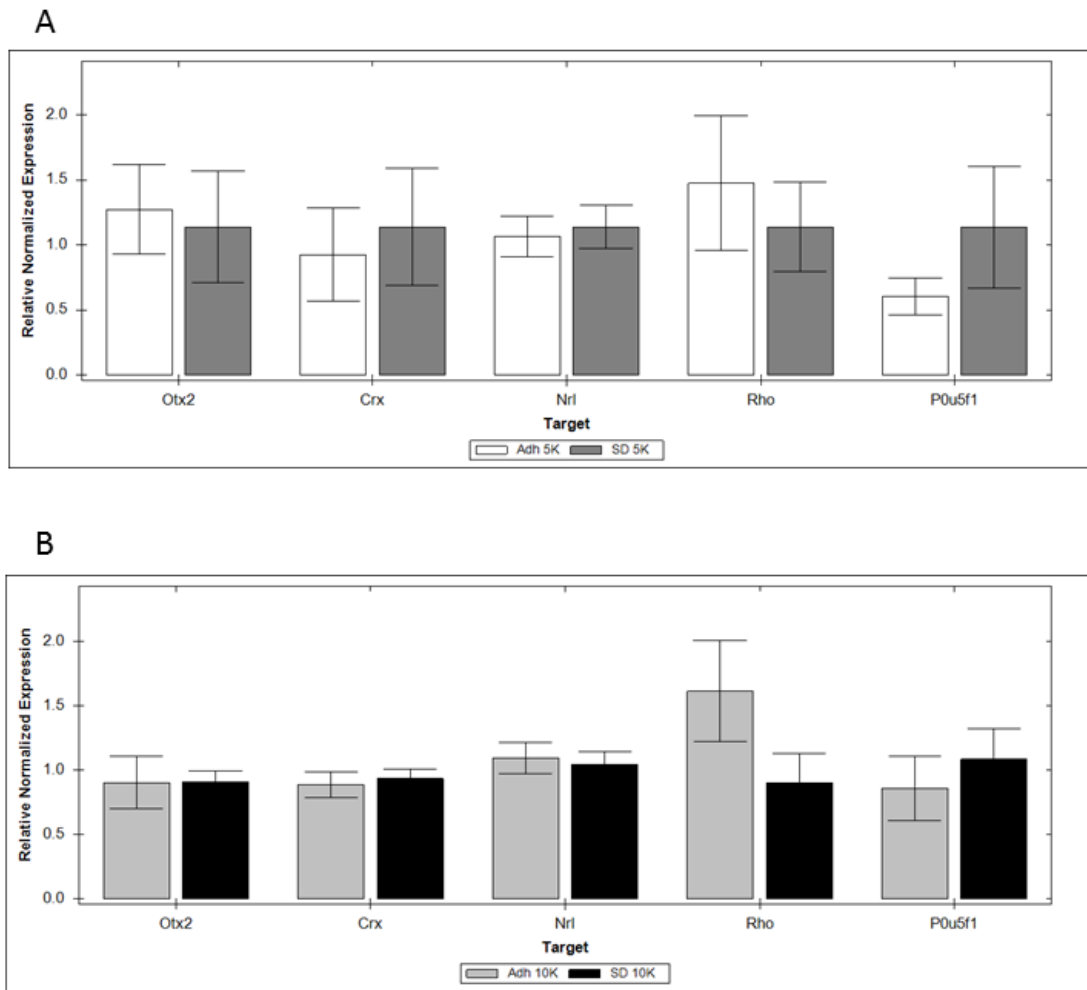


**Figure 5.11** The impact of orbital shaken culture on differentiation at day 10. A day 10 comparison of gene expression profiles between size-matched EBs of **(A)** 5K or **(B)** 10K cells cultured in control adherent (Adh 5k & Adh 10K) versus orbital shaken cultures (SD 5K & SD 10K). Relative expression of eye field transcription factor genes Otx2, Crx, Nrl, Rho and pluripotency marker POU5F1. EBs were produced using MSU001 cells.

## **5.5 Day 15: QPCR Analyses of EFTFs and POU5F1 expression**

### **5.5.1 The impact of varying EB size at day 15**

The impact of varying input EB size from 5K to 10K cells/EBs on differentiation at day 15 was measured by comparing the relative gene expression profiles of EBs of the same size cultured in either adherent or orbital shaken protocols (Figure 5.12).

#### Adherent cultures (Figure 5.12A)

EBs from matrigel containing adherent cultures at day 15 showed comparable levels of expression of the earlier retinal transcription factors Otx2 and Crx regardless of EB size by day 15 of retinal differentiation culture. However, by increasing EB size from 5K to 10K cells/EB we observed a significantly reduced expression of later photoreceptor markers Nrl (1.6 fold  $p=0.034$ ) and RHO (1.45 fold  $p=0.023$ ). In adherent cultures, 5K EBs also showed much higher expression of pluripotency marker POU5F1 than 10K EB populations (3.36 fold  $p=0.0007$ ). The data seem to suggest that 5K EBs were better suited to retinal differentiation in orbital shaken culture than larger 10K EBs.

#### Orbital shaken cultures (Figure 5.12B)

By day 15 EBs with either 5K or 10K starting sizes in orbital shaken cultures still showed a closer correlation in their retinal marker and POU5F1 expression, with the exception of one gene (Rho). The data show that 10K EBs in orbital shaken culture showed a 1.69 fold reduction in Rho expression compared to the 5K EB samples. All other genes were expressed at comparable levels, without any statistically significant changes observed.

In summary, the impact of increasing EB size from 5K to 10K EBs on differentiation at day 15, seemed to downregulate expression of pluripotency marker POU5F1 in both adherent and orbital shaken cultures. Interestingly, the downregulation of POU5F1 in larger EBs coincided with a reduction in Rho expression for both adherent and orbital shaken cultures. 5K EBs at day 15 therefore contain more pluripotent cells and more Rho positive photoreceptors than the 10K EBs.

### **5.5.2 The impact of orbital shaking culture on retinal marker expression in size matched EBs at day 15 of differentiation**

In order to fairly and separately analyse the impact of orbital shaking on progression of retinal differentiation at day 15, gene expression profiles from EBs of the same size cultured in either adherent or orbital shaken protocols are analysed separately.

#### Orbital shaking - 5K EBs (Figure 5.13A)

A comparison of the gene expression profiles of size-matched (5K) EBs between adherent and orbital shaken cultures revealed that at day 15, orbital shaking results in comparable levels of early retinal marker *Otx2* and photoreceptor precursor marker *Crx* between the culture techniques. For later photoreceptor-specific markers, *Nrl* expression is up-regulated in orbital shaken cultures (2.39 fold,  $p=0.026$ ), while the change in expression of *Rho* remained negligible. Interestingly, there was a much larger downregulation in expression of pluripotency marker *P0U5F1* in orbital shaking compared to adherent cultures (8.08 fold,  $p=0.000015$ ).

#### Orbital shaking - 10K EBs (Figure 5.13B)

In direct comparisons between size matched (10K) EB cultures across adherent and orbital shaken systems, at day 15 orbital shaken culture provides a greater impact on the expression of retinal markers and *P0U5F1* than in adherent cultures than in 5K EBs. For early eye field markers, orbital shaken culture of 10K EBs results in a 5.16 fold downregulation ( $p=0.00386$ ) of *Otx2* and expression of photoreceptor precursor marker *Crx* is also significantly reduced (6.36 fold  $p=0.00049$ ) compared to the adherent 10K EB controls. The photoreceptor marker *Nrl* however was expressed at 2.93 fold higher ( $p=0$ ) levels in orbital shaken cultures than adherent cultures with 10K EBs. Suggesting that 10K EBs cultured in orbital shaken cultures may have consisted of more mature retinal cell populations than their adherently cultured counterparts. Together with the down-regulation (3.6 fold,  $p=0.01$ ) of pluripotency marker *P0U5F1* in these cultures the data may indicate that orbital shaking cultures accelerate differentiation toward retinal lineages when compared to adherent cultures, without the addition of Matrigel.

Together the QPCR data show that when compared to size matched adherent cultures containing Matrigel, orbital shaking culture promoted a decrease in expression of

pluripotency marker POU5F1 whilst upregulating photoreceptor marker Nrl in both 5K and 10K EBs. For the larger 10K EBs, this pattern was accompanied by a coinciding reduction in the early markers of retinal differentiation Otx2 and photoreceptor precursor marker Crx, further supporting the hypothesis that these cultures contained more mature differentiated population of retinal cells.

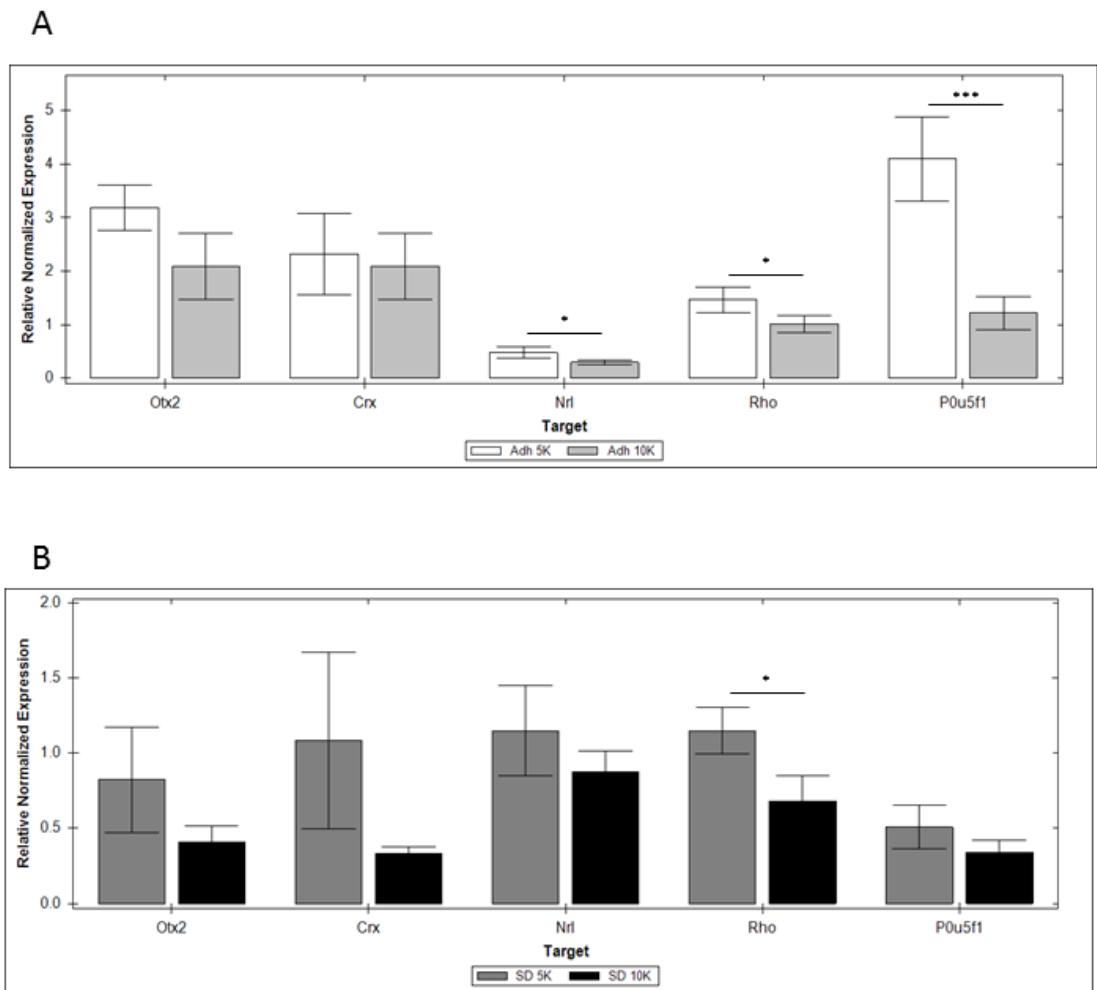


**Figure 5.12** The impact of EB size on differentiation in adherent and orbital shaken cultures at day 15. Relative expression of eye field transcription factor genes Otx2, Crx, Nrl, Rho and pluripotency marker POU5F1 in EBs at day 15 for (A) adherent (Adh 5K & Adh 10K) and (B) orbital suspension cultures (SD 5K & SD 10K). Retinal EBs with formation sizes of 5K or 10K cells/EB were produced using MSU001 cells.

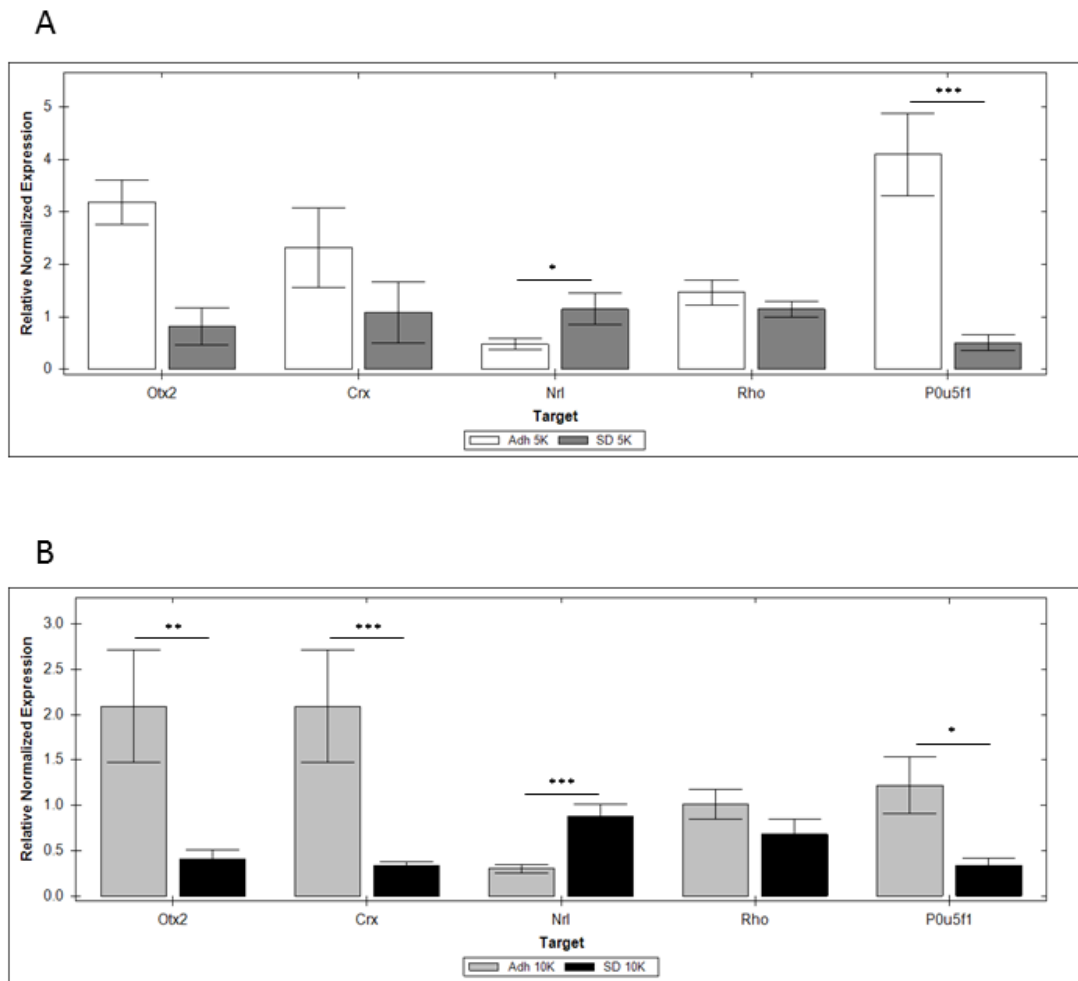


**Figure 5.13** The impact of orbital shaken culture on retinal differentiation of EBs made from 5K or 10K cells/EB at day 15. A day 15 comparison of gene expression profiles between size-matched EBs of **(A)** 5K or **(B)** 10K cells cultured in adherent (Adh 5K and Adh 10K) versus orbital shaken cultures (SD 5K & SD 10K). Relative expression of eye field transcription factor genes Otx2, Crx, Nrl, Rho and pluripotency marker POU5F1. EBs were produced using MSU001 cells

## **5.6 Day 21: QPCR Analyses of EFTFs and POU5F1 expression**

### **5.6.1 The impact of varying input EB size on retinal differentiation at day 21**

#### Adherent culture (Figure 5.14 A)

After 21 days in culture the gene expression profiles of adherent EBs show that the larger 10K EBs express less *Nrl* (1.28 fold,  $p=0.0217$ ) than the 5K EBs. In the 10K EBs, the reduced *Nrl* expression is accompanied by downregulation of *POU5F1* (1.83 fold,  $p=0.03127$ ) but no significant changes are observed in gene regulation of the other markers of differentiation in response to a change in EB size. In summary, the QPCR data at day 21 shows the impact of increasing EB size from 5K to 10K was to cause a reduction in the expression of pluripotency marker *POU5F1*, signaling a reduction in the presence of pluripotent cells in the cultures. The reduced expression of photoreceptor marker *Nrl* in adherent cultures but not in orbital shaken cultures was an interesting finding which warrants further immunohistochemical or FACS analyses to try and establish the identity of the cultured cells.

#### Orbital shaken cultures (Figure 5.14 B)

21 days in orbital shaken culture resulted in more homogenous gene expression profiles between both 5K and 10K EB sizes. The photoreceptor precursor marker *Crx* was the only significantly differentially expressed gene between the 10K and 5K EBs with a 1.79 fold ( $p= 0.04863$ ) reduced expression in larger 10K EBs. The rest of the markers for retinal differentiation (*Otx2*, *Nrl* and *Rho*) and marker of pluripotency *POU5F1*, were expressed at similar levels with no statistically significant differences observed between them. The higher expression reduced expression of *Crx* in larger EBs in orbital shaken culture, once again may support the idea that the cell populations within these 10K EBs may have differentiated to more mature types

With only one differentially expressed gene (*Crx*) between 5K and 10K EBs in orbital shaken culture, the data also suggests that by day 21, EBs in orbital shaken cultures may be composed of more homogenous cell populations than their adherent culture counterparts which showed differential expression in *Nrl* and *POU5F1*.

## 5.6.2 The impact of orbital shaken culture on EBs at day 21

### 5 K EBs in orbital shaken culture at day 21 (Figure 5.15 A)

For smaller 5K EBs at day 21, expression of the early eye field transcription factor Otx2 and photoreceptor precursor marker Crx were similar, with no statistically significant differences detected between adherent and orbital shaken cultures. Photoreceptor marker Nrl did show differential expression between the cultures with a downregulation of 1.4 fold ( $p=0.00188$ ) in orbital shaken cultures compared to adherent controls. No significant differences were observed in the expression of the later photoreceptor marker Rho.

Expression of the pluripotency marker POU5F1 was significantly reduced in orbital shaken cultures (8.14 fold,  $p=0.00029$ ). The large reduction in expression of pluripotency marker POU5F1 may provide some support for the hypothesis that orbital shaking can help accelerate differentiation but the coinciding evidence for downregulation in expression of Nrl may lie in contradiction. The reduced Nrl expression in 5K EBs in orbital shaken compared to adherent cultures, may suggest that orbital shaking may have ceased to support continued differentiation of photoreceptors by day 21. The higher expression of Nrl in adherent cultures at day 21 could also be a result arising from the effects of undefined ingredients present within Matrigel which have provided an advantage for Nrl expression at this time point.

### 10K EBs in orbital shaken culture at day 21(Figure 5.15 B)

As with the 10K EBs in orbital shaken culture at day 15, larger 10K EBs in orbital shaken culture at day 21 also showed a greater down-regulation in expression of early eye field marker Otx2 (3.21 fold,  $p=0.00336$ ) compared to their adherent controls. Also in line with the day 15 gene expression profiles, 10K EBs in orbital shaken culture showed significant downregulation in Crx expression (7.95 fold,  $p=0.00027$ ) when compared to their size-matched adherent controls. Unlike the day 15 10K EBs however, at day 21 Nrl expression between adherent and orbital shaken cultures was comparable without any statistically significant differential expression between the culture systems. Finally expression of the pluripotency marker POU5F1 also follows

the pattern from day 15 and a significant reduction in expression is observed in the 10K EBs in orbital shaken culture (4.37 fold,  $p=0.00032$ ) compared to their adherent controls.

Together the day 21 gene expression profiles of 10K EBs at day 21, also support the idea that cultures of larger EBs in the orbital shaken system may have consisted of more differentiated cell populations than their adherent counterparts. The downregulation of pluripotency (POU5F1) and early markers of retinal differentiation (Otx2 and Crx) support this claim and the similar expression of Nrl between the adherent and orbital shaken cultures for larger 10K EBs may also suggest orbital shaken culture supports later differentiation in larger EBs better than for smaller 5K EBs. Alternatively it may have been the case that both orbital shaken and adherent culture of 10K EBs at day 21 ceased to support continued differentiation of the EBS or that both systems had reached maximal expression of Nrl by this time point.

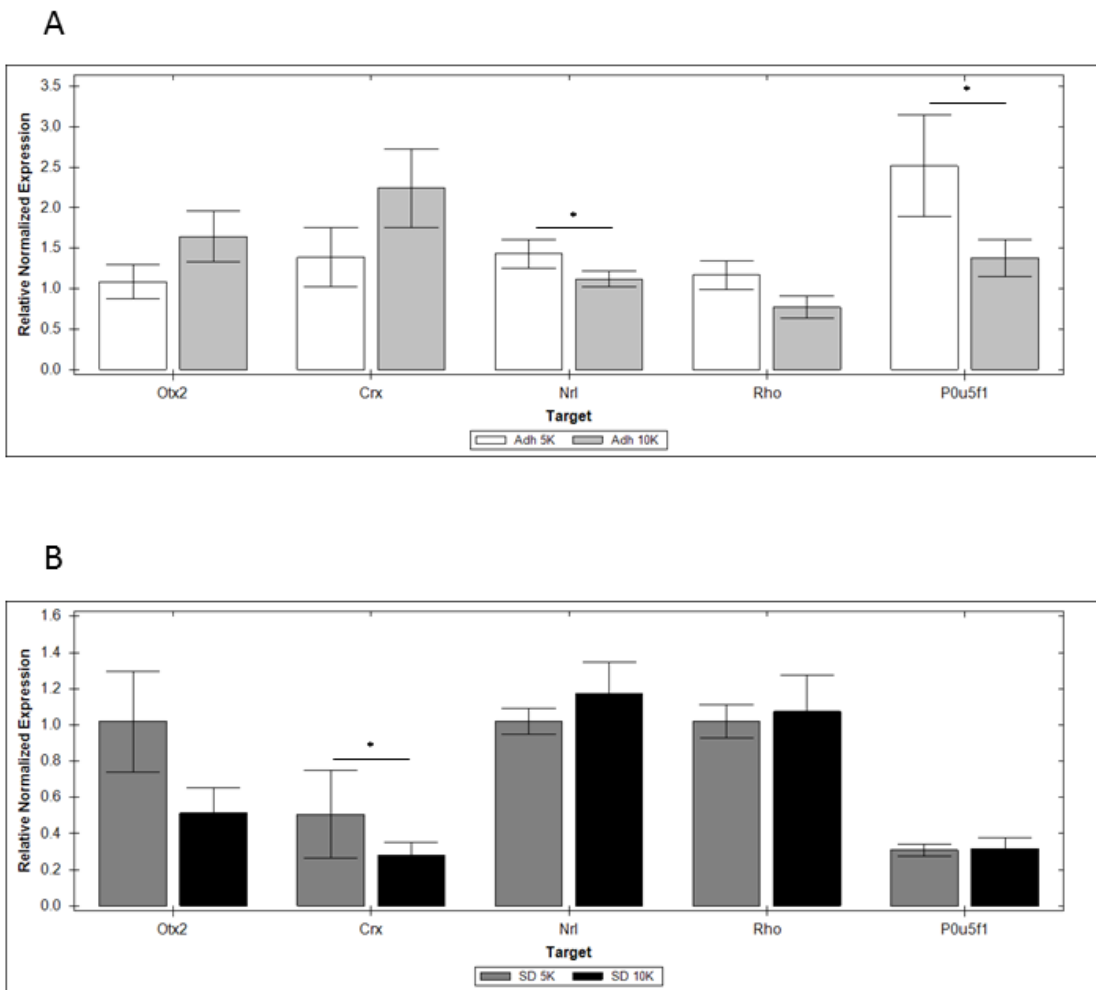


**Figure 5.14** Impact of EB size on differentiation in adherent (A) and orbital shaken (B) cultures at day 21. Relative normalized gene expression of eye field transcription factor genes *Otx2*, *Crx*, *Nrl*, *Rho* and pluripotency marker *P0U5F1* in EBs at day 21 for (A) adherent and (B) orbital suspension cultures. Retinal EBs with formation sizes of 5K or 10K cells/EB were produced using MSU001 cells

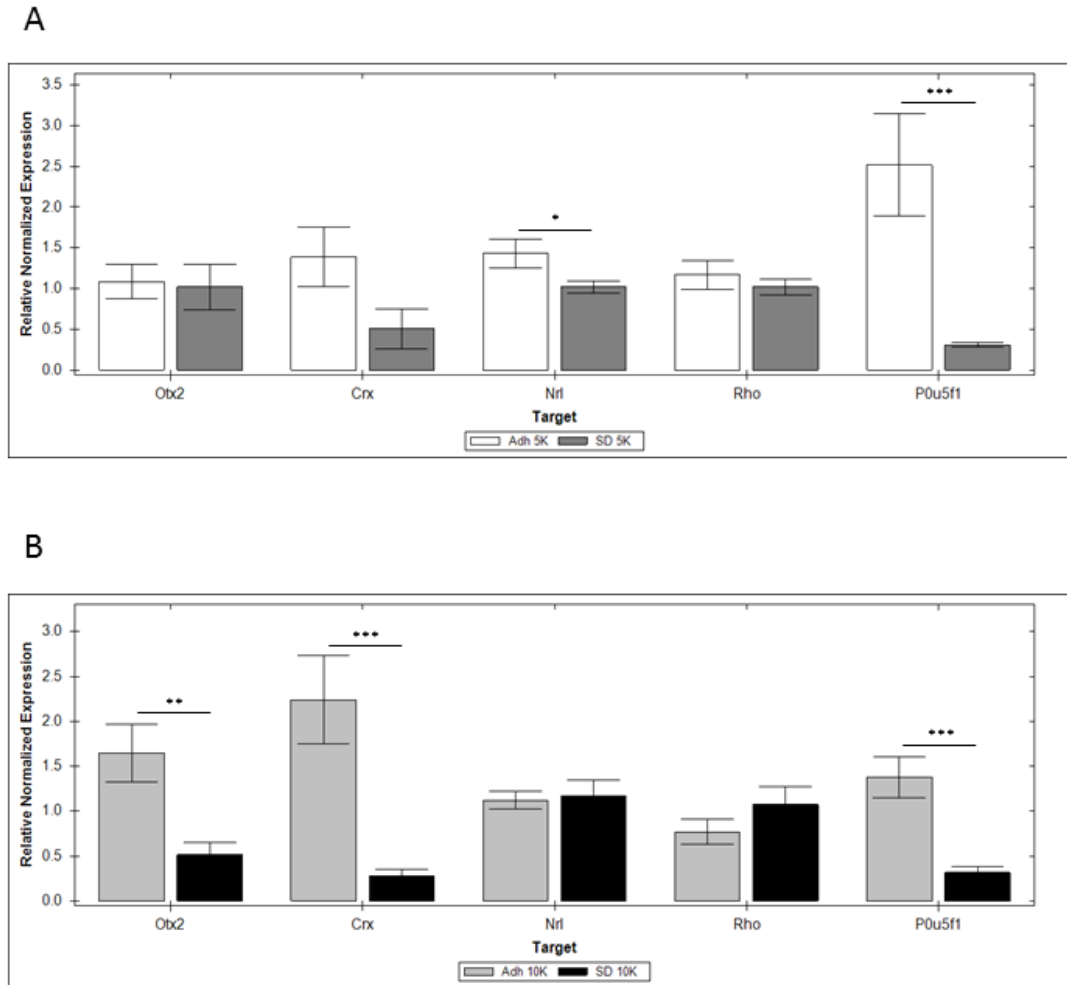


**Figure 5.15** The impact of orbital shaking culture on retinal differentiation at day 21. Comparison of relative normalized gene expression profiles at day 21, between size-matched EBs of (A) 5K or (B) 10K cells cultured in adherent versus orbital shaken systems. Relative expression of eye field transcription factor genes Otx2, Crx, Nrl, Rho and pluripotency marker POU5F1. EBs were produced using MSU001 cells

### **5.6.3 Time course analyses of pluripotency and retinal marker expression**

In order to appreciate the variation in expression of pluripotency marker POU5F1 and the retinal panel marker expression (Otx2, Crx, Nrl and Rho) with time Figure 5.16 presents the relative normalised expression profiles of the targeted genes in a clustergram. The clustergram allows a broad comparison of differential gene expression between adherent and orbital shaken culture techniques as well as between both EB sizes for all time points sampled (days 10, 15 and 21). In Figure 5.16 The dendrogram bars under the gene targets at the bottom of the clustergram show the shortest Dendrogram bars are observed between Crx and Otx2 expression indicating their expression profiles are the most closely related. The expression profile POU5F1 is the next most closely linked to the early retinal marker expression profiles, a pattern seen in most samples regardless of input EB size or culture technique. The longer Dendrogram bars adjoining POU5F1 and the grouped early markers of retinal differentiation Otx2 and Crx, with later markers Nrl and Rho show the hierarchical relationship between the expression profiles of these two sets of genes.

The dendrogram shows the relative similarity in gene expression profiles of all the target genes across culture techniques and regardless of input EB size at day 10. Suggesting that by 10 EBs in all culture environments were propagating almost uniformly toward retinal lineages. Day 15 of retinal differentiation culture seems to be an important timepoint for adherent samples, which express high levels of all retinal markers except Nrl coinciding with downregulation of POU5F1 at this time. In orbital shaken cultures day 15 also seems important, as all cultures seem to have switched expression from early to later retinal markers which coincides with downregulation of POU5F1. The improved homogeneity of retinal marker expression between EB sizes in orbital shaken culture is also apparent by day 15 and continues through to day 21. For adherent cultures at day 21 the gene expression profiles follow the same pattern of downregulation of early genes with upregulation of later retinal markers but persistence of expression of earlier retinal markers especially Crx shows the more heterogeneous nature of these cultures compared to orbital shaken culture.

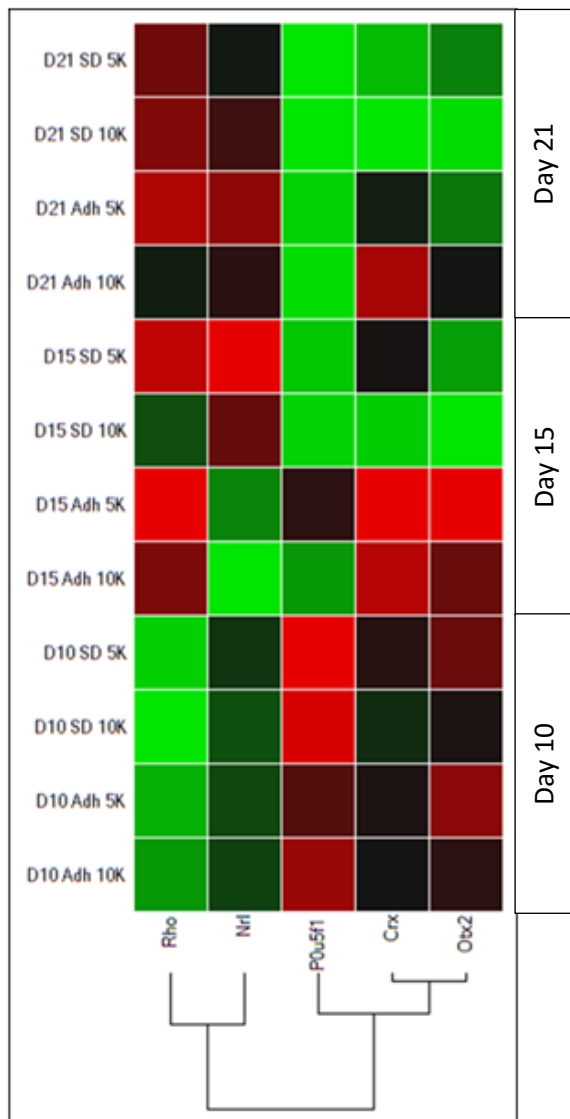


**Figure 5.16** Clustergram showing the levels of relative normalized gene expression of pluripotency marker POU5F1 and retinal markers OTX2, CRX, RHO and NRL across different EB sizes and culture techniques over days 10, 15 and 21. Samples are arranged according to sample time points on the y axis for days 10, 15 and 21. From left to right the row of squares at each time point shows the intensity of gene expression of pluripotency marker POU5F1, Otx2, Crx, Nrl and Rho. Sample nomenclature on the y axis indicates the culture day (D10), (D15) or (D21), whether the sample was from adherent (Adh) or orbital shaken culture (SD) with the input EB size of (5K) or (10K) cells/EB. The colour of each cell indicates the intensity of expression of a marker for each condition (green-low, red-high). Gene expression levels for all samples were normalised to internal reference genes Beta Actin and GAPDH. The samples are clustered by the targets to show the hierarchical relationship between these genes with time. The length of Dendreon bars under each target represent their linkage (longer bars for more dissimilarity).

## 5.7 Summary

In this chapter we tested the hypothesis that progression of retinal differentiation is possible in orbital shaken cultures without Matrigel supplementation up to 21 days. Immunohistochemistry was performed to show the presence of retinal cell populations, and differential gene expression profiles by QPCR helped to show the different impacts of adherent and orbital shaking cultures on EBs with input sizes of 5K or 10K cells/EB. We measured culture oxygen consumption rates and pH to understand the impact of orbital shaking culture on the microenvironment and performed cell quantification and LDH assays to assess the impact of EB size and culture technique on cell health and yields. The approach of using size matched EBs in control adherent cultures alongside orbital shaken cultures allowed us to separate the effects of orbital shaking from the effects of EB size on retinal differentiation respectively.

In characterising the effects of orbital shaking, we observed that a doubling in the cell numbers of input EBs from 5K to 10K cells/EB was not represented with observable differences between immunohistochemistry images or cell quantification experimental data, despite the fact that orbital shaken cultures for both EB sizes were subjected to the same medium exchange regimes throughout the culture period. It may therefore be possible that the EBs were adapting to the availability of nutrients. Detailed analysis of the medium metabolite profiles throughout the culture period might help future optimization experiments to determine ideal medium volumes and nutrient concentrations for these cultures.

Primary evidence for the differentiation and progression of EBs toward retinal specification, was provided by the immunostaining of retinal markers at the protein level in Figures 5.5 to 5.9. The retinal identities of constituent cell populations within differentiating EBs was also reflected in the QPCR data, summarized in the clustergram time course for adherent and orbital shaken cultures from days 10, 15 and 21 (Figure 5.16). The overview provided by the clustergram also showed the close fit between 5K and 10K EBs in both culture techniques in addition to showing the general pattern of changes in retinal marker expression from early to late markers over the culture period. The clustergram also showed downregulation of pluripotency marker expression with time, coincides with down-regulation of the early eye field marker

OTX2 and up-regulation of the later retinal markers NRL and RHO for both 5K and 10K EBs in both adherent and orbital shaken cultures.

If we consider adherent cultures as positive controls, the greater similarity observed in the relative normalised gene expression profiles between 5K adherent and 5K orbital shaken cultures compared to the same comparisons with larger 10K EBs may suggest, 5K EBs were better suited to orbital shaken culture than 10K EBs (Figure 5.15). The 10K EBs in orbital shaken culture however showed more intense downregulation of early retinal markers and POU5F1 expression when compared to their adherent controls suggesting, larger 10K EBs may have differentiated more rapidly in orbital shaken than adherent cultures.

Our data show that changing EB size had greater influence in adherent than orbital shaking EB cultures with larger EBs demonstrating higher expression of later retinal differentiation marker NRL and reduced pluripotency marker POU5F1 expression, than smaller 5K EBs (Figure 5.14) in orbital shaking cultures. The reduced impact of varying EB size in orbital shaken cultures is demonstrated by the similarity in retinal marker expression profiles for both sized EBs. The main difference in expression profiles between the two sizes under orbital shaken cultures was that larger EBs expressed less RHO at day 15 (Figure 5.12) and showed reduced expression of CRX at day 21 (Figure 5.14) than their 5K counterparts. These data could suggest that larger EBs consisted of later differentiated populations but more detailed FACS analyses would be necessary to confirm this hypothesis.

The broadly similar expression profiles of markers for retinal differentiation show the change in expression of pluripotency marker POU5F1 and early markers of retinal differentiation Otx2 and Crx reduces with time; as expression of later retinal markers Nrl and Rho are expressed toward the end of the culture period in both EB sizes, across culture techniques (Figure 5.16). The greater similarities in gene expression profiles between the 5K and 10K EBs in orbital shaken as opposed to adherent cultures might also indicate that orbital shaking cultures were more homogenous than adherent cultures. Appendix 1 and previous reports from this department also provide evidence for improved homogeneity of soluble factor gradients throughout the medium in orbital shaken cultures (Rodriguez et al. 2014). The improved mixing supported by orbital shaking may also explain the effect of reducing the impact of changing the

starting EB size on differentiating cells in orbital shaking cultures. Although the retinal gene expression profiles were more homogenous between different EB sizes in orbital shaken culture, larger EBs in orbital shaken culture deviated more from their adherent control retinal gene expression profiles (Figure 5.16). The greater fidelity between the retinal expression profiles of 5K EBs in orbital shaken culture and their adherent controls may suggest that 5K EBs were slightly better suited to orbital shaken culture than 10K EBs. Quantitative assessment of this hypothesis would require FACS analyses which were not performed in this report but together our data here, supports the hypothesis that orbital shaking reduces the impact of variation in differentiation, due to changes in starting EB size.

## **6.0 Orbital shaken culture of EBs for retinal differentiation with a feeder free cell line**

### **6.1 Introduction**

We have demonstrated orbital shaking culture in low-attachment 24 microwell plates is a successful platform for initiating retinal differentiation of EBs created from human IPS cells grown on mouse embryonic fibroblast cells (feeders) with the MSU001 IPS cell line in chapters 3 to 5. The feeder cell dependent nature of MSU001 hiPSC provided motivation to test whether orbital shaken culture could support the initiation of retinal differentiation in another feeder-free cell line.

A human foreskin fibroblast derived IPS cell line: BJ IPS (kindly gifted by Dr Amanda Carr, UCL, Institute of Ophthalmology) was sourced in an attempt to recapitulate differentiation toward retinal cell fates using the orbital shaken system described in chapter 5. The BJ IPS cells were cultured in a fully defined xeno free stem cell culture medium E8 (Invitrogen) which contains 8 components and was used in combination with a xeno-free defined substrate vitronectin to coat tissue culture vessels instead of animal derived Matrigel, or mouse embryonic fibroblasts. The only remaining animal derived components persisted in the adapted protocol for retinal differentiation from the early differentiation medium which contained FBS for the first 3 days of differentiation culture.

The removal of undefined and xenogeneic ingredients is an important step when considering potential clinical development as discussed Section 1.4, to improve culture purity and the safety of potential therapeutics. Additional benefits include the potential to improve the consistency of cultures, since guaranteeing exact quantities of undefined animal derived components is not possible. Though Matrigel and hiPSC cultured on animal feeders are still commonly used in differentiation protocols, it is foreseeable that a greater degree of definition and refinement will be important in future recommendations from regulatory bodies when governing the production of cellular or other biological therapeutics for human use. Better defined cultures will facilitate more accurate characterisation of cell populations. Ultimately defined cultures will also improve process understanding to identify and quantify which factors in the microenvironment of stem cell culture and processes, have the greatest impact

on differentiation into therapeutic cell types, cell health and cell yields as discussed in chapter 5.

In this chapter the BJ IPS feeder free cell line selected, is used to perform proof of principle experiments using one EB size (10K cells/EB) and culture over 15 days of retinal differentiation. Day 15 of culture was determined to be a key stage to assess progression to retinal differentiation from the relative gene expression results observed with MSU001 EBs in Chapter 5. By day 15 MSU001 EBs cultured in orbital shaken and adherent cultures showed expression of key markers of retinal differentiation with coinciding downregulation of pluripotency marker POU5F1. The aim of this chapter is to recapitulate these findings for the feeder free cell line to show initiation of retinal differentiation in orbital shaken culture in a similar system.

### **6.1.1 Aims and objectives**

- Test the impact of using Aggrewwells on the initiation of differentiation toward retinal cell fates in a second cell line.
- To determine whether orbital shaken culture of EBs supports retinal cell fate differentiation in a second feeder free IPS cell line.
- To characterise the impact of orbital shaking on differentiation toward retinal cell fates using immunohistochemistry and QPCR analyses.

## **6.2 Forced aggregation maintains consistent EB formation sizes with BJ hiPSC derived EBS which express early retinal markers at day 3**

The forced aggregation approach for forming EBs has been characterised for use with BJ IPS cells in Chapter 3 which demonstrated BJ IPS cells are also amenable to producing uniform controlled sized input EBs using the Aggrewell protocol. The protocol's suitability for uniform production of larger 10K EBs is shown in Figure 6.1, where light microscopy images of EBs formed by forced aggregation were compared to EBs formed by scraping (Figure 6.1(i)). The images demonstrate the expected improvements in uniformity of EB size as a result of using the forced aggregation to form EBs. The resulting EBs formed of 10K cells/EB, were cultured in retinal

differentiation medium in suspension without shaking for 3 days before further analysis. In keeping with the protocol used throughout this report the 10K BJ EB and scraped BJ EBs were also analysed by QPCR at day 3. The relative normalized gene expression profiles of both forced aggregation and scraped EBs show that scraped EBs outperformed forced aggregation EBs for the expression of all markers of retinal differentiation. Compared to scraped EBs the forced aggregation 10K EBs showed significantly reduced expression of early retinal field transcription factors Pax 6, Rx and Six3 (Pax6 2.51 fold,  $p=0.000002$ , Rx 8.96 fold,  $p=0$  and Six3 1.48 fold,  $p=0.031908$ ). The only gene expressed at similar levels between the scraped and forced aggregation EBs at day 3 was Otx2 which was the only insignificantly differentially expressed target between the two conditions (Figure 6.1(ii)).

Comparing scraped EBs against forced aggregation 10K EBs, the controlled sized EBs also showed reduced expression of pluripotency marker POU5F1 (3.64 fold,  $p<0$ ). The reduced expression in POU5F1 would be consistent with previous findings which showed reduced expression of POU5F1 coinciding with increased expression of retinal markers in EBs suspension culture with retinal differentiation medium in Chapter 4. The results were also consistent with the theory that differentiated cells downregulate POU5F1 expression. In light of this information results showing the greater reduction in POU5F1 expression for forced aggregation EBs were initially interpreted as indicating a faster differentiation toward retinal lineages for the larger more uniform 10K aggregates than their scraped BJ EB controls. However the greatly reduced expression of all other markers of retinal differentiation except Otx2 also suggest that the homogenous forced aggregate EBs may not have been differentiating as fast as the scraped EBs.

The precise molecular mechanisms governing human eye development are still largely unknown and the required levels of expression of retinal markers to initiate differentiation have not been determined. Consequently it was difficult to draw precise conclusions about the stage of eye development reached by EBs at day 3 of culture, based solely on the levels of gene expression detected (Figure 6.1(ii)). However, detection of the early markers of retinal differentiation albeit slight in the forced aggregates prompted further analyses to ascertain whether retinal marker expression might improve with more time in culture.

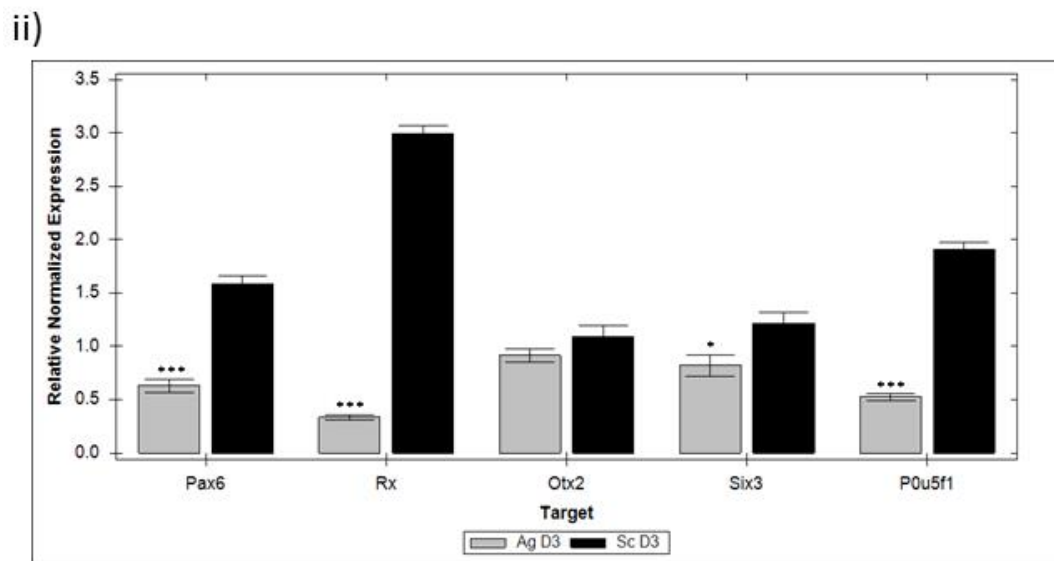
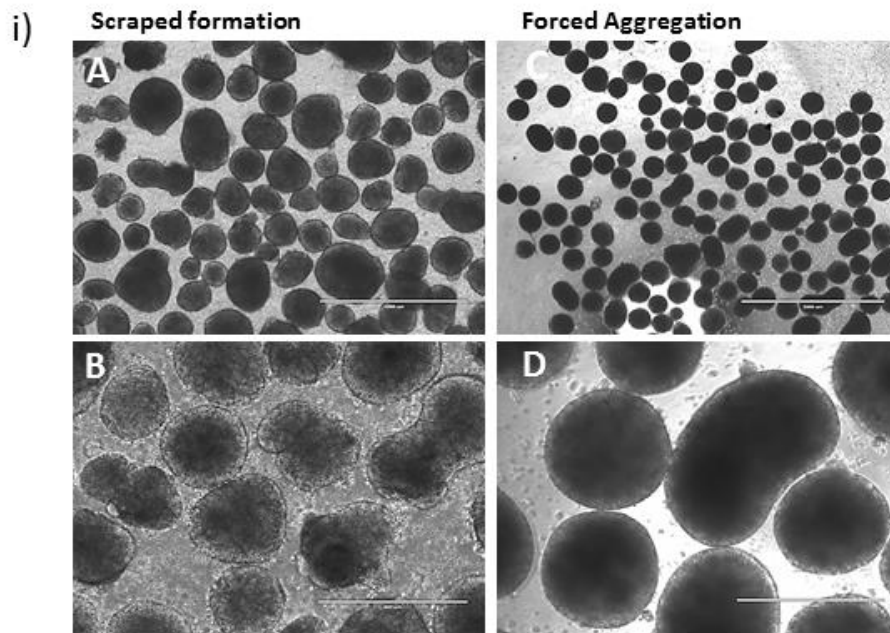


**Figure 6.1 (i)** Representative micrograph images of BJ retinal EBs made from 10K cells at day 3 of differentiation. EBs were formed by scraping (A and B) or forced aggregation (C and D). Scale bars = 1000  $\mu$ m (A and C) 400 $\mu$ m (B and D).

**(ii)** Relative expression of early retinal transcription factor genes Pax 6, Rx, Otx2 and Six3 with pluripotency marker POU5F1 in BJ EBs formed by forced (AgD3) or by scraped (ScD3) aggregation from 10K cells/EB at day 3. One way ANOVA analyses of gene expression levels in scraped EBs against forced aggregation EBs are shown (\* $p < 0.05$ , \*\* $p < 0.01$ , \*\*\* $p < 0.001$ )

### **6.3 Orbital shaken cultures support initiation of retinal differentiation in the feeder free cell line BJ IPS derived EBs**

EBs of 10K cells/EB formed by forced aggregation were cultured in adherent and orbital shaken systems for 15 days with 48 hourly medium exchanges and sampled at days 10 and 15 of differentiation. Microscopy analyses, immunohistochemical assays and QPCR assays were performed to assess how the progression of differentiation toward retinal cell fate is affected by the feeder free source of the BJ IPS cells and to test if a longer culture time could improve the detection of markers for retinal differentiation.

Light microscope images of EBs from days 10 and 15 in adherent and orbital shaken cultures were compared for the similarity of their morphological features to those observed in the MSU001 EBs (Chapter 5). Typical spherical shapes of floating EBs with the appearance of phase bright rings around dark centres were observed in most EBs and interpreted as signs for retinal lineage differentiation (Sridhar et al. 2013). Representative images of EBs in adherent and orbital shaken culture at days 10 and 15 illustrate these typical qualities of EBs differentiating along retinal fates (Figure 6.2).

In order to confirm the presence of retinal cells, in the differentiating EBs immunohistochemical were performed for EBs at day 15 of culture as presented in the figures below.

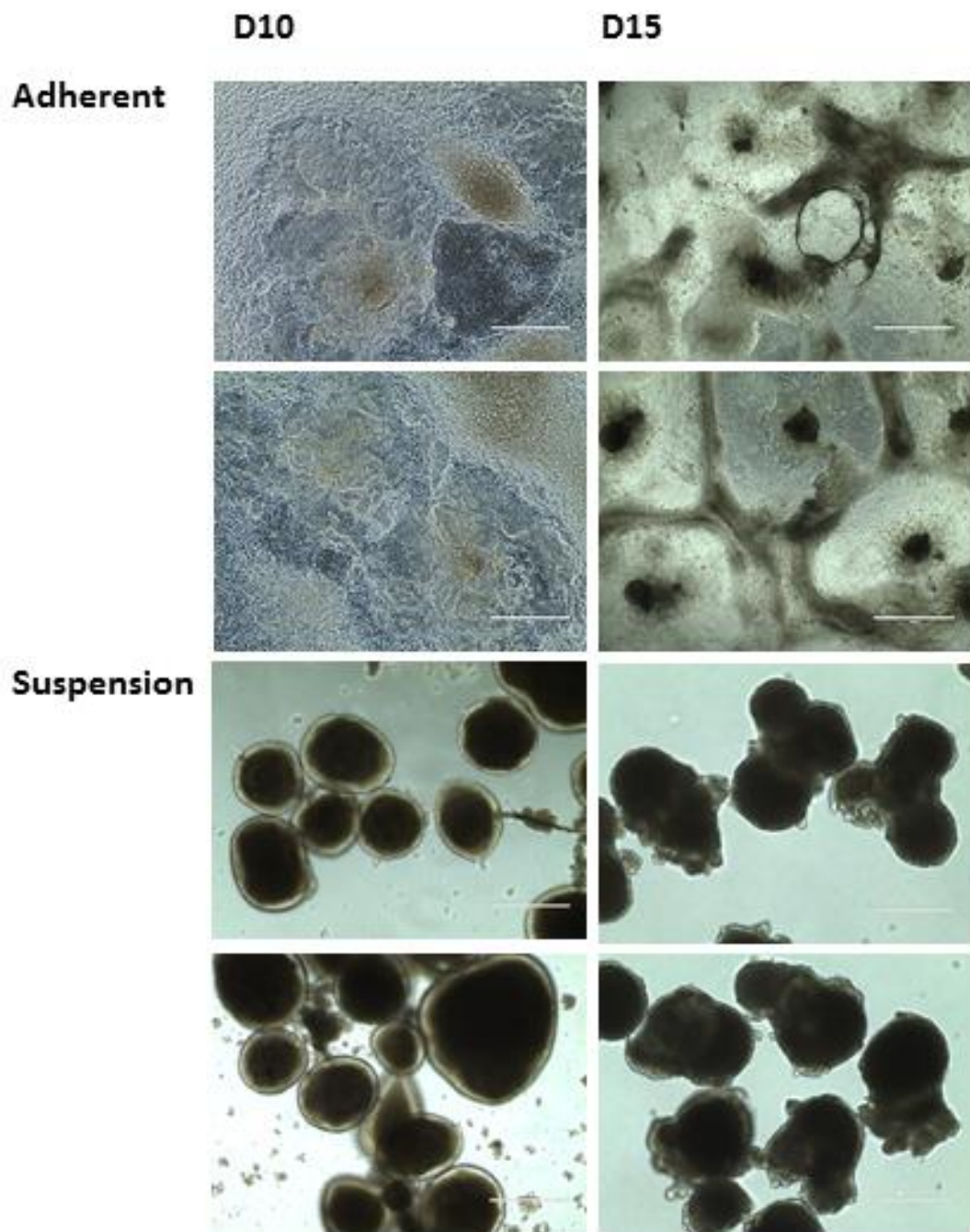


**Figure 6.2** Representative micrograph images of BJ EBs formed of 10K cells per EB grown in adherent or orbital shaken suspension cultures at days 10 and 15. Images were taken on an Evos microscope at 20x magnification scale bars = 1000um for adherent EBs and 400um for suspension EBs.

### **6.3.1 Immunohistochemical analyses demonstrate expression of key markers of retinal differentiation**

Immunofluorescence images of 10K EBs from orbital shaken or adherent control cultures confirm protein level expression of pluripotent populations from the low-level expression of transcription factor Nanog, another marker for pluripotency in Figure 6.4. In support of this observation, albeit with a different marker for pluripotency, the gene level expression of the pluripotency marker POU5F1 from QPCR analyses also shows POU5F1 expression and therefore pluripotent cell states persist at day 15 or adherent and orbital shaken culture.

Immunohistochemical detection of the expression of the early retinal differentiation marker Otx2 detected at days 3 and 15 by QPCR (Figure 6.3 and 6.5) provided confirmation that retinal cell types were present alongside the pluripotent cells detected in orbital shaken cultures. Furthermore, low expression of the later photoreceptor precursor marker Crx was also detected by immunohistochemistry of EBs from both adherent and orbital shaken cultures at day 15 of retinal differentiation. At day 15, the later photoreceptor marker Rho was also detected by immunohistochemistry at low levels in adherent but not orbital shaken cultures (Figure 6.4).

Together the images in Figure 6.3 together with findings from the phase contrast images (Figure 6.2) which showed typical morphologies of EBs undergoing retinal differentiation help support the idea that initiation of retinal differentiation is feasible in orbital shaken culture with EBs from the BJ feeder free IPS cell line.

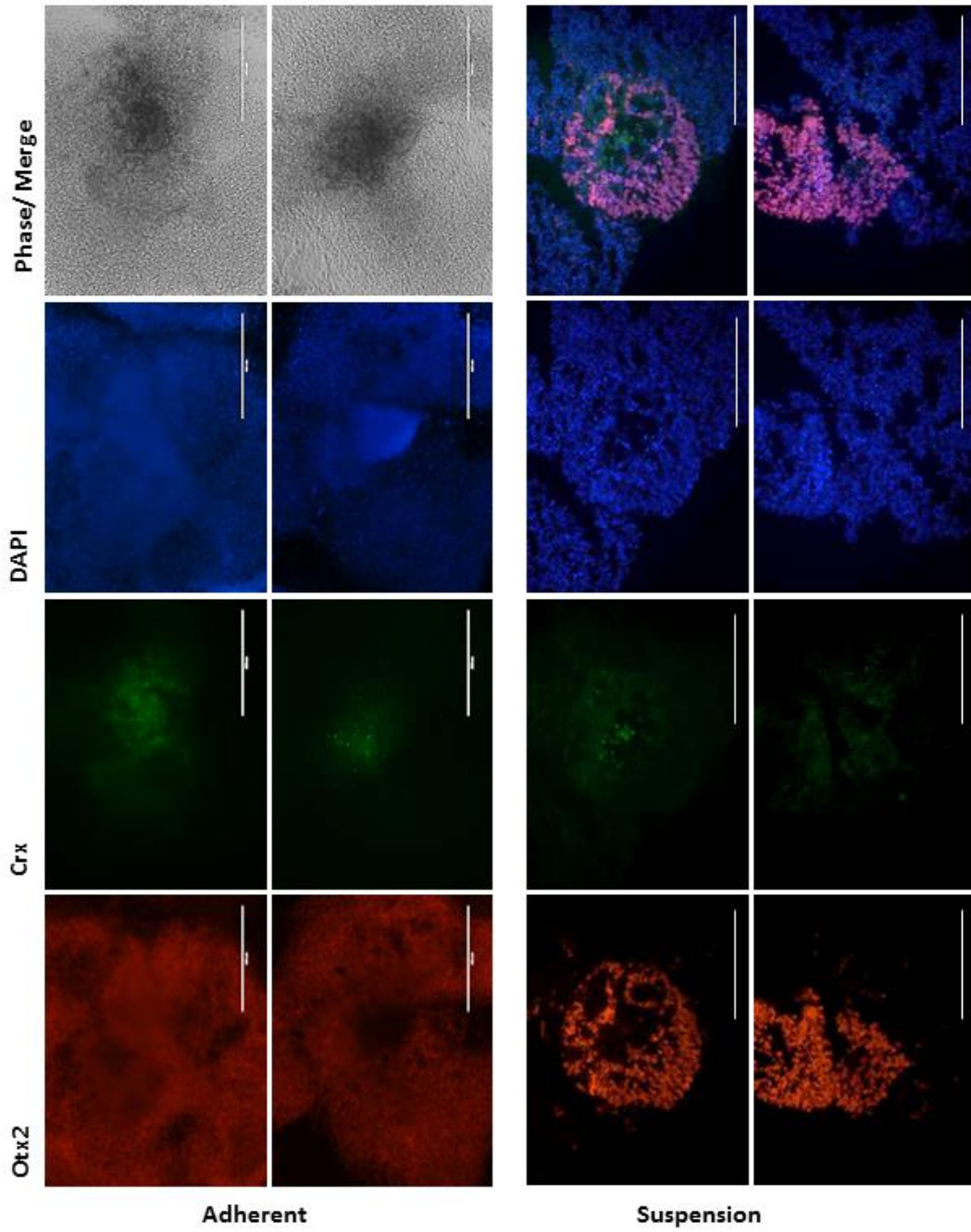
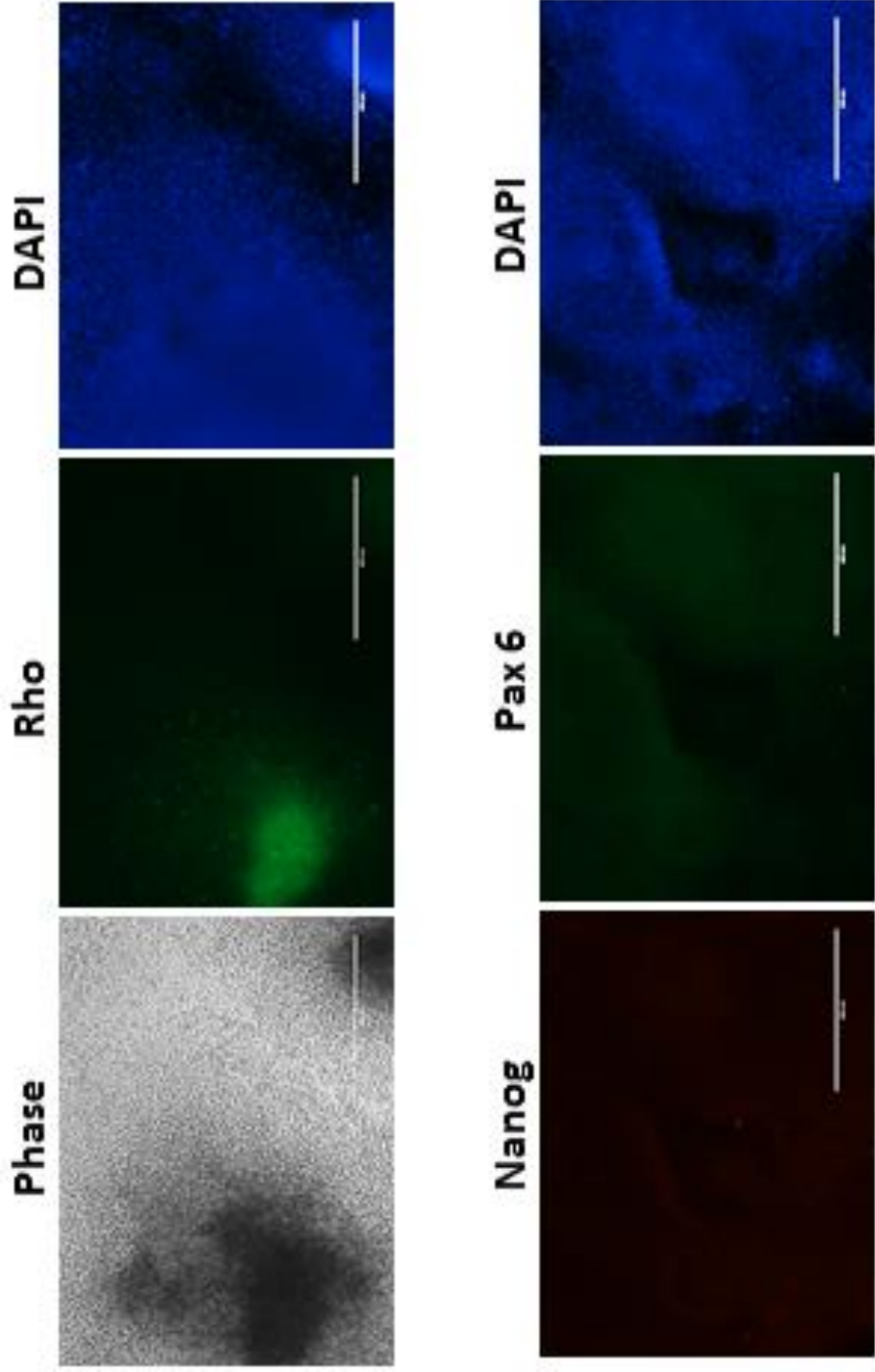


**Figure 6.3** Immunocytochemistry of adherent and orbital suspension BJ EBs made from 10K cells at day 15. Representative images show expression of retinal transcription marker Otx2 and photoreceptor precursor marker Crx. Immunocytochemistry of adherent cultures and cryosections performed as described in section 2.45-2.5. Images were taken at 20X magnification using an Evos microscope (adherent cultures) or an Olympus microscope (orbital suspension cultures) Scale bars = 400µm

**Figure 6.4**  
Immunohistochemistry of adherent EBs made from 10K cells/EB at day 15 showing expression of rod photoreceptor marker Rho, and relatively low expression of early eye field transcription factor Pax 6 and pluripotency marker Nanog.



## **6.4 QPCR analyses for retinal differentiation in orbital shaken cultures with BJ hiPSC derived EBs**

The QPCR analyses lend quantitative support for the immunohistochemical results showing evidence of retinal differentiation for EBs cultured under adherent and orbital shaken protocols at days 10 and 15. Orbital shaken EBs from cultures were compared for differential gene expression with control adherent cultured EB samples from the same time points. The adherent and orbital shaken samples were compared by the Pfaffl method to quantify relative gene expression using the delta delta CT method for consistency with the QPCR results in previous chapters. Relative quantification of gene expression of eye-field transcription factors *Otx2*, *Crx*, *Nrl* and *Rho* along with pluripotency marker *P0U5F1*, from adherent and orbital suspension cultures are presented for days 10 and 15 together in Figure 6.5 (A) and (B) respectively.

At day 10 of retinal differentiation a comparison of gene expression profiles between adherent and orbital shaken EBs (Figure 6.5 (A)) illustrates that expression of the early eye field marker *Otx2* in orbital shaken cultures is significantly reduced ( $p < 0.05$ ) compared to that of adherent control EBs. The reduced expression of *Otx2* in orbital shaken versus adherent controls at day 10 was not observed with MSU001 EBs (Figures 5.12), suggesting the BJ IPS cells may be following a different trend or timeframe for differentiation. Another difference between the day 10 expression profiles of BJ and MSU001 EBs was a significant downregulation of the photoreceptor precursor target *Crx* in orbital shaken cultures compared to adherent controls ( $p < 0.001$ ) for BJ EBs at day 10. Changes in gene expression of *P0U5F1*, *Rho* and *Nrl* between the orbital shaken and adherent cultures may suggest that BJ EB orbital shaken culture at day 10 may have supported more mature cell types than in adherent control cultures.

At day 15 retinal gene expression profiles between the adherent and orbital shaken cultures show only one significantly differentially expressed gene *Nrl* (Figure 6.5(B)). The expression of *Nrl* is expressed at 1.5 fold ( $p < 0.05$ ) higher levels in orbital shaken cultures compared to their adherent controls in 10K BJ EBs. Evidence of coinciding relative downregulation of pluripotency marker *P0U5F1* and *Otx2* were not observed

at day 15 for orbital shaken BJ EBs, showing a deviation from the trend established with orbital shaken MSU001 EBs at day 15 (Figure 5.15(B)). Consequently, interpreting the significance of the increased expression of *Nrl* is challenging. The increased expression of *Nrl* in orbital shaken EBs at day 15 compared to adherent controls suggests the presence of more differentiated cell types in these cultures.

The trend of decreased expression of *Otx2* and *P0U5F1* with comparatively increased expression of *Nrl* observed at day 15 in orbital shaken cultures for the MSU001 EBs (Figure 5.15(B)) is however still echoed in the day 15 gene expression profiles of the feeder free line for orbital shaken cultures in this chapter but without statistical significance (Figure 5.16). The lack of a statistically significant reduction in the expression of *Otx2* and *P0U5F1* in the orbital shaken BJ EBs, may also be indicative of the persistence of more pluripotent cells and immature early retinal cell types by day 15 in BJ EBs compared to orbital shaken MSU001 EBs at day 15 (Figure 5.16(B) and 6.5 (B)).

The QPCR data together show BJ orbital shaken EBs have a unique time frame and pattern of expression of retinal differentiation genes distinct from the trends observed in MSU001 EBs. These results may also indicate the BJ IPS cell line may be less suited to orbital shaken culture with 10K EBs than MSU001 EBs. The observed differences in gene expression profiles may be attributable to inherent biases within the cell line, the removal of feeders from the cell expansion phase or the use of vitronectin instead of Matrigel in the feeder free cultures.

Additionally, the expression profiles of *P0U5F1* in the day 10 and 15 cultures were unfortunately more variable either due to less accurate detection or technical errors during work with the feeder free cell line as indicated by the large error bars (Figure 6.5(B)). An alternate explanation may be there was much greater variability in *P0U5F1* expression between samples but this was not possible to verify during the scope of this work. A future improvement might include flow cytometry analyses of the cells in addition to the QPCR analyses, to better verify the observed trends and allocate proportions of the cell populations to their respective cell markers.

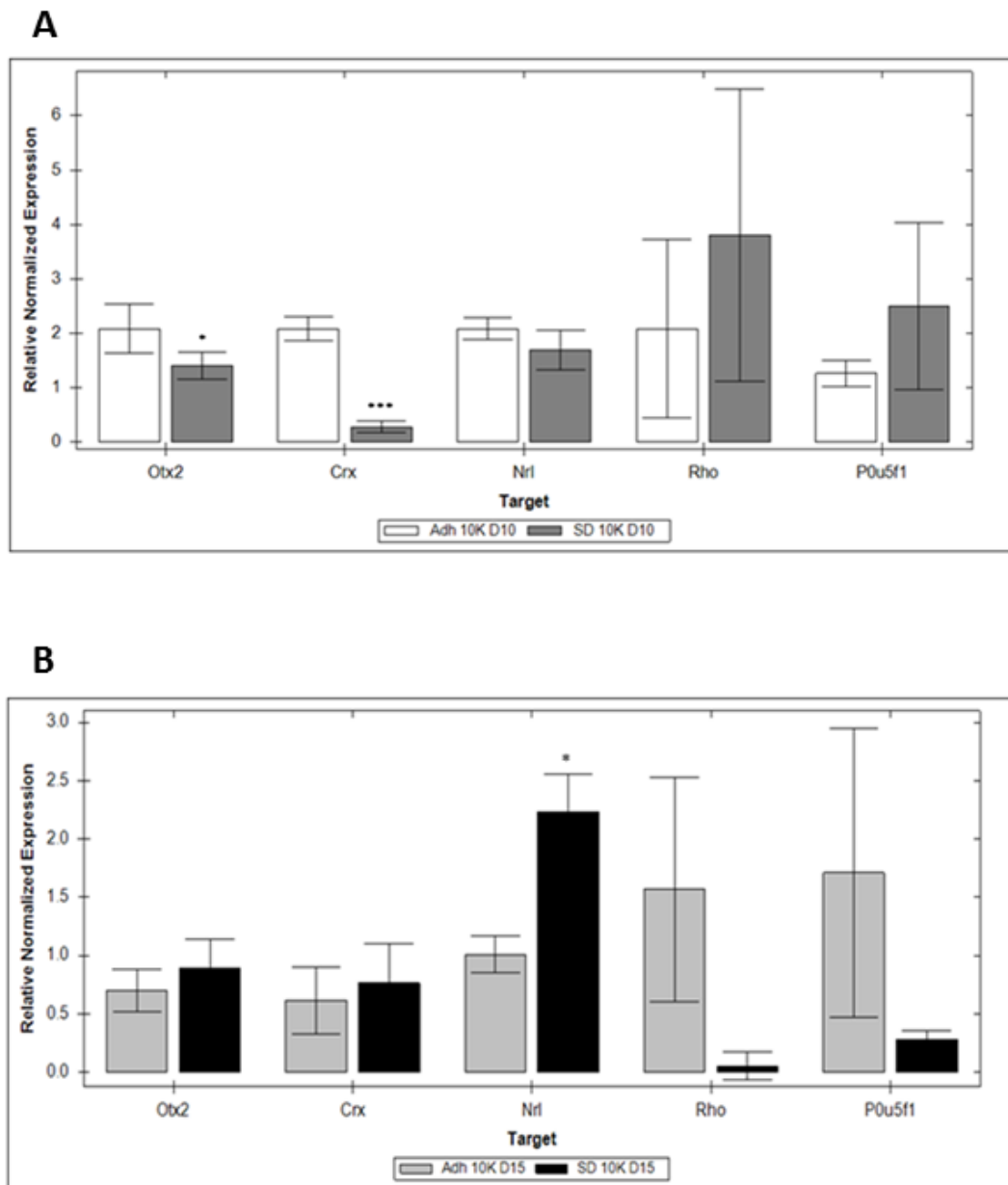


**Figure 6.5** Relative expression of early retinal transcription factor gene Otx2, photoreceptor precursor marker Crx, rod photoreceptor markers Nrl and Rho and pluripotency marker POU5F1 in differentiated BJ EBs made from 10K cells at day 10 (**A**) and 15 (**B**) for adherent and orbital suspension cultures. One way ANOVA analyses of gene expression levels against adherent EBs cultures made from 10K cells are presented (\* $p < 0.05$ , \*\* $p < 0.01$ , \*\*\* $p < 0.001$ ).

## 6.5 Summary

The aim of this chapter was to ascertain whether orbital shaken culture is a technique which can be applied to support retinal differentiation in a feeder free cell line. It was hoped the effects of relatively faster expression of early retinal markers and relatively increased expression of later retinal markers would be observed in comparisons with adherent control samples as they were in Chapter 5. Though the retinal gene expression patterns differed between orbital shaken MSU001 EBs and BJ EBs, this chapter demonstrated that orbital shaken culture is a system which can be utilised across different cell lines to observe the initiation of retinal differentiation as evidenced by the expression of retinal markers by immunohistochemistry and QPCR. We observed the expression of all the retinal markers investigated in previous chapters but with differing expression profiles to those observed in the MSU001 cell line. The inherent propensities of different cell lines and the lineage biases they confer has been documented before (Bauwens et al. 2008) and more recently differences in differentiation capacities due to changing EB sizes has also been reported (Moon et al. 2014). Therefore it may be the case that both EB size and cell line biases were factors which need to be independently optimised specifically with retinal differentiation in mind.

## 7.0 Conclusions and future work

### 7.1 Conclusions

The aim of this thesis was to test whether improving process control in a commonly used retinal differentiation protocol can improve the initiation of induced pluripotent stem cell differentiation toward retinal lineages. The experimental work aimed to show control over input EB size could be utilised using commercially available technology (Aggrewell plates, StemCell technologies) to improve the consistency of the initiation of differentiation. It was also our aim to test whether it was possible to adapt a commonly used 2D adherent retinal differentiation protocol to an orbital shaken suspension culture system in 24 well microwell plates. By adaptation of this culture technique our goal was to improve the uniformity of the microenvironment and test the hypothesis that orbital shaking can accelerate differentiation (Burrige et al., 2007 ; Carpenedo, Sargent, et McDevitt, 2007). Orbital shaken culture is known to improve mixing which led to the hypothesis such a system may also help eliminate the requirement for exogenous factors such as animal derived Matrigel from the culture medium. We monitored the impact of these process changes on the onset of hiPSC fate specification toward retinal differentiation using a commonly used protocol for retinal differentiation as the model system (Lamba et al. 2006).

The work in this thesis has shown evidence for successful retinal differentiation of control sized IPS derived EBs in orbital shaken culture by adaptation of an established adherent process for retinal differentiation (Lamba et al., 2006). By introducing controlled sized EBs (5K and 10K cells/EB) into an orbital shaken process it was possible to demonstrate more homogeneous initiation of retinal differentiation compared to static adherent cultures through retinal gene expression profiling. Furthermore, the results provide evidence that orbital shaken culture is capable of supporting retinal differentiation for up to 21 days, at shaking speeds of 120rpm. Additionally, by implementing the orbital shaken platform, it has been possible to eliminate the requirement for Matrigel supplementation to the culture medium.

**Review of methodology and results:** Although methods for uniform EB production are available many protocols for retinal differentiation recommend scraping which results in the production of variable sized EBs. Primarily to address the challenge of

variable sized EB production associated with scraped EB formation, we achieved control over EB formation efficiency and size by characterising a forced aggregation protocol for EB formation in chapter 3. Control over EB formation was achieved using forced aggregation and tight control over EB sizes (Figure 3.4 and 3.5). Forced aggregation improved the efficiency of aggregation and therefore the yield of cells incorporated for differentiation by >3fold ( $p<0.05$ ) (Section 3.2, Figure 3.3).

Comparisons of the levels of expression of markers of pluripotency and early retinal differentiation provided evidence that forced aggregation can be beneficial for the onset of retinal fate specification in EBs. Scraped EBs with uncontrolled sizes provided control samples to compare against forced aggregation EBs. The results first provided evidence that controlled sized EBs expressed key markers of retinal differentiation at comparable levels to their scraped controls (Figure 3.7). Having demonstrated EB size can be successfully determined by using specific numbers of cells available for aggregation in Chapter 3, the next aim was to determine if EB size impacts initiation of retinal differentiation.

Controlled size EBs also facilitated the selection of a permissive shaking speed of 120rpm for orbital shaken EB cultures (Figure 4.2). Determining a range of EB sizes practical for and amenable to orbital shaking culture conditions enabled the demonstration of the influence of initial EB size on progression and acceleration to retinal lineage specification (Figure 4.3). To track progression towards retinal specification QPCR analysis showed reduced expression of pluripotency markers coincided with upregulation of early retinal markers, indicating the initiation of retinal differentiation. Comparing orbital shaken cultures against scraped EB controls, the former showed higher expression of early eye field transcription factors Rx and Six3 ( $p<0.05$ ) with further reduced expression of the pluripotency marker POU5F1 ( $p<0.05$ ) (Figure 4.3). Forced aggregation EBs demonstrated a superior ability to initiate retinal differentiation and were consequently taken forward in experiments to select EB sizes amenable to retinal differentiation in orbital shaken culture.

The orbital shaken culture system is not only suitable for initiating retinal differentiation but it also eliminates the requirement for supplementing the medium with the murine Engelbreth-Holm-Swarm tumour derived substrate, Matrigel (discussed in chapter 4). Matrigel is a commonly used research tool in many stem cell

differentiation protocols (see table 1.5). Its undefined and xenogeneic status however make it a subject of controversy which is hotly debated (Polykandriotis et al. 2008). The motivation to remove xenogeneic materials becomes important when considering developing clinical-grade cells (Sun et al. 2010). In addition to reducing the risk of exposure to animal pathogens, the demonstrated ability to exclude Matrigel from cultures helps observe and measure the effect of other changes made to the microenvironment, with reduced risk of influence from its undefined ingredients. In this report, simplifying the micro-environment by removing Matrigel helped observe and more confidently attribute measured effects to the impact of changing EB size and introducing orbital shaking to the culture system. By reducing or eliminating undefined ingredients from cultures the orbital shaken culture system succeeds in improving reproducibility, predictability and ultimately increases the potential for translation to clinically relevant good manufacturing practices.

With evidence that orbital shaken culture supports retinal fate specification and improve the homogeneity of the microenvironment, through eliminating the requirement for Matrigel, the next objective was to apply these findings to yield improvements over the process of retinal differentiation. Combining control over the number of cells entering the process, the size of starting aggregates and the homogeneity of the microenvironment made it possible to directly compare the impact of EB size and culture technique (adherent or orbital shaken) on retinal differentiation (Chapter 5). Comparisons of orbital shaking cultures in 24 SRW microwell plates on an orbital shaking platform were conducted with size-matched adherent EB culture controls in standard 24 well culture plates. The 24SRW microwell platform was chosen as it has been previously validated for use as a scale-down model for translating mammalian cell cultures into pilot and commercial scale bioprocesses (Silk et al. 2010). Another important consideration was that the 24SRW platform format provided sufficient throughput, to investigate the impact of two EB sizes (5K and 10K cells per EB) on retinal differentiation over 3 time-points days 10, 15 and 21 of retinal differentiation culture.

In order to measure the effects of EB size and orbital shaking on differentiation, a key challenge faced was, the difficulty in achieving single cell suspensions from differentiated EBs. Using Tryple Xpress (Invitrogen) with manual pipetting in a water bath at 37<sup>0</sup>C was sufficient for newly formed EBs as demonstrated in chapter 3. For

later EBs, older than 5 days however, the technique resulted in large quantities of fragmented cells and subsequent agglutination of the remainder of the samples into large clumps. This was likely due to increased viscosity from the release of DNA into the medium. Attempts to resolve clumps using DNase (Sigma) with Tryple (Invitrogen) had little impact and persistent clumps prompted new attempts to obtain reliable single cell numbers. Two alternate methods tested were sonication with the E450 Sonicator (Covaris) and an Embryoid Body Dissociation Kit and device (Miltneyi Biotec). Both proved to be no better than manual dissociation as neither was able to resolve the clumps. The inconsistent quality of single cell suspensions achieved by these methods in our hands disqualified them from inclusion in flow cytometry analyses to acquire cell numbers linked to retinal marker expression in order to identify and quantify retinal cell populations within the culture. Future experiments to progress the work in this study would benefit from a thorough exploration of other available tissue digestion techniques. Identification and quantification of cell populations is a critical step in generating characterized purified cells for basic research as well as for potential clinical applications (Davie et al. 2012).

The potential yields achievable by cell manufacturing processes is another key factor in assessing the suitability of methods, to understand if they are fit for purpose and determine if novel approaches offer potential for improved cell yields over existing platforms. To assess the impact of orbital shaking and EB size on the yield of cells, the Pico-Green Quant-iT assay helped determine relative cell numbers derived from total DNA quantification (Figure 5.4A). The data showed a close correlation between total cell quantities of EBs cultured in the 24 SRW microwells for adherent and orbital shaken systems (Figure 5.4A). The close fit between total cell numbers across samples irrespective of variation in EB size and culture technique ( $P > 0.05$ ) found using ANOVA, also presents an avenue for further enquiry. A follow-on study might investigate if the system exhibited a method of self-regulation in response to nutrient availability or whether the doubled difference in EB sizes investigated was insufficient to observe a clear effect (discussed in section 5.6).

Results showing the cell health throughout differentiation in orbital shaken cultures, using LDH assays also demonstrated a close fit between the 5K and 10K EB samples (Figure 5.4B). Our data showed no statistical differences of LDH activity for each time point between both EB sizes over 21 days of retinal differentiation ( $p > 0.05$ ) for

all comparisons made with one way ANOVA). Together the size distribution data and the LDH results show that homogeneity exists between the 5K and 10K EBs and could form the basis of establishing optimal ranges of EB sizes from which to initiate retinal differentiation in future experiments.

Evidence for the improved homogeneity of differentiation, achieved by using orbital shaking suspension cultures, also draws support from data analyses of the changes in size distribution with time of differentiating EBs. Throughout the culture our findings indicate that the majority of orbital shaken EBs (~80%) were evenly distributed across 3 narrow size ranges by day 15 (200-400 $\mu$ m, 401-600  $\mu$ m and 601-800 $\mu$ m) with no statistically significant differences between the size populations ( $p>0.05$ ) (Figures 5.2 and 5.3). Further investigation of the EBs within the 3 size ranges may reveal subpopulations of EBs differentiating at different rates or in slightly different ways and which could provide information on the role of EB self-regulation in microenvironments with limited resources.

The well documented conservation of retinal marker expression throughout mammalian retinogenesis helped to define the panel of genes used in our approach for tracking differentiation (Heavner & Pevny 2012; Hsieh & Yang 2009). The use of conserved genes validated the approach of using immunocytochemistry coupled with QPCR analyses to qualitatively and quantitatively demonstrate progression toward retinal differentiation in adherent and orbital shaken cultures (chapter 5). Our data showed the impact of both orbital shaking and size variation (between 5K and 10K EBs) on progression of retinal differentiation. Comparing gene expression profiles over the 21 day differentiation between adherent and orbital shaken cultures, provided evidence that expression patterns for the markers of retinal differentiation were conserved across culture techniques and between different EB sizes (Figure 5.16). The results also provide data to show increasing EB size (from 5K to 10K cells/EB) had greater influence on increasing later retinal marker expression in adherent cultures than in orbital shaken cultures (Figures 5.12 – 5.15). Orbital shaken cultures demonstrated greater homogeneity in retinal gene expression profiles irrespective of starting EB size highlighting the utility of the system as a means to reduce variability in retinal differentiation cultures.

Taken together, the EB size distribution data (Figures 5.2-3) along with evidence of earlier down-regulation of pluripotency marker POU5F1, faster up-regulation of early retinal markers Rx and Six 3 at day 3 (Figure 4.3), speedier down-regulation of Otx2 and the earlier peak expressions of later retinal markers Crx, Nrl and Rho (Figure 5.16); these results provide evidence that orbital shaken cultures demonstrate accelerated and more consistent initiation of retinal differentiation compared to adherent controls. Furthermore, as orbital shaken cultures diminished the requirement for Matrigel in the medium composition there is a case for using this platform to develop more defined retinal cell manufacturing processes.

Pioneering orbital shaken stem cell culture studies demonstrated murine ESCs benefit from such a system which supports increased cell yields and homogeneity of the microenvironment without injurious effects on differentiation (Carpenedo, Sargent, et McDevitt, 2007). In testing the utility of early proof of principle studies the work in this report provides supporting evidence for the previous findings, whilst extending their applicability to hiPSC derived EB culture and retinal differentiation over extended culture periods. Orbital shaking cultures offer EB derived cell processes a system for improving the homogeneity of the microenvironment whilst also reducing the requirement for undefined animal components. Reducing variability in cell manufacturing processes by using the orbital shaken platform addresses a key requirement for cell therapy manufacture to maximise the potential for consistent and reproducible quality products.

## **7.2 Future work**

The ultimate aim of work to develop bioprocesses from regenerative medicine research such as *in vitro* retinal cell generation, is to enable the production of safe, pure, potent, effective and stable products in cGMP compliant reproducible processes. In order to test the wider applicability of the orbital shaken culture system, better characterisation of the current model would be necessary. The following discussion includes suggestions for future lines of investigation arising from the work in this study to address the challenges faced herein as well as those which could arise from advancing the work for industrial application.

Greater resolution into the impact of EB size and orbital shaking would require the implementation of an effective method for resolving differentiated EBs into live single cell suspensions. Readily available single cell suspensions from differentiated EBs would enable detailed characterization of the sub-populations arising within the cultures and would help quantify the biases for specific retinal cell lineages inferred by the QPCR results in Chapters 4 -6 to provide more definitive data for cell characterization. Measuring the impact of microenvironmental changes at the cellular level rather than cell population level would also be an important addition to the work to identify stage specific markers of differentiation as well as process dependent changes to the cells in culture. Successful evaluation of the distribution of different cell populations making up retinal EBs in response to changes to their microenvironment due to the orbital shaken system will depend on novel assays to determine the quality of the cells in terms of their phenotypic identity as well as functionality. These additions would form an important intermediary step before the inclusion of cells produced by orbital shaken culture in further studies intended for process development for clinical translation.

Comprehensive characterisation of cells and processes is often dependent on the discovery of more biomarkers to specify identity. Cells sourced from hiPSC which undergo multiple stages of differentiation would benefit from biomarkers for each stage. Correlating biomarkers for the finer stages of differentiation with markers for cell health throughout the process could be particularly useful in identifying areas for improvement in developing efficient bioprocesses for cell based products. The recently reviewed approach of applying high-throughput methods such as transcriptomics to identify transcripts involved in retinal degeneration in age-related macular degeneration and glaucoma may also be applied to *in vitro* hiPSC derived retinogenesis to help find biomarkers for stages of differentiation (Tian et al. 2015). A transcriptomic approach combined with a proteome level assessment of retinogenesis would be beneficial in assuring protein level expression of key genes (Pripuzova et al. 2015). A panel of specific quantifiable biomarkers with causative rather than associative relationships to the specific stages of (retinal) differentiation would therefore facilitate more accurate measurements of changes to the microenvironment and therefore help determine optimal culture conditions for therapeutic cell production.

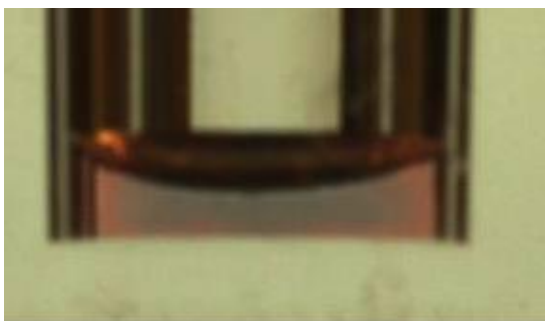
A deeper understanding of the impact of orbital shaking on developing EBs and the influence of growing EBs on the fluid dynamics of medium in 24 SRW microwell plates, would also benefit from further study to follow on from work in this report and that from the work of McDevitt and others (Sargent et al. 2010; Kinney et al. 2012; Rodrigues et al. 2011). Detailed mathematical models using computational fluid dynamics programmes should be validated with laboratory experiments to develop more accurate models of the fluid dynamics which take into account the presence of and changing sizes of EBs over time. Such a model would be beneficial in helping to determine the most suitable adaptive shaking regimes in a predictive and therefore more cost-effective manner for novel cell lines and target cell types amenable to orbital shaking culture. Such a model once created, might also ideally be used to develop a database correlating EB sizes and shaking regime combinations specific to different target cell derivation systems. This approach could produce a resource that would be of great use in accelerating the translation of differentiation protocols for clinical relevance.

The demand for cell manufacture processes in therapeutic scenarios is rising. Currently 53 cell therapy clinical trials are underway in the UK of which a majority of 34 (64%) are patient specific (autologous) treatments ([www.clinicaltrials.gov](http://www.clinicaltrials.gov)). Autologous cell products require manufacturing approaches to produce smaller numbers of cells than allogeneic therapies but depending on the indication this range varies from thousands to billions of cells per patient (Serra et al. 2012). The orbital shaken culture platform using 24 SRW plates is a manufacturing approach amenable to scale-up to 250ml shaken flasks providing sufficient scope to produce cell numbers in line with cell therapy requirements (Silk et al. 2010; Barrett et al. 2010). Additionally since the 24 SRW orbital shaken system offers a 30-fold reduction in scale of operation and consumable requirements, it represents a cost effective tool for developing further scale-up strategies (Barrett et al. 2010). Furthermore, the simplicity of the orbital shaken culture system combined with elimination of animal derived Matrigel from retinal cell derivation systems shown in this report suggests it is suitable for scalable manufacturing process development for retinal cell production from hiPSC derived EBs.

Our approach of selecting EB sizes amenable to shaking culture and determining corresponding shaking speeds to develop cell differentiation systems, is one which

could be readily applied to other cell derivation systems, since EBs give rise to all three germ layers responsible for the development of all tissues in the body (Thomson et al. 1998). In order to maximise the potential of the system, a recommendation would be to start with the EB size range of 5K and 10K cells/EB combined with the orbital shaking speed of 120rpm found to be permissive for 21 days of retinal differentiation. Taking advantage of the EB size to orbital shaking combination found to work for two hiPSC cell lines in this report could save time and therefore cost in applying the platform for the derivation of other cell types. The potential for applicability to other cell types can only be determined experimentally by substituting exogenous retinal induction factors for those determined to be appropriate for deriving another target cell type. A subsequent systematic categorisation of EB diameters at different stages of differentiation towards the new cell fate should be linked to key stage specific biomarkers. In this way identifying optimal EB sizes to initiate and progress through different stages of differentiation along other cell fate specification pathways in orbital shaken cultures might also be possible. The value of such a process is in facilitating adaption of adherent differentiation protocols to 3D orbital shaken suspension systems and in acting as a method for eliminating Matrigel from other differentiation protocols; to help translate cell derivation practices to scalable manufacturing processes.

## Appendix I



### Appendix 1

Representative images of the liquid surface in a single well of a 24 well microwell plate during measurement of mixing times using the dual indicator system for mixing time (DISMT) (Melton et al. 2002). With a fill volume of 500 $\mu$ l with water like viscosities, at an orbital shaking frequency of 120rpm the mixing of 50 $\mu$ l of thymol blue (Applichem) and 500 $\mu$ l methyl red (Fischer Scientific) both in a final concentration of 4.3mg/L in deionised water provided the colour change captured to indicate a visually determined mixing time of under 3 minutes. The colour of the liquid changes initially to blue before transitioning to yellow on complete mixing from pink to yellow as depicted in the images. Images were taken using a high-speed CCD video camera mounted on an orbital shaken stage

This work was carried out with the kind aid of Gregorio Rodriguez (UCL, Biochemical Engineering.)

## **Appendix II Considerations for industrial uptake of retinal differentiation in the Matrigel-free orbital shaken microwell platform**

### **Introduction**

The purpose of this chapter is to evaluate the applicability of the process of orbital shaken culture for initiating retinal differentiation in hiPSC derived EBs in an industrial context. The objective of the research in this report has been to adapt a 2D adherent retinal differentiation protocol for deriving retinal cells to a 3d mixed system. Adaption to a mixed system with the orbital shaken 24 microwell platform improved homogeneity of differentiation by day 10 and appeared to improve the speed of differentiation for later time points with expression of later markers of retinal differentiation. Importantly retinal differentiation was achieved in orbital shaken cultures whilst removing reliance on animal derived Matrigel and adding potential scalability.

Improved control over retinal differentiation was achieved in two parts; first by introducing specific input EB sizes for initiating retinal differentiation and secondly by introducing orbital shaking to the culture system. Forced aggregation provided reproducible EB formation sizes (Chapter 3). The formation of specific sized EBs, facilitated the identification of suitable EB sizes (5K and 10K cells/EB) able to improve the initiation of retinal differentiation, compared to heterogeneous sized EBs formed by manual scraping techniques (Chapter 4). The second half of the work involved adapting the adherent protocol to a mixed culture system. The 24 microwell orbital shaking platform was selected for this purpose as it had been previously validated for scalability of mixing dynamics with mammalian cell cultures to shake flasks and stirred tank lateral vessels (Silk et al. 2010; Barrett et al. 2010).

The utility of the orbital shaken system for improving future scalability was shown not only in its ability to improve the homogeneity and speed of retinal differentiation cultures, but also in helping to reduce reliance on animal derived raw materials such as Matrigel. Reduction of animal components is key requirement in considering future

clinical applications of the work. Attempts to show broader applicability of the Matrigel-free orbital shaken system were made in chapter 6, to show the system could initiate retinal differentiation in a different feeder-free hiPSC line. The different gene expression profiles observed in the feeder free cell line brought one of the first key challenges for wider applicability into focus: the issue of cell line variability. The objectives of this chapter are to highlight such challenges facing uptake of Matrigel-free orbital shaking culture for retinal differentiation and consider pragmatic approaches to address them.

### **Reducing reliance on animal derived raw materials**

The reduction of animal derived raw materials from bioproduction processes intended for the production of human therapeutics is a regulatory requirement in validating new cell products and processes. The introduction of mixing through orbital shaking facilitated the removal of a key potential source of variability in stem cell differentiation protocols, arising from the common use of the xenogeneic material Matrigel. Matrigel could be a key source of variability unsuitable for scale up procedures due to its undefined status. Removal of Matrigel was accomplished in trying to address challenges associated with static culture. In particular the increased variability of the microenvironment arising from the creation of concentration gradients due to a lack of mixing, which make static cultures inherently limited for scalability (Côme et al. 2008b). The implementation of orbital shaken culture in the pre-validated 24-microwell shaking platform to improve mixing and show amenability to scale up, allowed the complete exclusion of Matrigel from this system.

Other animal derived ingredients routinely used in stem cell culture, include porcine skin derived gelatine, mouse embryonic fibroblasts (MEF) and bovine albumin present in knockout serum replacement (KOSR). These can be eliminated by switching to a feeder free cell line as shown in chapter 6. Eliminating MEFs commonly used as feeder cells for hiPSC maintenance and expansion is in compliance with regulatory recommendations from the EMA and FDA (PAS 83:2012). A feeder free hiPSC lines derived by transient over-expression of non-integrating episomal reprogramming plasmids would also avoid risks of genomic integration associated with viral reprogramming techniques. Using larger panels of feeder free hiPSC lines for

differentiation in the orbital shaken platform would be a key improvement to understanding the applicability of the system to different cell lines. Doing so would help explore its potential utility for autologous cell therapy manufacturing processes.

### **Cell-line variability**

The derivation of a pluripotent cell line from a donor, or selection of a commercially available pluripotent cell line is the first step in the process of developing a stem cell differentiation process. The importance of variability arising from cell line selection draws on the experiences from mammalian cell manufacturing processes and cell line development where clonal variations can result in the production of different quantities and qualities of proteins such as monoclonal antibodies (Lai et al., 2013). Unlike in mammalian cell process development, for regenerative medicine, live cells themselves are usually the products and variabilities arising from different cell lines can result in varying differentiation propensities (Osafune et al. 2008).

A potential source of increased variability in hiPSC lines can arise from using different methods to derive and reprogram the somatic donor cells, as was the case for the MSU001 and BJ IPS cell lines used in this report. The major source of transcriptional variation arising from cell line specific variability is less connected to reprogramming method and more a result of the inherent genetic variations in cells, epigenetic memory from donor cells has also been found to be an insignificant factor (Rouhani et al. 2014). To account for donor to donor genetic cell line specific variability cell differentiation processes should conduct studies with much larger numbers of hiPSC lines. Ensuring the use of hiPSC lines derived from multiple donors but sourced from the same tissue and reprogrammed by identical techniques, should help account for this potential source of variation in developing differentiation processes.

The effects of potential genetic variation from starting pluripotent cells are demonstrated in chapter 6 which showed that cell line variation can result in unique differentiation profiles of target cell types. The different gene expression profiles for retinal cell fate specification observed in the feeder free cell line may have been a response to the changes in cell culture conditions for expanding and maintaining feeder free cells. The effects of using different matrix substrates such as Vitronectin used to

support pluripotent cell cultures together with the E8 Stem Cell Medium system (Invitrogen) should also be characterised for potential effects on retinal differentiation. Evaluating a series of different stem cell maintenance systems for their impact on retinal differentiation profiles could help to identify a gold standard procedure for feeder-free cell culture of hiPSC intended for retinal differentiation. On establishing a standard protocol for pluripotent cell culture it would be possible to compare larger numbers of hiPSC lines in parallel in the orbital shaken culture system for retinal differentiation to find suitable conditions for a majority of cell lines. This would be important to establish differentiation systems to produce a variety of cells with different haplotypes from genetically diverse cell lines to represent large populations of patients.

### **Cell characterisation**

Cell characterisation is required for clinical application of hiPSCs and their derivatives. Characterisation is important to ensure comparability between the cells' identity and character can be demonstrated before and after manufacturing processes for starting cell materials and target differentiated cells, to demonstrate control over manufacturing processes. In this report, initial pluripotent cells were characterised for expression of markers of pluripotency at the gene and protein expression levels (Chapter 3). As pluripotent cells differentiated toward retinal fates, challenges associated with deriving consistent single cell suspensions from cultured EBs limited cell characterisation to population level analyses. Gene expression profiling, LDH assays and expression of markers for retinal differentiation by immunohistochemistry within EBs were tested in order to achieve this in Chapter 5.

Characterising target cells at different stages with cellular and population level resolution will facilitate specific definition of the critical quality attributes of target cells. Additionally, this would help to identify contaminating cell populations, such as pluripotent cells which require removal. The use of commercially available micro-array tests and wider transcriptional profiling approaches would help future development of robust panels of markers for cell characterisation (Fergus et al. 2014; Tian et al. 2015).

Ensuring cells have normal karyotypes is also important for characterisation and to minimise associated risks of tumorigenesis and develop laboratory scale research with clinical relevance (Harrison, et al., 2007). Karyotypic analyses are particularly important for pluripotent cells, which can undergo random chromosomal rearrangements in long term culture (Fazeli et al. 2011). Frequent karyotypic analyses of the hiPSC lines at different stages of differentiation and at different steps of processing would form an important addition to cell characterisation efforts.

### **Identifying target cell populations**

To define the target cell populations for development in the orbital shaken platform for retinal differentiation it will be important to establish a rapid method for identifying retinal cells at various stages of differentiation and through different stages of bioprocessing. Identification and purification of cell populations rests on the ability to separate target cells from mixed populations of differentiating cells in 3D aggregates. In this report after 10 days of differentiation in orbital shaken culture target retinal cells in EBs were entangled in tough extracellular matrix which made achieving single cell suspensions difficult without large losses. While other reports have shown successful isolation of photoreceptors from adherent cultures using trypsin and manual pipetting, these techniques were not repeated in our lab where EBs were cultured in a suspension system (Lamba et al. 2010). Optimising cell separation with more specific digestive enzymes would be a key improvement required for the development of cell therapies from heterogeneous suspension cultures such as the target retinal cells from EBs in this report. On development of appropriate cell separation techniques, the cells could be purified by fluorescence activated cell sorting (FACS) or magnetic activated cell sorting (MACS) to enrich for target cell populations to demonstrate purity and perform toxicity, potency and functionality assays.

### **Differentiation and purification of desired cell types**

In order to enrich for target cell populations a comprehensive set of cell surface biomarkers is an essential requirement for cell therapy development. The recent discovery of a set of 5 cell surface markers for photoreceptor precursor cells conserved

between mice and human retinæ may provide great promise for the ability to efficiently purify targeted retinal cell types from this report (Lakowski et al., 2015).

The development of similar sets of markers for key stages of differentiation to track progress of differentiating cells throughout their time in culture would help to better understand and control differentiation processes. In combination with efficient cell quantification techniques such as FACS or MACS to quantify cell populations in differentiating EBs, it would may then be possible to select optimal culture conditions for different retinal cell types in the culture. Optimised culture conditions for retinal differentiation in the 24 microwell orbital shaken culture would in turn help achieve maximal purities of target cells such as photoreceptors. Photoreceptors intended for therapeutic use could then be isolated more to demonstrate purity using the panels of markers and separation techniques discussed above.

The identification of cell surface biomarkers for assessing cell health and degradation in retinal differentiation would be another useful development. These could help monitor cellular responses to potential toxic or metabolic insults arising from unsuitable, sub-optimal or anomalous culture conditions through different stages of differentiation in orbital shaken cultures. Such markers could be used to determine the impacts of differing concentrations/ combinations of exogenous factors, altering EB sizes or changing orbital shaking speeds on the identity, purity and health of final differentiated cell populations. Apart from their value in informing process development, and optimisation decisions for retinal differentiation in orbital shaken cultures, such data would ultimately help enable processes to maintain target product quality profiles of target retinal cell based therapeutics manufactured in the orbital shaken microwell system.

### **Scalable process development**

The 24 microwell approach is a pre-validated approach for scale up of mammalian cultures to larger vessels (Barrett et al. 2010; Silk et al. 2010). However, the use of this platform for stem cell differentiation protocols is a novel application which would benefit from further study to evaluate scale-up approaches to larger vessels. While the fluid dynamics of migrating in scales from 24 microwells to larger vessels (shake

flasks and 5L STLVs) have been explored in previous reports, these also do not include the potential impact of growing aggregates of differentiating stem cells in these cultures (Barrett et al., 2010 ; Weheliye et al., 2012). Studies to investigate the unique hydrodynamic environment of orbital shaking EBs would be required to understand the demonstrated applicability of the 24 microwells shaking platform to a system incorporating differentiating EBs. Better understanding and characterisation of the hydrodynamic environment at the small 24 microwell scale with operating conditions relevant to EB differentiation protocols would facilitate a smoother transition to larger scales and help identify scale dependent variables to highlight opportunities for improvement.

The integration of the orbital shaken microwell platform into an automation platform would also help improve potential scalability of the system. In this report changing the medium in 24 microwells every 48 hours for the first 15 days and then every 24 hours for the remaining 6 days of culture in laminar flow tissue culture hoods was prone to operator variability and associated risks of culture contaminations. Previously demonstrated culture of stem cells in an automated platform provides within a sterile system provide the proof of principle for this approach (Hussain et al. 2013). Integrating the orbital shaken system with an automated platform would reduce risks of contamination involved with manual handling and improve reproducibility by eliminating operator bias. If incorporated with a temperature and CO<sub>2</sub> regulated sterile chamber an automation platform could minimise the time cells spend outside optimal culture conditions, to avoid potentially detrimental fluctuations in pH and oxygen consumption that are inevitable during medium exchanges (Veraitch et al. 2008).

## **Conclusion**

Advances in laboratory scale culture techniques are required as retinal cell therapy research and development approach clinical translation with difficult to culture cell types such as photoreceptors (MacLaren et al. 2006; West et al. 2012; Lamba et al. 2010; Reichman et al. 2014). Derivation of retinal cell types currently rely on complex and lengthy protocols in mostly adherent systems and some static suspension systems (Table 1.4). Clinical trials using live human retinal progenitor cells are currently underway and recruiting patients for phase II studies (Clinicaltrials.gov ref:

NCT02320812). If this and similar studies are successful there is likely to be an increase in demand for processes to differentiate retinal cells in systems with improved reproducibility, reduced reliance on animal derived ingredients and with potential for scalability.

The results chapters in this report demonstrate adaption of an adherent culture system for retinal differentiation to an orbital shaken 24 well microwell approach. The adaption has resulted in improved potential for scalability, elimination of animal derived Matrigel from the differentiation process and improved speed of differentiation. In order to consider the use of this platform for the manufacture of clinically relevant material a cGMP compliant method to separate cells from 3D aggregates and a comprehensive set of biomarkers to characterise target retinal cell types would need to be established. Overcoming this hurdle will help identify and purify target populations and aid removal of contaminant cell populations. The orbital shaken system could then provide a high-throughput, rapid and accessible approach with low product costs to assess several different factors affecting stem cell differentiation toward retinal fates in parallel. Doing so could help establish a universally applicable system for retinal differentiation from hiPSCs, which could be used to develop larger scale manufacturing processes for therapeutic retinal cell types.

## Bibliography

- Adewumi, O. et al., 2007. Characterization of human embryonic stem cell lines by the International Stem Cell Initiative. *Nature biotechnology*, 25(7), pp.803–816.
- Allegrucci, C. & Young, L.E., 2007. Differences between human embryonic stem cell lines. *Human reproduction update*, 13(2), pp.103–120.
- Amit, M. et al., 2000. Clonally derived human embryonic stem cell lines maintain pluripotency and proliferative potential for prolonged periods of culture. *Developmental biology*, 227(2), pp.271–278.
- Amit, M. et al., 2004. Feeder layer- and serum-free culture of human embryonic stem cells. *Biology of reproduction*, 70(3), pp.837–845.
- Andersson, E.R. & Lendahl, U., 2014. Therapeutic modulation of Notch signalling--are we there yet? *Nature reviews. Drug discovery*, 13(5), pp.357–78.
- Andres M. Bratt-Leal, Richard L. Carpenedo, T.C.M., 2009. Engineering the Embryoid Body Microenvironment to Direct Embryonic Stem Cell Differentiation. *NIH Public Access*, 25(1), pp.43–51.
- Azarin, S.M. & Palecek, S.P., 2010. Development of scalable culture systems for human embryonic stem cells. *Biochemical Engineering Journal*, 48(3), pp.378–384.
- Bae, D. et al., 2011. Hypoxia Enhances the Generation of Retinal Progenitor Cells from Human Induced Pluripotent and Embryonic Stem Cells. *Stem cells and development*, 21(8), pp.1344–1355.
- Bailey, T.J. et al., 2004. Regulation of development by Rx genes. *International Journal of Developmental Biology*, 48(8-9), pp.761–770.
- Ban, H. et al., 2011. Efficient generation of transgene-free human induced pluripotent stem cells (iPSCs) by temperature-sensitive Sendai virus vectors. *Proceedings of the National Academy of Sciences of the United States of America*, 108(34), pp.14234–9.
- Barrett, T. a et al., 2010. Microwell engineering characterization for mammalian cell culture process development. *Biotechnology and bioengineering*, 105(2), pp.260–75.
- Bauwens, C.L. et al., 2008. Control of human embryonic stem cell colony and aggregate size heterogeneity influences differentiation trajectories. *Stem cells*, 26(9), pp.2300–2310.
- Beachy, P. a. et al., 2010. Interactions between Hedgehog proteins and their binding partners come into view. *Genes and Development*, 24(18), pp.2001–2012.
- Becker, A.J. McCulloch, E.A. Till, J., 1963. Cytological Demonstration of the Clonal Nature of Spleen Colonies Derived from Transplanted Mouse Marrow Cells. *Nature*, 197, pp.452–454.
- Billingham, R.. & Boswell, T., 1952. Studies on the problem of myoneurotization. *Proceedings of The Royal Society of London*, pp.392–407.
- Bock, C. et al., 2011. Reference maps of human es and ips cell variation enable high-throughput characterization of pluripotent cell lines. *Cell*, 144(3), pp.439–452.
- van den Bos, C. et al., 2013. Therapeutic Human Cells: Manufacture for Cell

- Therapy/Regenerative Medicine. , pp.61–97.
- Boucherie, C. et al., 2012. Self-organising Neuroepithelium from Human Pluripotent Stem Cells Facilitates Derivation of Photoreceptors. *Stem cells (Dayton, Ohio)*, 44(0).
- Bradley, a et al., 1984. Formation of germ-line chimaeras from embryo-derived teratocarcinoma cell lines. *Nature*, 309(5965), pp.255–256.
- Buchs, J. et al., 2000. Power consumption in shaking flasks on rotary shaking machines: I. Power consumption measurement in unbaffled flasks at low liquid viscosity. *Biotechnology and Bioengineering*, 68(6), pp.589–593.
- Buchs, J., Lotter, S. & Milbradt, C., 2001. Out-of-phase operating conditions, a hitherto unknown phenomenon in shaking bioreactors. *Biochemical Engineering Journal*, 7(2), pp.135–141.
- Burridge, P.W. et al., 2007. Improved human embryonic stem cell embryoid body homogeneity and cardiomyocyte differentiation from a novel V-96 plate aggregation system highlights interline variability. *Stem cells (Dayton, Ohio)*, 25(4), pp.929–38.
- Buta, C. et al., 2013. Reconsidering pluripotency tests: Do we still need teratoma assays? *Stem Cell Research*, 11(1), pp.552–562.
- Campbell, K.H.S., 1996. Sheep cloned by nuclear transfer from a cultured cell line. *Letter to Nature*, 380(7), pp.64–66.
- Carpenedo, R.L., Sargent, C.Y. & McDevitt, T.C., 2007. Rotary suspension culture enhances the efficiency, yield, and homogeneity of embryoid body differentiation. *Stem cells*, 25(9), pp.2224–2234.
- Casaroli-marano, R.P. & Vilarrodona, A., 2014. Regulatory Issues in Cell-Based Therapy for Clinical Purposes. , 53, pp.189–200.
- Chen, G. et al., 2011. Chemically defined conditions for human iPS cell derivation and culture. *Nature methods*, 8(5), pp.424–429.
- Choi, Y.Y. et al., 2010. Controlled-size embryoid body formation in concave microwell arrays. *Biomaterials*, 31(15), pp.4296–4303.
- Christiane, N. & Moens, H., 2013. Expansion and differentiation of human embryonic stem cells on an automated microwell platform ( PhD ) in Biochemical Engineering.
- Cimetta, E. et al., 2009. Micro-bioreactor arrays for controlling cellular environments: design principles for human embryonic stem cell applications. *Methods (San Diego, Calif.)*, 47(2), pp.81–9.
- Côme, J. et al., 2008a. Improvement of culture conditions of human embryoid bodies using a controlled perfused and dialyzed bioreactor system. *Tissue engineering. Part C, Methods*, 14(4), pp.289–98.
- Côme, J. et al., 2008b. Improvement of culture conditions of human embryoid bodies using a controlled perfused and dialyzed bioreactor system. *Tissue engineering. Part C, Methods*, 14(4), pp.289–98.
- Coppola, D., Ouban, A. & Gilbert-Barness, E., 2009. Expression of the insulin-like growth factor receptor 1 during human embryogenesis. *Fetal and pediatric pathology*, 28(2), pp.47–54.

- Crook, J.M., Hei, D. & Stacey, G., 2010. The International Stem Cell Banking Initiative (ISCBI): raising standards to bank on. *In vitro cellular & developmental biology. Animal*, 46(3-4), pp.169–72.
- Curcio, C. a et al., 1990. Human photoreceptor topography. *The Journal of comparative neurology*, 292(4), pp.497–523.
- Curcio, C.A., Medeiros, N.E. & Millican, C.L., 1996. Photoreceptor Loss in Age-Related Macular Degeneration. *Investigative ophthalmology & visual science*, 37(7), pp.1236–1249.
- Cyranoski, D., 2012. Stem-cell pioneer banks on future therapies. *Nature*, 488, p.139.
- Dang, S.M. et al., 2004. Controlled, scalable embryonic stem cell differentiation culture. *Stem cells*, 22, pp.275–282.
- Dang, S.M. et al., 2002. Efficiency of Embryoid Body Formation and Hematopoietic Development from Embryonic Stem Cells in Different Culture Systems.
- Davie, N.L. et al., 2012. Streamlining Cell Therapy Manufacture. *BioProcess International*, 10(3), pp.24–49.
- Davis, a a, Matzuk, M.M. & Reh, T. a, 2000. Activin A promotes progenitor differentiation into photoreceptors in rodent retina. *Molecular and cellular neurosciences*, 15(1), pp.11–21.
- Devito, L. et al., 2014. Cost-effective master cell bank validation of multiple clinical-grade human pluripotent stem cell lines from a single donor. *Stem cells translational medicine*, 3(10), pp.1116–24.
- Doetschman, T.C. et al., 1985. The in vitro development of blastocyst-derived embryonic stem cell lines: formation of visceral yolk sac, blood islands and myocardium. *Journal of embryology and experimental morphology*, 87, pp.27–45.
- Doig, S.D. et al., 2005. Modelling surface aeration rates in shaken microtitre plates using dimensionless groups. *Chemical Engineering Science*, 60(10), pp.2741–2750.
- Dowling, J.E., 2009. Retina : An Overview. , pp.159–169.
- Ducci, A; Weheliye, W., 2014. Orbitally shaken bioreactors - viscosity effects on flow characteristics. *American Institue of Chemical Engineers*, 60(11), p.3951.
- Dutt, K. et al., 2003. Generation of 3D retina-like structures from a human retinal cell line in a NASA bioreactor. *Cell transplantation*, 12(7), pp.717–31.
- Dutt, K. & Cao, Y., 2009. Engineering retina from human retinal progenitors (cell lines). *Tissue engineering. Part A*, 15(6), pp.1401–13.
- Earls, J.K., Jin, S. & Ye, K., 2013. Mechanobiology of human pluripotent stem cells. *Tissue engineering. Part B, Reviews*, 19(5), pp.420–30.
- Eiraku, M. et al., 2008. Self-Organized Formation of Polarized Cortical Tissues from ESCs and Its Active Manipulation by Extrinsic Signals. *Cell Stem Cell*, 3(5), pp.519–532. Available at: <http://dx.doi.org/10.1016/j.stem.2008.09.002>.
- Eiraku, M. et al., 2011. Self-organizing optic-cup morphogenesis in three-dimensional culture. *Nature*, 472(7341), pp.51–6.
- Eiraku, M., Adachi, T. & Sasai, Y., 2012. Relaxation-expansion model for self-driven retinal morphogenesis: a hypothesis from the perspective of biosystems dynamics

- at the multi-cellular level. *BioEssays : news and reviews in molecular, cellular and developmental biology*, 34(1), pp.17–25.
- Elmahdi, I. et al., 2003. pH control in microwell fermentations of *S. erythraea* CA340: Influence on biomass growth kinetics and erythromycin biosynthesis. *Biochemical Engineering Journal*, 16(3), pp.299–310.
- Evans, M.J.K.M., 1981. Establishment in culture of pluripotential cells from mouse embryos.pdf.
- Faísca, P. & Desmecht, D., 2007. Sendai virus, the mouse parainfluenza type 1: a longstanding pathogen that remains up-to-date. *Research in veterinary science*, 82(1), pp.115–25.
- Fazeli, A. et al., 2011. Altered patterns of differentiation in karyotypically abnormal human embryonic stem cells. *The International journal of developmental biology*, 55(2), pp.175–80.
- Fergus, J., Quintanilla, R. & Lakshmipathy, U., 2014. Characterizing Pluripotent Stem Cells Using the TaqMan(®) hPSC Scorecard (TM) Panel. *Methods in molecular biology (Clifton, N.J.)*.
- Finlay, B.L., 2008. The developing and evolving retina: Using time to organize form. *Brain Research*, 1192, pp.5–16.
- Fridley, K., Nair, R. & McDevitt, T., 2014. Differential Expression of extracellular matrix and growth factors by embryoid bodies in hydrodynamic and static cultures. *Tissue Engineering*, 6647(12), pp.1–35.
- Fridley, K.M. et al., 2010. Unique differentiation profile of mouse embryonic stem cells in rotary and stirred tank bioreactors. *Tissue engineering. Part A*, 16(11), pp.3285–98.
- Fuhrmann, S., 2010. Eye morphogenesis and patterning of the optic vesicle. *Current Top Dev Biol*, 93, pp.61–84.
- Fusaki, N. et al., 2009. Efficient induction of transgene-free human pluripotent stem cells using a vector based on Sendai virus, an RNA virus that does not integrate into the host genome. *Proceedings of the Japan Academy, Series B*, 85(8), pp.348–362.
- Gamm, D.M. & Meyer, J.S., 2010. Directed differentiation of human induced pluripotent stem cells: a retina perspective. *Regenerative medicine*, 5(3), pp.315–317.
- Genaro, P. De et al., 2013. Retinoic Acid Promotes Apoptosis and Differentiation in Photoreceptors by Activating the P38 MAP Kinase Pathway.
- Gerecht-Nir, S., Cohen, S. & Itskovitz-Eldor, J., 2004. Bioreactor cultivation enhances the efficiency of human embryoid body (hEB) formation and differentiation. *Biotechnology and Bioengineering*, 86(5), pp.493–502.
- Gill, N.K. et al., 2008. Design and characterisation of a miniature stirred bioreactor system for parallel microbial fermentations. *Biochemical Engineering Journal*, 39(1), pp.164–176.
- Girard, P. et al., 2001. Small-scale bioreactor system for process development and optimization. *Biochemical Engineering Journal*, 7(2), pp.117–119.
- Gonzalez-Cordero, A. et al., 2013. Photoreceptor precursors derived from three-

- dimensional embryonic stem cell cultures integrate and mature within adult degenerate retina. *Nature biotechnology*, 31(8), pp.741–747.
- Haeckel, E., 1868. *Natürliche Schöpfungsgeschichte*. *Natürliche Schöpfungsgeschichte*, pp.282–283.
- Harrison, N.J., Baker, D. & Andrews, P.W., 2007. Culture adaptation of embryonic stem cells echoes germ cell malignancy. *International Journal of Andrology*, 30(4), pp.275–281.
- Hazeltine, L.B., Selekman, J. a. & Palecek, S.P., 2013. Engineering the human pluripotent stem cell microenvironment to direct cell fate. *Biotechnology Advances*, 31(7), pp.1002–1019.
- Heath, J.K. & Rees, a R., 1985. Growth factors in mammalian embryogenesis. *Ciba Foundation symposium*, 116, pp.3–22.
- Heavner, W. & Pevny, L., 2012. Eye development and retinogenesis. *Cold Spring Harbor perspectives in biology*, 4(12).
- Hendrickson, A. et al., 2008. Rod photoreceptor differentiation in fetal and infant human retina. *Experimental eye research*, 87(5), pp.415–26.
- Heng, B.C. et al., 2007. Mechanical dissociation of human embryonic stem cell colonies by manual scraping after collagenase treatment is much more detrimental to cellular viability than is trypsinization with gentle pipetting. *Biotechnology and applied biochemistry*, 47(Pt 1), pp.33–37.
- Heng, B.C. et al., 2012. Translating Human Embryonic Stem Cells from 2-Dimensional to 3-Dimensional Cultures in a Defined Medium on Laminin- and Vitronectin-Coated Surfaces. *Stem Cells and Development*, 21(10), pp.1701–1715.
- Hermann, R., Lehmann, M. & Buchs, J., 2003. Characterization of gas-liquid mass transfer phenomena in microtiter plates. *Biotechnology and Bioengineering*, 81(2), pp.178–186.
- Hernandez, D., Ruban, L. & Mason, C., 2011. Feeder-free culture of human embryonic stem cells for scalable expansion in a reproducible manner. *Stem cells and development*, 20(6), pp.1089–1098.
- Hirami, Y. et al., 2009. Generation of retinal cells from mouse and human induced pluripotent stem cells. *Neuroscience Letters*, 458(3), pp.126–131.
- Hong, S.-K. et al., 2011. Embryonic mesoderm and endoderm induction requires the actions of non-embryonic Nodal-related ligands and Mxtx2. *Development (Cambridge, England)*, 138(4), pp.787–95.
- Horbelt, D., Denkis, A. & Knaus, P., 2012. A portrait of Transforming Growth Factor ?? superfamily signalling: Background matters. *International Journal of Biochemistry and Cell Biology*, 44(3), pp.469–474.
- Hough, S.R. et al., 2009. A continuum of cell states spans pluripotency and lineage commitment in human embryonic stem cells. *PLoS ONE*, 4(11), p.e7708.
- Hsieh, Y.-W. & Yang, X.-J., 2009. Dynamic Pax6 expression during the neurogenic cell cycle influences proliferation and cell fate choices of retinal progenitors. *Neural development*, 4, p.32.
- Hua, J. & Sidhu, K., 2008. Recent advances in the derivation of germ cells from the

- embryonic stem cells. *Stem cells and development*, 17(3), pp.399–411.
- Hussain, W. et al., 2013. Reproducible culture and differentiation of mouse embryonic stem cells using an automated microwell platform. *Biochemical Engineering Journal*, 77, pp.246–257.
- Hwang, N.S., Varghese, S. & Elisseeff, J., 2008. Controlled differentiation of stem cells. *Advanced Drug Delivery Reviews*, 60(2), pp.199–214.
- Hwang, Y.-S. et al., 2009. Microwell-mediated control of embryoid body size regulates embryonic stem cell fate via differential expression of WNT5a and WNT11. *Proceedings of the National Academy of Sciences of the United States of America*, 106, pp.16978–16983.
- Hyatt, G. a et al., 1996. Retinoic acid alters photoreceptor development in vivo. *Proceedings of the National Academy of Sciences of the United States of America*, 93(23), pp.13298–13303.
- Ikeda, H. et al., 2005. Generation of Rx+/Pax6+ neural retinal precursors from embryonic stem cells. *Proceedings of the National Academy of Sciences of the United States of America*, 102(32), pp.11331–11336.
- Ilic, D. & Stephenson, E., 2013. Promises and challenges of the first clinical-grade induced pluripotent stem cell bank. *Regenerative medicine*, 8(2), pp.101–2.
- Itskovitz-Eldor, J. et al., 2000. Differentiation of human embryonic stem cells into embryoid bodies compromising the three embryonic germ layers. *Molecular medicine (Cambridge, Mass.)*, 6(2), pp.88–95.
- Jayakody, S. a. et al., 2015. Cellular strategies for retinal repair by photoreceptor replacement. *Progress in Retinal and Eye Research*, (February), pp.1–36.
- Karp, J.M. et al., 2007. Controlling size, shape and homogeneity of embryoid bodies using poly(ethylene glycol) microwells. *Lab on a chip*, 7(6), pp.786–794.
- Keller, G., 2005. Embryonic stem cell differentiation: Emergence of a new era in biology and medicine. *Genes and Development*, 19(10), pp.1129–1155.
- Keller, G.M., 1995. In vitro differentiation of embryonic stem cells. *Current opinion in cell biology*, 7(6), pp.862–9..
- Kelley, M.W., Turner, J.K. & Reh, T. a, 1994. Retinoic acid promotes differentiation of photoreceptors in vitro. *Development (Cambridge, England)*, 120(8), pp.2091–2102.
- Kim, D. et al., 2009. Generation of human induced pluripotent stem cells by direct delivery of reprogramming proteins. *Cell stem cell*, 4(6), pp.472–476.
- Kinney, M. a & McDevitt, T.C., 2013. Emerging strategies for spatiotemporal control of stem cell fate and morphogenesis. *Trends in biotechnology*, 31(2), pp.78–84.
- Kinney, M. a. & McDevitt, T.C., 2012. Emerging strategies for spatiotemporal control of stem cell fate and morphogenesis. *Trends in Biotechnology*, 31(2), pp.78–84.
- Kinney, M. a., Saeed, R. & McDevitt, T.C., 2012. Systematic analysis of embryonic stem cell differentiation in hydrodynamic environments with controlled embryoid body size. *Integrative Biology*, 4(6), p.641.
- Klößner, W. et al., 2012. Power input correlation to characterize the hydrodynamics of cylindrical orbitally shaken bioreactors. *Biochemical Engineering Journal*, 65, pp.63–69. Available at: <http://dx.doi.org/10.1016/j.bej.2012.04.007>.

- Klößner, W. & Büchs, J., 2012. Advances in shaking technologies. *Trends in Biotechnology*, 30(6), pp.307–314.
- Kopper, O. et al., 2010. Characterization of gastrulation-stage progenitor cells and their inhibitory crosstalk in human embryoid bodies. *Stem cells (Dayton, Ohio)*, 28(1), pp.75–83.
- Kumar, M. et al., 2007. Neurospheres derived from human embryoid bodies treated with retinoic Acid show an increase in nestin and ngn2 expression that correlates with the proportion of tyrosine hydroxylase-positive cells. *Stem cells and development*, 16(4), pp.667–81.
- Kurosawa, H., 2007. Methods for inducing embryoid body formation: in vitro differentiation system of embryonic stem cells. *Journal of bioscience and bioengineering*, 103(5), pp.389–398.
- Kwan, K.M., 2014. Coming into focus: The role of extracellular matrix in vertebrate optic cup morphogenesis. *Developmental Dynamics*, pp.1242–1248.
- Lai, M.I. et al., 2011. Advancements in reprogramming strategies for the generation of induced pluripotent stem cells. *Journal of assisted reproduction and genetics*, 28(4), pp.291–301.
- Lai, T., Yang, Y. & Ng, S.K., 2013. Advances in mammalian cell line development technologies for recombinant protein production. *Pharmaceuticals*, 6(5), pp.579–603.
- Lamba, D. a et al., 2010. Generation, purification and transplantation of photoreceptors derived from human induced pluripotent stem cells. *PloS one*, 5(1), p.e8763.
- Lamba, D. a., Gust, J. & Reh, T. a., 2009. Transplantation of Human Embryonic Stem Cell-Derived Photoreceptors Restores Some Visual Function in Crx-Deficient Mice. *Cell Stem Cell*, 4(1), pp.73–79.
- Lamba, D.A. et al., 2006. Efficient generation of retinal progenitor cells from human embryonic stem cells. *Proceedings of the National Academy of Sciences of the United States of America*, 103(34), pp.12769–12774.
- Lancaster, M. a. & Knoblich, J. a., 2014. Organogenesis in a dish: modeling development and disease using organoid technologies. *Science (New York, N.Y.)*, 345(6194), p.1247125.
- Lara, A.R. et al., 2006. Living with heterogeneities in bioreactors: understanding the effects of environmental gradients on cells. *Molecular biotechnology*, 34(3), pp.355–381.
- Larsen, K.B. et al., 2009. Expression of the homeobox genes PAX6, OTX2, and OTX1 in the early human fetal retina. *International journal of developmental neuroscience : the official journal of the International Society for Developmental Neuroscience*, 27(5), pp.485–92.
- Li, H. et al., 1997. A single morphogenetic field gives rise to two retina primordia under the influence of the prechordal plate. *Development (Cambridge, England)*, 124, pp.603–615.
- Li, T.-S. & Marbán, E., 2010. Physiological levels of reactive oxygen species are required to maintain genomic stability in stem cells. *Stem cells (Dayton, Ohio)*, 28(7), pp.1178–85.
- Lim, H.-J. et al., 2011. Biochemical and morphological effects of hypoxic environment

- on human embryonic stem cells in long-term culture and differentiating embryoid bodies. *Molecules and cells*, 31(2), pp.123–132.
- Lund, R.D. et al., 2006. Human embryonic stem cell-derived cells rescue visual function in dystrophic RCS rats. *Cloning and stem cells*, 8(3), pp.189–199.
- Lye, G.J. et al., 2003. Accelerated design of bioconversion processes using automated microscale processing techniques. *Trends in Biotechnology*, 21(1), pp.29–37.
- MacLaren, R.E. et al., 2006. Retinal repair by transplantation of photoreceptor precursors. *Nature*, 444(7116), pp.203–207.
- Macosko, E.Z. et al., 2015. Highly Parallel Genome-wide Expression Profiling of Individual Cells Using Nanoliter Droplets. *Cell*, 161(5), pp.1202–1214.
- Manuscript, A., Stem, E. & Differentiation, C., 2010. NIH Public Access. *Artificial Cells Blood Substitutes And Immobilization Biotechnologyartif Cells Blood Substit Immobi*, 25(1), pp.43–51.
- Meir, Y.J.J. et al., 2013. A versatile, highly efficient, and potentially safer piggyBac transposon system for mammalian genome manipulations. *FASEB Journal*, 27, pp.4429–4443.
- Mellough, C.B. et al., 2012. Efficient stage-specific differentiation of human pluripotent stem cells toward retinal photoreceptor cells. *Stem cells (Dayton, Ohio)*, 30(4), pp.673–86.
- Mellough, C.B. et al., 2014. Lab generated retina: Realizing the dream. *Visual neuroscience*, pp.1–16.
- Melton, L. a. et al., 2002. Dismt - Determination of mixing time through color changes. *Chemical Engineering Communications*, 189(March 2015), pp.322–338.
- Meng, X. et al., 2014. Stem cells in a three-dimensional scaffold environment. *SpringerPlus*, 3(1), p.80.
- Meyer, J.R., 2008. The significance of induced pluripotent stem cells for basic research and clinical therapy. *Journal of medical ethics*, 34(12), pp.849–851.
- Meyer, J.S. et al., 2009. Modeling early retinal development with human embryonic and induced pluripotent stem cells. *Proceedings of the National Academy of Sciences of the United States of America*, 106(39), pp.16698–16703.
- Meyer, J.S. et al., 2012. Optic vesicle like structures derived from human pluripotent stem cells facilitate a customized approach to retinal disease treatment. *NIH Public Access*, 29(8), pp.1206–1218.
- Mfopou, J.K. et al., 2010. Recent advances and prospects in the differentiation of pancreatic cells from human embryonic stem cells. *Diabetes*, 59(9), pp.2094–101.
- Micheletti, M. & Lye, G.J., 2006. Microscale bioprocess optimisation. *Current Opinion in Biotechnology*, 17(6), pp.611–618.
- Militante, J.D. & Lombardini, J.B., 2002. Taurine: evidence of physiological function in the retina. *Nutritional neuroscience*, 5(2), pp.75–90.
- Moon, S.H. et al., 2014. Optimizing human embryonic stem cells differentiation efficiency by screening size-tunable homogenous embryoid bodies. *Biomaterials*, 35(23), pp.5987–5997.
- Moon, S.-H. et al., 2011. Gene expression profiles in CHA3 and CHA4 human embryonic stem cells and embryoid bodies. *Molecules and cells*, pp.1–10.

- Nakano, T. et al., 2012. Self-formation of optic cups and storable stratified neural retina from human ESCs. *Cell stem cell*, 10(6), pp.771–85.
- Niebruegge, S. et al., 2009. Generation of human embryonic stem cell-derived mesoderm and cardiac cells using size-specified aggregates in an oxygen-controlled bioreactor. *Biotechnology and Bioengineering*, 102(2), pp.493–507.
- Niederhorn, J.Y. & Wang, S., 2005. Immune privilege of the eye and fetus: parallel universes? *Transplantation*, 80(9), pp.1139–1144.
- Nowak, J.Z., 2006. Age-related macular degeneration (AMD): pathogenesis and therapy. *Pharmacological reports : PR*, 58(3), pp.353–63.
- Okita, K. et al., 2011. A more efficient method to generate integration-free human iPS cells. *Nature methods*, 8(5), pp.409–12.
- Okita, K. & Yamanaka, S., 2011. Induced pluripotent stem cells: opportunities and challenges. *Philosophical transactions of the Royal Society of London. Series B, Biological sciences*, 366(1575), pp.2198–2207.
- Osafune, K. et al., 2008. Marked differences in differentiation propensity among human embryonic stem cell lines. *Nature biotechnology*, 26(3), pp.313–315.
- Osakada, F. et al., 2009. Stepwise differentiation of pluripotent stem cells into retinal cells. *Nature protocols*, 4(6), pp.811–824.
- Osakada, F. & Takahashi, M., 2015. Challenges in Retinal Circuit Regeneration : Linking Neuronal Connectivity to Circuit Function. , 38(3), pp.341–357.
- Pal, R. et al., 2009. Propensity of human embryonic stem cell lines during early stage of lineage specification controls their terminal differentiation into mature cell types. *Experimental biology and medicine (Maywood, N.J.)*, 234(10), pp.1230–43.
- Pan, Y. et al., 2011. Regulation of photoreceptor gene expression by the retinal homeobox (Rx) gene product. , 339(2), pp.494–506.
- Papayioannou, V.E. et al., 1975. Fate of teratocarcinoma cells injected into early mouse embryos. *Nature*, 258(5530), pp.70–73.
- Pearson, R. a., 2014. Advances in repairing the degenerate retina by rod photoreceptor transplantation. *Biotechnology Advances*, 32(2), pp.485–491.
- Pekkanen-Mattila, M. et al., 2010. Spatial and temporal expression pattern of germ layer markers during human embryonic stem cell differentiation in embryoid bodies. *Histochemistry and cell biology*, 133(5), pp.595–606.
- Pittack, C., Grunwald, G.B. & Reh, T. a, 1997. Fibroblast growth factors are necessary for neural retina but not pigmented epithelium differentiation in chick embryos. *Development (Cambridge, England)*, 124(4), pp.805–816.
- Polykandriotis, E. et al., 2008. To matrigel or not to matrigel. *The American journal of pathology*, 172(5), p.1441; author reply 1441–1442.
- Pripuzova, N.S. et al., 2015. Development of a protein marker panel for characterization of human induced pluripotent stem cells (hiPSCs) using global quantitative proteome analysis. *Stem Cell Research*, 14(3), pp.323–338.
- Puskeiler, R., Kaufmann, K. & Weuster-Botz, D., 2005. Development, parallelization, and automation of a gas-inducing milliliter-scale bioreactor for high-throughput bioprocess design (HTBD). *Biotechnology and Bioengineering*, 89(5), pp.512–

- Ramsden, C.M. et al., 2014. Neural retinal regeneration with pluripotent stem cells. *Developments in ophthalmology*, 53, pp.97–110.
- Reichman, S. et al., 2014. From confluent human iPS cells to self-forming neural retina and retinal pigmented epithelium. *Proceedings of the National Academy of Sciences of the United States of America*, 111(23), pp.8518–23.
- Rodin, S. et al., 2010. Long-term self-renewal of human pluripotent stem cells on human recombinant laminin-511. *Nature Biotechnology*, 28(6), pp.611–615.
- Rodrigues, C. a V et al., 2011. Stem cell cultivation in bioreactors. *Biotechnology Advances*, 29(6), pp.815–829.
- Rodriguez, G. et al., 2013. Mixing time and kinetic energy measurements in a shaken cylindrical bioreactor. *Chemical Engineering Research and Design*, 91(11), pp.2084–2097.
- Rodriguez, G. et al., 2014. On the measurement and scaling of mixing time in orbitally shaken bioreactors. *Biochemical Engineering Journal*, 82, pp.10–21.
- Rodriguez-de la Rosa, L. et al., 2012. Age-related functional and structural retinal modifications in the Igf1<sup>-/-</sup> null mouse. *Neurobiology of Disease*, 46(2), pp.476–485..
- Rouhani, F. et al., 2014. Genetic Background Drives Transcriptional Variation in Human Induced Pluripotent Stem Cells. *PLoS Genetics*, 10(6).
- Rungarunlert, S. et al., 2009. Embryoid body formation from embryonic and induced pluripotent stem cells: Benefits of bioreactors. *World journal of stem cells*, 1(1), pp.11–21.
- Sachlos, E. & Auguste, D.T., 2008. Embryoid body morphology influences diffusive transport of inductive biochemicals: A strategy for stem cell differentiation. *Biomaterials*, 29(34), pp.4471–4480.
- Saha, K. et al., 2011. Surface-engineered substrates for improved human pluripotent stem cell culture under fully de fi ned conditions.
- Sakai, Y., Yoshiura, Y. & Nakazawa, K., 2011. Embryoid body culture of mouse embryonic stem cells using microwell and micropatterned chips. *Journal of Bioscience and Bioengineering*, 111(1), pp.85–91.
- Sargent, C.Y. et al., 2010. Hydrodynamic modulation of embryonic stem cell differentiation by rotary orbital suspension culture. *Biotechnology and Bioengineering*, 105(3), pp.611–626.
- Sasai, Y., Eiraku, M. & Suga, H., 2012. In vitro organogenesis in three dimensions: self-organising stem cells. *Development*, 139, pp.4111–4121.
- Sato, N. et al., 2004. Maintenance of pluripotency in human and mouse embryonic stem cells through activation of Wnt signaling by a pharmacological GSK-3-specific inhibitor. *Nature medicine*, 10(1), pp.55–63.
- Sato, N. et al., 2003. Molecular signature of human embryonic stem cells and its comparison with the mouse. *Developmental Biology*, 260(2), pp.404–413.
- Serra, M. et al., 2009. Integrating human stem cell expansion and neuronal differentiation in bioreactors. *BMC biotechnology*, 9, p.82.
- Serra, M. et al., 2012. Process engineering of human pluripotent stem cells for clinical

- application. *Trends in biotechnology*, pp.1–10.
- Sharp, B., 1885. the Development of the Eye. *Science (New York, N.Y.)*, 6(135), pp.194–195.
- Sher, F. et al., 2012. Dynamic changes in Ezh2 gene occupancy underlie its involvement in neural stem cell self-renewal and differentiation towards oligodendrocytes. *PLoS ONE*, 7(7).
- Silk, N.J. et al., 2010. Fed-batch operation of an industrial cell culture process in shaken microwells. *Biotechnology letters*, 32(1), pp.73–8.
- Soldner, F. et al., 2009. Parkinson's Disease Patient-Derived Induced Pluripotent Stem Cells Free of Viral Reprogramming Factors. *Cell*, 136(5), pp.964–977.
- Somers, A., 2010. NIH Public Access. *NIH Public Access*, 28(10), pp.1728–1740.
- Sommer, A.C., 2009. Induced Pluripotent Stem Cell Generation Using a Single Lentiviral Stem Cell Cassette. *Stem Cells*, 27, pp.543–549.
- Sridhar, A., Steward, M.M. & Meyer, J.S., 2013. Nonxenogeneic growth and retinal differentiation of human induced pluripotent stem cells. *Stem cells translational medicine*, 2(4), pp.255–64.
- Stadtfeld, M. et al., 2008. Pluripotent Generated Without Induced Stem Viral Integration. *Science*, 322(5903), pp.945–949.
- Stevens, L.C., 1970. The development of transplantable teratocarcinomas from intratesticular grafts of pre- and postimplantation mouse embryos. *Developmental biology*, 21(3), pp.364–382.
- Sun, N., Longaker, M.T. & Joseph, C., 2010. Considerations before clinical applications. , 9(5), pp.880–885.
- Tada, M. et al., 2001. Nuclear reprogramming of somatic cells by in vitro hybridization with ES cells. , 11(1), pp.1553–1558.
- Takahashi, K. et al., 2007. Induction of Pluripotent Stem Cells from Adult Human Fibroblasts by Defined Factors. *Cell*, 131(5), pp.861–872.
- Takahashi, K. & Yamanaka, S., 2006. Induction of Pluripotent Stem Cells from Mouse Embryonic and Adult Fibroblast Cultures by Defined Factors. *Cell*, 126(4), pp.663–676.
- Thomson, J. a et al., 1998. Embryonic stem cell lines derived from human blastocysts. *Science (New York, N.Y.)*, 282(5391), pp.1145–1147.
- Thomson, J. a et al., 1995. Isolation of a primate embryonic stem cell line. *Proceedings of the National Academy of Sciences of the United States of America*, 92(17), pp.7844–7848.
- Tian, L. et al., 2015. Transcriptome of the human retina, retinal pigmented epithelium and choroid. *Genomics*.
- Tucker, B. a. et al., 2013. Patient-specific iPSC-derived photoreceptor precursor cells as a means to investigate retinitis pigmentosa. *eLife*, 2, pp.e00824–e00824.
- Ungrin, M.D. et al., 2008. Reproducible, ultra high-throughput formation of multicellular organization from single cell suspension-derived human embryonic stem cell aggregates. *PLoS ONE*, 3(2).
- Valamehr, B. et al., 2011. Developing defined culture systems for human pluripotent

- stem cells. *Regenerative medicine*, 6(5), pp.623–634.
- Valamehr, B. et al., 2008. Hydrophobic surfaces for enhanced differentiation of embryonic stem cell-derived embryoid bodies Results. *Pnas*.
- Vallier, L. et al., 2009. Signaling pathways controlling pluripotency and early cell fate decisions of human induced pluripotent stem cells. *Stem Cells*, 27(11), pp.2655–2666.
- Vallier, L. & Pedersen, R., 2008. Differentiation of human embryonic stem cells in adherent and in chemically defined culture conditions. *Current Protocols in Stem Cell Biology*, Chapter 1(SUPPL. 4), p.Unit 1D.4.1–1D.4.7.
- Vallier, L. & Pedersen, R. a, 2005. Human embryonic stem cells: an in vitro model to study mechanisms controlling pluripotency in early mammalian development. *Stem cell reviews*, 1(2), pp.119–130.
- VandenDriessche, T. et al., 2009. Emerging potential of transposons for gene therapy and generation of induced pluripotent stem cells. *Blood*, 114(8), pp.1461–1468.
- Veraitch, F.S. et al., 2008. The impact of manual processing on the expansion and directed differentiation of embryonic stem cells. *Biotechnology and Bioengineering*, 99(5), pp.1216–1229.
- Waldrep, J.C. & Kaplan, H.J., 1983. Anterior chamber-associated immune deviation induced by TNP-splenocytes (TNP-ACAIID). II. Suppressor T-cell networks. *Investigative Ophthalmology and Visual Science*, 24, pp.1339–1345.
- Walia, B. et al., 2012. Induced Pluripotent Stem Cells: Fundamentals and Applications of the Reprogramming Process and its Ramifications on Regenerative Medicine. *Stem Cell Reviews and Reports*, 8(1), pp.100–115.
- Warren, L. et al., 2010. Highly efficient reprogramming to pluripotency and directed differentiation of human cells with synthetic modified mRNA. *Cell Stem Cell*, 7(5), pp.618–630.
- Watanabe, K. et al., 2007. A ROCK inhibitor permits survival of dissociated human embryonic stem cells. *Nature biotechnology*, 25(6), pp.681–686.
- Weheliye, W., Yianneskis, M. & Ducci, A., 2012a. On the Fluid Dynamics of Shaken Bioreactors — Flow Characterization and Transition. *American Institute of Chemical Engineers*, 00(0), pp.1–11.
- Weheliye, W., Yianneskis, M. & Ducci, A., 2012b. PIV measurements in a shaken cylindrical bioreactor. , (1997), pp.9–12.
- West, E.L. et al., 2012. Defining the Integration Capacity of ES Cell-Derived Photoreceptor Precursors. *Stem cells (Dayton, Ohio)*, (0), pp.1424–1435.
- Wilson, J.L. & McDevitt, T.C., 2012. Stem cell microencapsulation for phenotypic control, bioprocessing, and transplantation. *Biotechnology and bioengineering*, 110(3), pp.667–682.
- Wilson, S.W. & Houart, C., 2004. Early steps in the development of the forebrain. *Developmental Cell*, 6(2), pp.167–181.
- Van Winkle, A.P., Gates, I.D. & Kallos, M.S., 2012. Mass transfer limitations in embryoid bodies during human embryonic stem cell differentiation. *Cells Tissues Organs*, 196(1), pp.34–47.
- Woltjen, K., 2009. piggyBac transposition reprograms fibroblasts to induced

- pluripotent stem cells.pdf. *Nature Letters*, 458(9 April), pp.766–771.
- Xu, R. et al., 2009. Signaling in Human ES Cells. *October*, 3(2), pp.196–206.
- Yanai, A. et al., 2013. Differentiation of human embryonic stem cells using size-controlled embryoid bodies and negative cell selection in the production of photoreceptor precursor cells. *Tissue Engineering Part C: Methods*, Epub ahead(10).
- Yi, X. et al., 2005. Insulin receptor substrate 2 is essential for maturation and survival of photoreceptor cells. *The Journal of neuroscience : the official journal of the Society for Neuroscience*, 25(5), pp.1240–1248.
- Yirme, G. et al., 2008. Establishing a dynamic process for the formation, propagation, and differentiation of human embryoid bodies. *Stem cells and development*, 17(6), pp.1227–1241.
- Yu, J. et al., 2007. Induced pluripotent stem cell lines derived from human somatic cells. *Science (New York, N.Y.)*, 318(5858), pp.1917–1920.
- Zhang, P. et al., 2008. Short-term BMP-4 treatment initiates mesoderm induction in human embryonic stem cells. *Blood*, 111(4), pp.1933–1941.
- Zheng, Z. et al., 2010. A requirement for FGF signalling in the formation of primitive streak-like intermediates from primitive ectoderm in culture. *PloS one*, 5(9), p.e12555.
- Zhong, X. et al., 2015. Generation of three dimensional retinal tissue with functional photoreceptors from human iPSCs. *HHS Public Access*, 5(4047), pp.1–31.
- Zhou, W. & Freed, C.R., 2009. Adenoviral gene delivery can reprogram human fibroblasts to induced pluripotent stem cells. *Stem cells (Dayton, Ohio)*, 27(11), pp.2667–74.
- Zuber, M.E. et al., 2003. Specification of the vertebrate eye by a network of eye field transcription factors. *Development (Cambridge, England)*, 130, pp.5155–5167.